FINAL REPORT
AQRP Project 10-006

Quantification of industrial emissions of VOCs, NO_2 and SO_2 by SOF and Mobile DOAS

John Johansson[1], Johan Mellqvist[1], Jerker Samuelsson[1,2] Brian Offerle[1,2]

Bernhard Rappenglück[3], Darrell Anderson, Barry Lefer[3], Sergio Alvarez[3] and James Flynn[3]

[1] Earth and Space Science Chalmers University of Technology, Hörsalsvägen 11, SE-41296 Göteborg, E-mail: johan.mellqvist@chalmers.se

[2] FluxSense AB, Hörsalsvägen 11, SE-41296 Göteborg, Sweden

[3]Department of Earth and Atmospheric Sciences, University of Houston
4800 Calhoun Rd Houston, TX 77204-5007

The preparation of this report is based on work supported by the State of Texas through the Air Quality Research Program administered by The University of Texas at Austin by means of a Grant from the Texas Commission on Environmental Quality.

Date: 2011-11-30

Title:

Authors: John Johansson, Johan Mellqvist, Jerker Samuelsson, Brian Offerle, Bernhard Rappenglück, Darrell Anderson, Barry Lefer, Sergio Alvarez and James Flynn

Department of Earth and Space Science
Chalmers University of Technology
Hörsalsvägen 11
SE-412 96 Göteborg
Sweden

E-mail: johan.mellqvist@chalmers.se

Executive summary

A measurement study was performed from April 6 to June 18, 2011, in southeast Texas, with the aim to study direct emission of VOCs (Volatile Organic Compounds), SO_2, NO_2, and formaldehyde (HCHO) from refineries and petrochemical industries. Several methods were used, i.e. SOF (Solar Occultation Flux), Mobile DOAS (Differential Optical Absorption Spectroscopy), thermal FTIR (Fourier Transform InfraRed) spectroscopy and canister sampling with gas chromatography analysis. These methods were complemented by meteorological measurements by GPS sondes, a sonic anemometer positioned on the measurement car and a 17 m high mobile mast on a trailer.

In addition, measurements of methane, ethane, propane CO and other VOCs were made in the Fort Worth area from May 9 to May 15, to study emissions from natural gas production and to investigate whether these are relevant for the frequently high levels of tropospheric ozone in the Fort Worth area. The methods used for this were Mobile extractive FTIR (MeFTIR) and tracer gas correlation combined with canister sampling. In addition, SOF measurements were carried out.

Several sites in SE Texas have been surveyed with SOF and Mobile DOAS before, i.e. Houston Ship Channel (HSC), Mont Belvieu and Texas City. When comparing the 2011 results with measurements from previous years i.e. 2006 and 2009, as shown in Table ES 1 below, some general patterns can be seen. For alkanes and ethene the overall emissions seems fairly constant over the 5 years, with the exception for Mont Belvieu showing variable alkane emissions. For propene the emissions seems to have decreased, especially between 2006 and 2009, for the HSC. However, during a significant part of the 2011 AQRP study the propene channel was underperforming which limits the available propene data. This is especially true for Mont Belvieu, one of the largest sources in previous studies.

The Beaumont and Port Arthur area was surveyed for the first time with SOF in this campaign. Alkane emissions as summed up from seven individual plant areas, averaged about 6700 kg/h.. In terms of alkenes, four plants in the Beaumont Port Arthur area contributed with 148 kg/h of ethene emissions on average, whereas no major propene emissions were observed. From one source in Port Arthur relatively high emissions of 1.3-butadiene and isobutene were measured on different days, corresponding to 190 kg/h and 43 kg/h, respectively. This can be compared to TCEQ 2011 inventory data of 1 kg/h and 2 kg/h, respectively.
The adjacent petrochemical site in Orange was measured to have ethene emissions of on average 197 kg/h. A major alkene source was found in Longview, also surveyed for the first time with SOF. The site showed an ethene emission of 452 kg/h and a propene emission 282 kg/h.

A comparison of the 2011 measurements with the 2009 TCEQ inventory, Table ES 1 below, shows good overall agreement for NO_x ((-20)–50)% and SO_2 (18–44)%, with the exception for Texas city (260%). However, for the VOCs there are larger discrepancies with (400–1500)% for alkanes, (300–1500)% for ethene and (170–800)% for propene. For the two new areas observed here, Port Arthur/Beaumont and Longview the discrepancies are (300–700)% for ethene, (200–800)% for propene and (900–1500)% for alkanes. Hence, for VOCs it appears to be a persistent difference between inventories and measurements, independent of industrial area or region.

To investigate whether high alkene emissions, observed in the HSC and Mont Belvieu, can be explained by flaring from petrochemical industries, as speculated in earlier studies, a special thermal emission FTIR system was assembled and applied for measurements on individual petrochemical flares. From these measurements it is possible to detect, qualitatively, the presence of alkenes and roughly estimate a relative concentration of alkenes in the flare emission plume. Thermal emission measurements of 20 petrochemical flares (and 4 other point sources) were carried out and out of these 4 flares showed significant detectable amounts of ethene and propene after flaring, and for 6 of the flares studied, weak signatures of the two species were found. This indicates that more than one fifth of the flares show incomplete combustion of alkenes and that flaring indeed is a potentially large source of alkenes. This indicates the need for further petrochemical flare studies. (It is also possible to quantify the amount of gas species more precisely but this was outside the scope of this study).

Emission measurements of formaldehyde were carried out with the mobile DOAS since this is an important ozone precursor. Most of the formaldehyde sources found were detected also in a former campaign in 2009, with similar magnitude, indicating that these emissions are not temporary occurrences. Three sources were found in Texas City, averaging at 25 kg/h, 10 kg/h, and 15 kg/h respectively. One source was found in Mont Belvieu, averaging at 20 kg/h; and two sources were found in the Houston Ship Channel, averaging at 34 kg/h and 31 kg/h respectively. In the Beaumont/Port Arthur area, which had not been surveyed before, three formaldehyde sources were found with average emissions of 20 kg/h, 9 kg/h and 23 kg/h, respectively. Many of the formaldehyde sources are associated with industries emitting also alkenes.

In the Fort Worth study mobile measurements were carried out from a van, carrying out real time concentration measurements of methane and ethane with the MeFTIR system. When high concentrations of methane were encountered the emission source was located and tracer gas releases were conducted in vicinity of the source to be able to estimate the emission source strength. In addition, canister samples were taken to investigate the VOC composition. The largest single sources of methane and other species in this study were the treatment facilities combined with large compressor stations. Three such sites were measured and typical emissions are 100 kg/h of methane, 40 kg/h of CO, 10 kg/h of ethane, 1 kg/h of ethane and 0.4 kg/h of ethene; see Table ES 2.

Another emission source category is smaller compressor stations with an order of magnitude lower emission than the large stations, obtained from measuring 3 individual stations. A third emission category is well pads, i.e. sites where the natural gas is extracted and the condensates are separated in a tank. Continuous emissions typically correspond to 1 kg/h of methane, and 0.1 kg/h of ethane and little else. However, gases dissolved in the condensate are regularly flashed out by venting the condensate tanks (flashing emissions). There are reports in the literature claiming that such flashing emissions from well pads are the dominant emission source from natural gas production, due to the large amount of well pads. Flashing emissions from a condensate tank was measured on one occasion in this study with emissions of 140 kg/h methane, 10 kg/h ethane and 2 kg/h of ethene and other species; see Table ES 2. Noteworthy is the importance of ethene for tropospheric ozone formation. To our knowledge ethene emissions has not been reported by other studies and this should be further studied.

Table ES 1 Emissions obtained by SOF and mobile DOAS in this study and in earlier campaigns together with TCEQ inventory data.

Source region	Species	SOF/DOAS 2011 (kg/h)	SOF/DOAS 2009 (kg/h)	SOF/DOAS 2006 (kg/h)	Inventory 2009 (kg/h)	Inventory 2006 (kg/h)	Inventory 2004 (kg/h)
Total HSC	Ethene	612	580	804	74	64	60
	Propene	563**	624	1653	77	140	80
	Alkane	11569	10134	11528	851	1483	1500
	SO_2	2328	3364		1967	2585	2552
	NO_2	1829			1297*		
Mont Belvieu	Ethene	545	429	443	65	81	45
	Propene	58**	310	488	28	35	12
	Alkane	1319	1837	863	244	190	261
	NO_2	305	168		192*	189*	268*
Texas City	Ethene	177	118	83	4	7	9
	Propene	56**	54	ND	8	9	11
	Alkane	2342	2598	2889	318	372	240
	SO_2	1209	834		327	596	613
	NO_2	492	283		387*	452*	883*
Beaumont / Port Arthur	Ethene	179			24		
	Propene	54**			20		
	Alkane	7412			457		
	SO_2	1611			1114		
	NO_2	1421			1145*		
Longview	Ethene	452			113		
	Propene	282			32		
	Alkane	841			87		
	NO_2	176			207*		

* NO_x is reported, ** degraded measurement quality

Table ES 2 Emission data obtain from natural gas production in the Fort Worth area, obtained by combining MeFTIR, tracer gas releases and canister sampling. The data summarizes data from three large compressor stations and treatment facilities, 3 smaller compressor stations including also well pads, and emissions from three different well pads with one or several condensate tanks. Data also includes flashing emission from a condensate tank with an open valve.

Emission category	Comment	Emission (kg/h)
Compressor station, and treatment facility	6–12 compressors	CH_4: 80-150 CO: 0-40 C_2H_6: 5-10 C_3H_8: 0.03-0.8 C_2H_4: 0-0.4
Small Compressor station, and gas separators and well pad	1–3 compressor	CH_4: 8-17 CO: 0.4-10 C_2H_6:1
Well pads	2–3 condensate tanks	CH_4: 1 CO: 0.1±0.05 C_2H_6: 0-0.12
Well pad	Flashing emission from condensate tank with open valve	CH_4: 138.7 CO: 0 C_2H_6: 10.6 C_3H_8: 0.40 C_2H_4: 2.04 C_3H_6:0.04 C_5H_6: 0.01

Table of Contents

1. Introduction

A measurement study was carried out from April 6–June 18, 2011 in southeast Texas, including Houston Ship Channel (HSC), Texas City, Mont Belvieu, Beaumont, Port Arthur, and Longview (see Table 1 for specific dates for each area). The aim was to study direct emission of VOCs (Volatile Organic Compounds), SO_2, NO_2, and formaldehyde (HCHO) from refineries and petrochemical industries. Several methods were used, i.e. SOF (Solar Occultation Flux), Mobile DOAS (Differential Optical Absorption Spectroscopy), thermal FTIR (Foutrier Transform InfraRed) Spectroscopy and canister sampling.

In addition, measurements of methane, ethane, propane CO, NO and other VOCs were made in the Fort Worth area, to study emissions from natural gas production. The methods used for this were Mobile extractive FTIR (MeFTIR) and tracer correlation combined with canister sampling. In addition, SOF measurements were carried out.

Table 1 Overview of measurements

Apr 6–27	*HSC, Mont Belvieu and Texas city*	*SOF and Mobile DOAS*
6 days April 21–26	*HSC, Mont Belvieu and Texas City*	*Thermal FTIR measurements of olefins by FTIR*
Apr 28 to May 6	*Port Arthur and Beaumont*	*SOF and Mobile DOAS Alkenes, alkanes, NO2 and SO2*
May 7	*Longview*	*SOF and Mobile DOAS Alkenes, alkanes, NO2, SO2, HCHO*
May 9 to 15	*Fort Worth area*	*SOF, MeFTIR and canister*
May 16 and 17	*Port Arthur , Beaumont, Orange*	*SOF training UH , MeFTIR + canister*
June 9,10,11,12,13,14,16,18	Mont Belvieu and Texas city	alkanes (limited alkene) measurements.

The background for the project is that earlier measurements in the TexAQS 2006 campaign [Mellqvist 2007, 2008b, 2010; Rappenglück 2008a, 2008b; De Gouw 2009; Wert 2003; Ryerson 2003] showed high alkene and alkane emissions from the industrial areas in the vicinity of Houston as well occasional large plumes of formaldehyde [Rivera 2009a, 2009b; Rappenglück 2008a; Buhr 2006]. The VOC measurements were 5–10 higher than inventory values. As well as carrying out measurements in the Houston area, as in earlier studies, we have extended the area of observations to Port Arthur, Beaumont and Longview. To investigate whether flares are the cause for high and variable alkene emissions thermal FTIR were carried out on 20 flares in areas with generally high emissions.

The second objective of this study was to investigate the emissions of air pollutants from oil and gas production in the Barnett Shale area. Emissions were estimated for fugitive and intermittent sources, which include production equipment fugitives, well drilling and well completions, gas processing, and transmission fugitives. Pollutants analyzed included smog forming emissions (NOx and VOC), greenhouse gases, and air toxic compounds.

Natural gas production in the Barnett Shale region of Texas has increased rapidly since 1999, and as of June 2008, over 7700 oil and gas wells had been installed and another 4700 wells

were pending. Gas production in 2007 was approximately 923 BCF (billion cubic feet) from wells in 21 counties. Natural gas is a critical feedstock to many chemical production processes, and it has many environmental benefits over coal as a fuel for electricity generation. Nevertheless, oil and gas production from the Barnett Shale can impact local air quality and release greenhouse gases into the atmosphere.

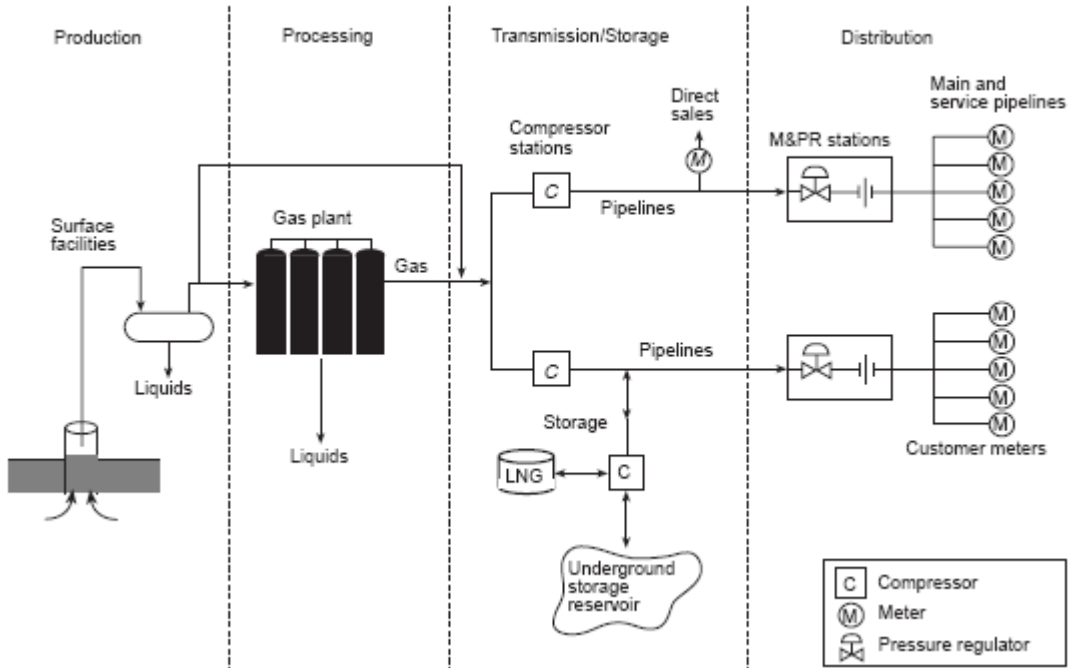

Figure 1 The main processes involved in the natural gas production in the Barnett Shale. Adapted from Armendariz, 2008

The main processes involved in the natural gas production are shown in Figure 1. Fluids that are brought to the surface at Barnett Shale natural gas wells are a high-pressure mixture of natural gas, other gases, water, and hydrocarbon liquids. The high pressure mixture is typically first sent to a separator unit, which reduces the pressure of the fluids and separates the natural gas and other gases from the water and hydrocarbon liquids. The gases are collected off the top of the separator, while the water and hydrocarbon liquids fall to the bottom and are then stored on-site in storage tanks. The hydrocarbon liquid is known as condensate. The condensate tanks at Barnett Shale wells are typically 10,000 to 20,000 gallons and hydrocarbons vapors from the condensate tanks can be emitted to the atmosphere through vents on the tanks (flashing emission). Condensate liquid is periodically collected by truck and transported to refineries for incorporation into liquid fuels, or to other processors. At oil wells, tanks are used to store crude oil on-site before the oil is transported to refiners. Like the condensate tanks, oil tanks can be sources of hydrocarbon vapor emissions to the atmosphere through tank vents.

2. Methods

The main methods used in this project were the two optical remote sensing methods, i.e. the SOF to measure emissions of VOCs (alkenes and alkanes) and Mobile DOAS to measure formaldehyde, NO_2 and SO_2. In addition, a third instrument was used, i.e. MeFTIR, to measure distributed concentrations of methane, alkanes and other tracer species such as CO. The optical measurements were complemented by canister sampling at the various sites. Meteorological measurements were obtained from GPS (Global Positioning System) sondes and Continuous Air Monitoring Stations (CAMS) operated by TCEQ (Texas Commission on Environmental Quality).

Figure 2 The SOF van and the meteorological tower.

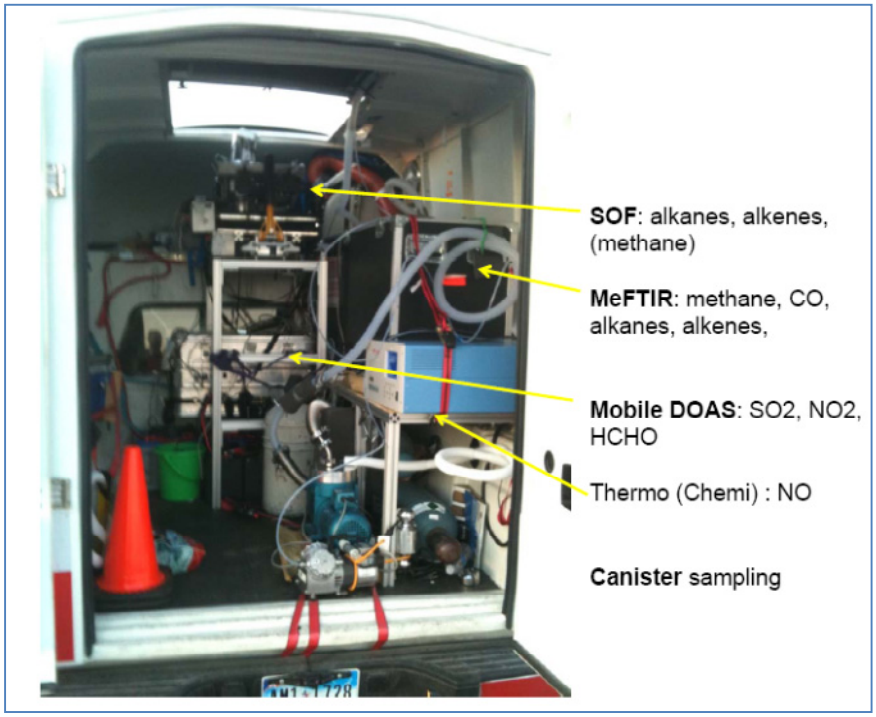

Figure 3 Overview of the instrument setup on the inside of the measurement van.

Table 2 Overview of the main measurement methods used in the study.

Method	Measurement principle	Species measured	Type of quantity	Auxiliary measurements	Derived quantity
SOF (Solar Occultation Flux)	Molecular absorption of direct sun light, Mid-IR 3–15 µm	Alkanes and alkenes	Column	GPS-coordinates, wind velocity	Mass flux
Mobile DOAS	Molecular absorption of scattered sun light, UV 310–350 nm	Formaldehyde , SO_2 and NO_2	Column	GPS-coordinates, wind velocity	Mass flux
MeFTIR	Molecular absorption of light from active source in multi-pass cell, Mid-IR 3–15 µm	Methane, other alkanes and N_2O	Concentration	Tracer gas release rate (N_2O)	Mass flux
Thermal FTIR	Molecular thermal emission of light, Mid-IR 8–15 µm	Ethene and Propene	Column	GPS-coordinates, telescope heading,	-
Canisters/GC-FID	Gas chromatography and flame ionization detection	59 different NMHCs (non-methane hydrocarbons)	Concentration	-	-

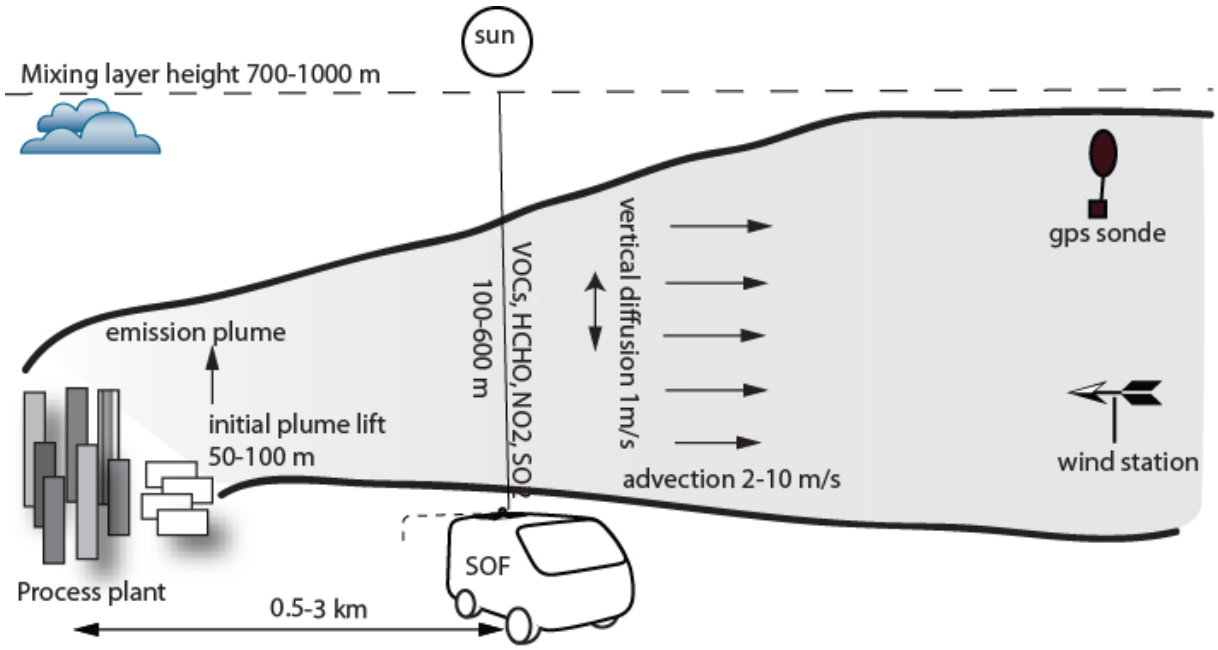

Figure 4 The SOF and Mobile DOAS experiment during the FLAIR campaign is illustrated here. In general the average wind between ground to 500 m was used, obtained from GPS sondes or from up-scaled wind station data. In the measurement car also a Mobile extractive FTIR was operated.

2.1 The SOF method

2.1.1 General

The Solar Occultation Flux (SOF) method is relatively new and was developed from a number of different research projects [Mellqvist 1999a, 1999b; Galle 1999]. The method utilizes the sun as the light source and gas species that absorb in the infrared portion of the solar spectrum are measured from a mobile platform.

The method is today used to screen and quantify VOC emissions from industrial conglomerates down to sub-areas in individual plants. The SOF method is usually combined with an extractive FTIR instrument in the same measurement vehicle, see section 2.3, by which it is possible to carry out complementary measurements, for instance night time measurements of tanks and ship loading operations. Tracer gas is then positioned at the location of the leak and then the ratio of tracer gas and leaking VOC is measured by extracting the gas plume into a gas cell and then analyzing the gas concentrations by infrared spectroscopy.

The SOF method has been applied in several larger campaigns in both Europe and the US and in more than 45 individual plant surveys over the last 7 years. In the various campaign studies it has been found that the measured emissions obtained with SOF are 5–10 times higher than the reported emission obtained by calculations. For instance in a recent study in Houston, TexAQS 2006, it was shown that the industrial releases of alkenes for the Houston Galveston area, on average, were 10 times higher than what was reported [Mellqvist 2010]. These results were supported by airborne measurements [De Gouw 2009]. For alkanes the discrepancy factor was about 8 [Mellqvist 2007]. The data obtained in the TexAQS 2006 campaign were later used in a ozone modelling study [Kim et al. 2011] showing improved results when upscaling the emission data according to the SOF study.
In a SOF measurement study for the conglomerate of refineries and oil storage in the Rotterdam harbor during 2008 [Mellqvist 2009a], a discrepancy factor of 4.4 was found between the alkane measurements and the reported VOC emission values, with individual sites varying between a factor of 2–14. A SOF study, was also carried out in France during 2008 for which large discrepancies were obtained. Also for Swedish refineries the emissions can be considerably higher than calculations and the measurements show that the VOC emissions typically correspond to 0.03–0.09 % of their throughput of oil, with more than half of the emissions originating from oil and product storage [Kihlman 2005a, 2005b]. The SOF method is also described in a recent optical remote sensing handbook by the US EPA (EPA ORS Handbook, 2011).

2.1.2 Details of the method

The SOF method is based on the recording of broadband infrared spectra of the sun with a Fourier transform infrared spectrometer (FTIR) that is connected to a solar tracker. The latter is a telescope that tracks the sun and reflects the light into the spectrometer independent of its position. From the solar spectra it is possible to retrieve the path-integrated concentration (column, see Eq. 1) in the unit mg/m^2 of various species between the sun and the spectrometer. In Figure 5 a measurement system is shown built into a van. The system consists of a custom built solar tracker, transfer optics and a Bruker EM27 FTIR spectrometer with a spectral resolution of 0.5 cm^{-1}, equipped with a combined MCT (mercury cadmium telluride) detector or an InSb (indium antimonide) detector. Optical filters were used to reduce the bandwidth when conducting alkene and alkane measurements.

Figure 5 The SOF system elevated through the roof top of the mobile van. The solar tracker (front left) transmits the solar light into the infrared spectrometer (mid right with a GPS on top) independent of the vehicle's position.

To obtain the gas emission from a source, the car is driven in such way that the detected solar light cuts through the emission plume. This is illustrated in Figure 4 and Figure 8. To calculate the gas emission the wind direction and speed is also required and these parameters are usually measured from high masts and towers.

The spectral retrieval is performed by a custom software, QESOF [Kihlman 2005b], in which calibration spectra are fitted to the measured spectra using a nonlinear multivariate fitting routine. Calibration data from the HITRAN database [Rothman 2003] are used to simulate absorption spectra for atmospheric background species at the actual pressure, temperature and instrumental resolution of the measurements. The same approach is applied for several retrieval codes for high resolution solar spectroscopy [Rinsland 1991; Griffith 1996] and QESOF has been tested against these with good results. For the retrievals, high resolution spectra of ethene, propene, propane, n-butane, n-octane and other VOCs (e.g. isobutene, 1,3-butadiene) were obtained from the PNL (Pacific Northwest Laboratory) database [Sharpe 2004]. These are degraded to the spectral resolution of the instrument by convolution with the instrument lineshape. The uncertainty in the absorption strength of the calibration spectra is about 3.5 % for the five species.

During the campaign the SOF system was operated in two parallel optical modes, one for alkenes and one for alkanes. The former mode was specifically targeted at ethene and propene and these species were retrieved simultaneously in the wavelength region between 900 and 1000 cm^{-1}, taking into account the interfering species water, CO_2 and ammonia. Ethene is also evaluated separately from propene over a shorter wave number interval. In Figure 6 solar spectra corresponding to a measurement downwind of an industrial facility in Longview are shown. The solar spectra were measured both outside and inside the emission plume. In addition spectral fits of ethene and propene are shown obtained using the QESOF spectral retrieval algorithm. The fit shown here was evaluated between 900 cm^{-1} and 1000 cm^{-1} to show both ethene and propene. A similar picture is shown in Figure 7 for 1,3-butadiene and butene measured downwind of an industrial facility in Port Arthur. During the campaign the retrievals for ethene, propene, NH_3 and butane had 1σ-variabilities (unsystematic RMS error)

in mg/m^2 of about 0.85, 1.15, 0.07 and 1.73 mg/m^2, respectively, for good measurement conditions over a transect of around 1.5 km with average speeds of 30–40 km/h. The variability is caused by interference effects and noise due to instrument vibrations while driving. Under more typical measurement conditions, occasional shadowing, road induced vibration and solar tracking also increase measurement noise. The evaluation of propene is more prone to noise due to driving conditions and other mechanically induced vibrations. This was particularly true after installing the instrument in the new measurement vehicle. Thus during the earlier part of the campaign, when most of the measurements in southeast Texas were made, the quality of the spectral evaluation of propene was not within acceptable limits and therefore propene column data are unavailable. Periodic "spikes" in the obtained column concentrations, with absolute values considerably higher than the noise values given above, often cause higher RMS (root mean square) errors in the spectral fit and are consequently removed from flux calculations.

The alkane optical mode corresponds to measurements in the infrared region between 3.3–3.7 µm (2700–3005 cm^{-1}), using the vibration transition in the carbon and hydrogen bond (CH-stretch). The absorption features of the different alkanes are similar and interfere with each other, but since the number of absorbing C-H-bonds is directly related to the molecule mass, the total alkane mass can be retrieved despite the interference. In the analysis we therefore use calibration spectra of propane, n-butane, and n-octane and fit these to the recorded spectra, using a resolution of 8 cm^{-1}. Aromatics and alkenes also have absorption features in the CH-stretch region, but mainly below 3.33 µm for the most abundant species. A sensitivity study of the SOF alkane retrieval was made for the TexAQS 2006 [Mellqvist 2007], taking into account the typical matrix of VOCs, and this study showed that total alkane mass obtained by the SOF was overestimated by 6.6 %. Here we assume the same uncertainty.

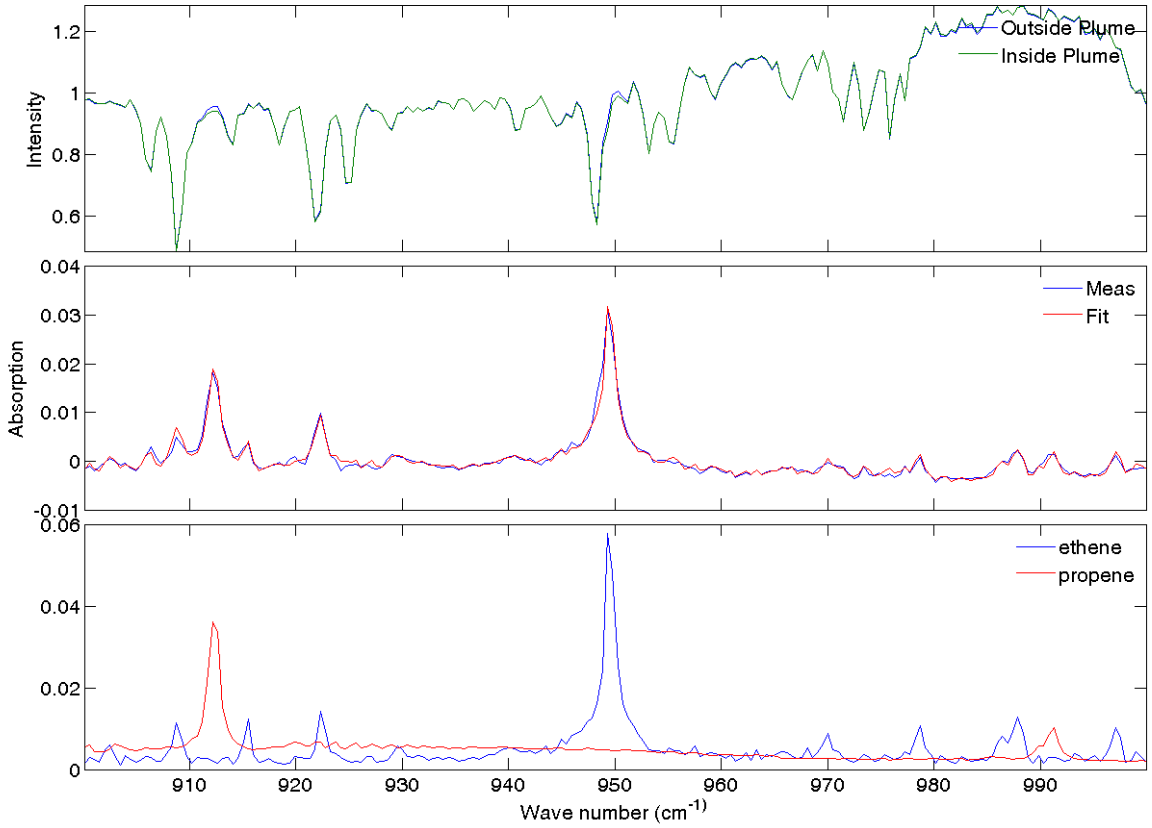

Figure 6 Solar spectra measured outside and inside the emission plume of an industrial plant in arbitrary intensity units (upper). Measured and fitted spectral evaluation for ethene and propene (calibrated spectra, lower) using the QESOF spectral retrieval algorithm is also shown (middle).

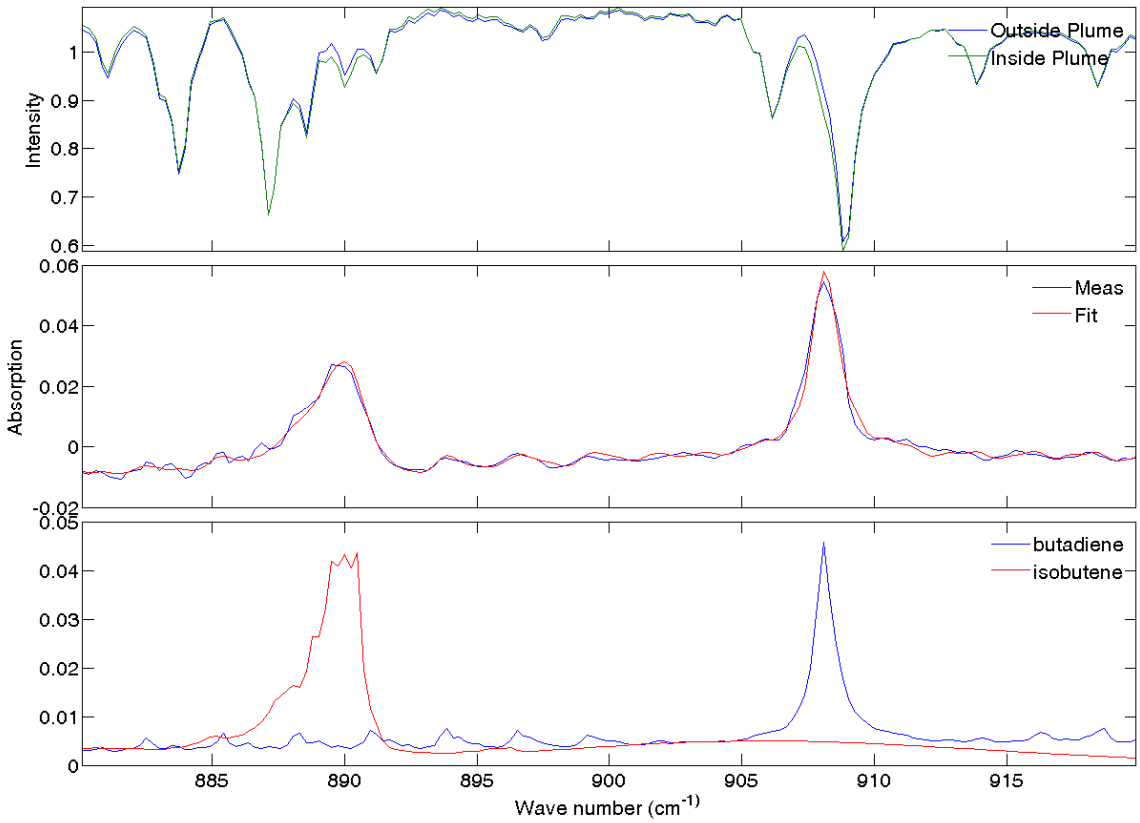

Figure 7 Solar spectra measured outside and inside the emission plume of an industrial plant in arbitrary intensity units (upper). Measured and fitted spectral evaluation for 1,3-butadiene and isobutene (calibrated spectra, lower) using the QESOF spectral retrieval algorithm is also shown (middle).

2.1.3 Flux calculation

To obtain the gas emission from a target source, SOF transects, measuring vertically integrated species concentrations, are conducted along roads oriented crosswind and close downwind (0.5–3 km) of the target source so that the detected solar light cuts through the emission plume as illustrated in Figure 2. The gas flux is obtained first by adding the column measurements and hence the integrated mass of the key species across the plume is obtained. To obtain the flux this value is then multiplied by the mass average wind speed of the plume, u'_{mw}. The flux calculation is shown in Eq. 1. Here, **x** corresponds to the travel direction, **z** to the height direction, **u'** to the wind speed orthogonal to the travel direction (x), $\mathbf{u'_{mw}}$ to the mass weighted average wind speed and $\mathbf{H_{mix}}$ to the mixing layer height. The slant angle of the sun is compensated for, by multiplying the concentration with the cosine factor of the solar zenith angle.

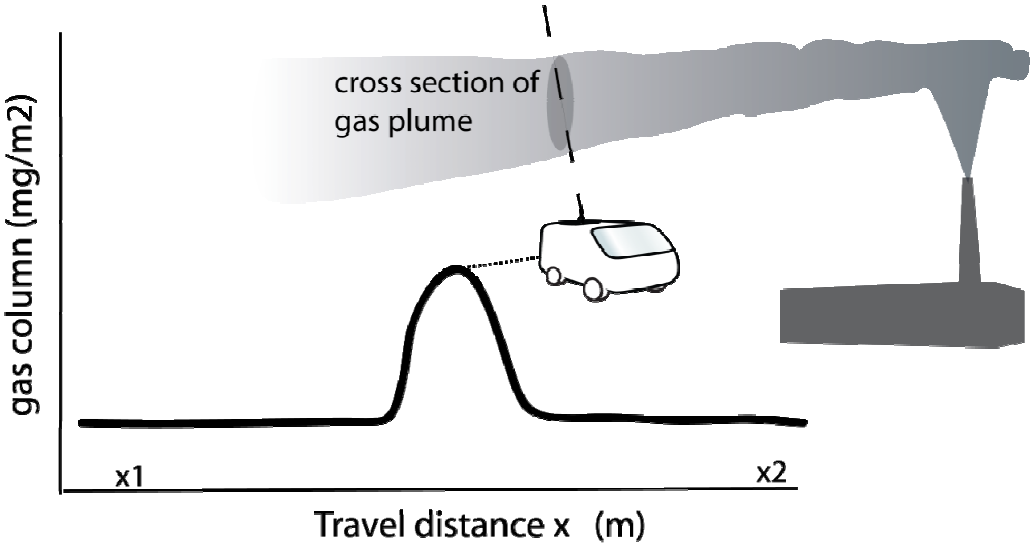

Figure 8 Illustration of the SOF measurement

$$flux = \int_{x1}^{x2}\left(\int_{0}^{Hmix} conc(z)\cdot u'(z)\cdot dz\right)dx = u'_{mw}\int_{x1}^{x2} column(x) \qquad \text{(Eq. 1)}$$

$$\text{where } u'_{mw} = \frac{\int_{0}^{Hmix} conc(z)u'(z)\cdot dz}{\int_{o}^{Hmix} conc(z)dz} \quad \text{and } column = \int_{0}^{Hmix} conc(z)\cdot dz$$

The wind is not straightforward to obtain since it is usually complex close to the ground and increases with the height. The situation is helped by the fact that SOF measurements can only be done in sunny conditions. This is advantageous since it corresponds to *unstable meteorological conditions* for which wind gradients are smoothed out by convection. Over relatively flat terrain with turbulence inducing structures the mean wind varies less than 20 % between 20 and 100 m height using standard calculations of logarithmic wind. This is illustrated for the harbor of Göteborg in Figure 9. Here the average daytime wind velocity and wind direction profile for all sunny days during August of 2004 have been simulated [Kihlman 2005a] using a meteorological flow model denoted TAPM [Hurley 2005].

In addition, for meteorological conditions with considerable convection, the emission plume from an industry mixes rather quickly vertically giving a more or less homogeneous distribution of the pollutant versus height through the mixing layer even a few kilometers downwind. In addition to the atmospheric mixing, the plumes from process industries exhibit an initial lift since they are usually hotter than the surrounding air.

The rapid well-mixed assumption agrees with results from airborne measurements made by NOAA (National Oceanic and Atmospheric Administration) [De Gouw 2009] and Baylor University [Buhr 2006] during the TexAQS 2006 in which also SOF measurements were conducted [Mellqvist 2010]. The NOAA measurements indicate that the gas plumes from the measured industries mix evenly from the ground to 1000 m altitude, i.e. throughout the entire

mixing layer, within 1000–2000 s (~25 min) transport time downwind the industrial plants. This indicates a vertical mixing speed of the plume between 0.5 to 1 m/s. This is further supported by Doppler LIDAR (Light Detection And Ranging) measurements by NOAA showing typical daytime vertical mixing speeds of ±(0.5–1.5) m/s [Tucker 2007].

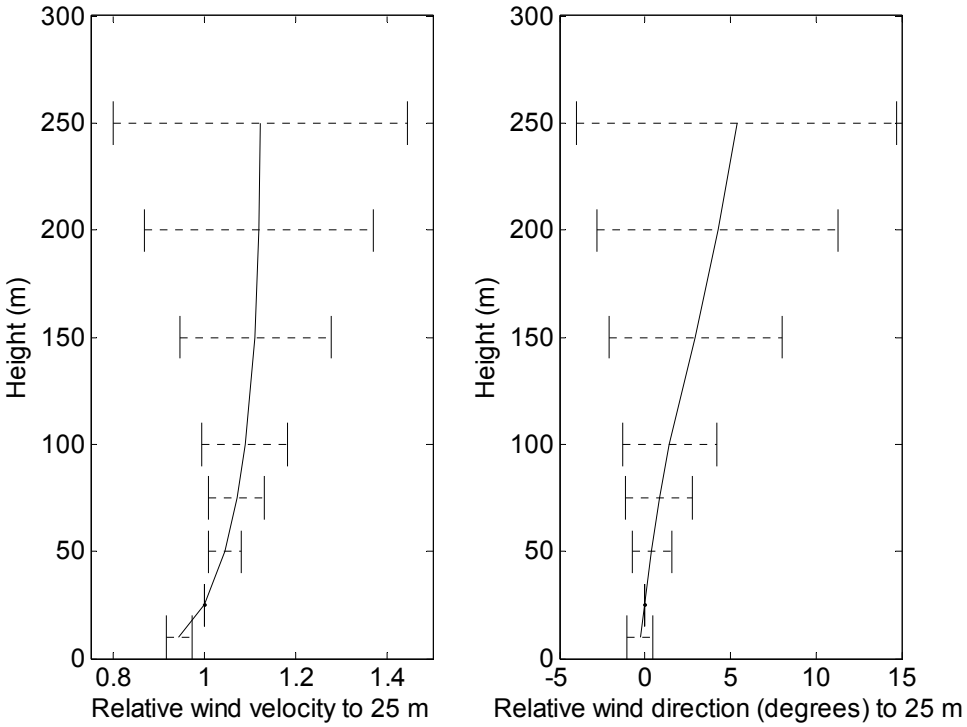

Figure 9 Average daytime wind velocity and wind direction profile retrieved by simulation above Göteborg harbor area averaged over all sunny days during a month with a wind-speed of 3–6 m/s at ground. The error bars indicate standard deviation between daily averages [Kihlman 2005a].

In this study, the measurements were conducted downwind of the industries at a typical plume transport time of 100–1000 s. According to the discussion above this means that the emission plumes have had time to mix up to heights of several hundred meters above the ground, above the first 50–100 m where the wind is usually disturbed due to various structures. For this reason we have used the average wind from 0 to 500 m height in the flux calculations. This wind was obtained from wind profiles measured by GPS balloon sondes within this project at the areas studied. Wind data from three TCEQ CAMS sites near the study areas were also used but adjusted to be comparable to the GPS wind balloons, since the latter systematically measure lower winds, see section 3. Note that it only affects the wind speed very little if the 0–100, 0–200 or 0–500 m wind is chosen. This can be seen in section 3.

Figure 10 shows a real measurement example illustrating the principle for the SOF and Mobile DOAS measurements. Here a measurement of alkanes, a transect across the plume downwind of a refinery, is shown. The measured gas column of alkanes in the unit mass/area (mg/m^2), as measured by the SOF in the solar light, is plotted versus distance across the plume. The wind was measured simultaneously by a GPS balloon, in the vicinity of the measurement as shown in Figure 11 and the 0–200 m value corresponds to 7.9 m/s, while the 0–500 value corresponds to 8.4 m/s. In the flux calculation the columns are integrated across the transect, whereby the integrated mass in unit mass per length unit in the plume (mg/m) is

obtained. This value corresponds to an average column value of 48 mg/m^2 across the whole transect, over 1300 m. This mass value is then multiplied by the wind speed, to obtain mg/s.

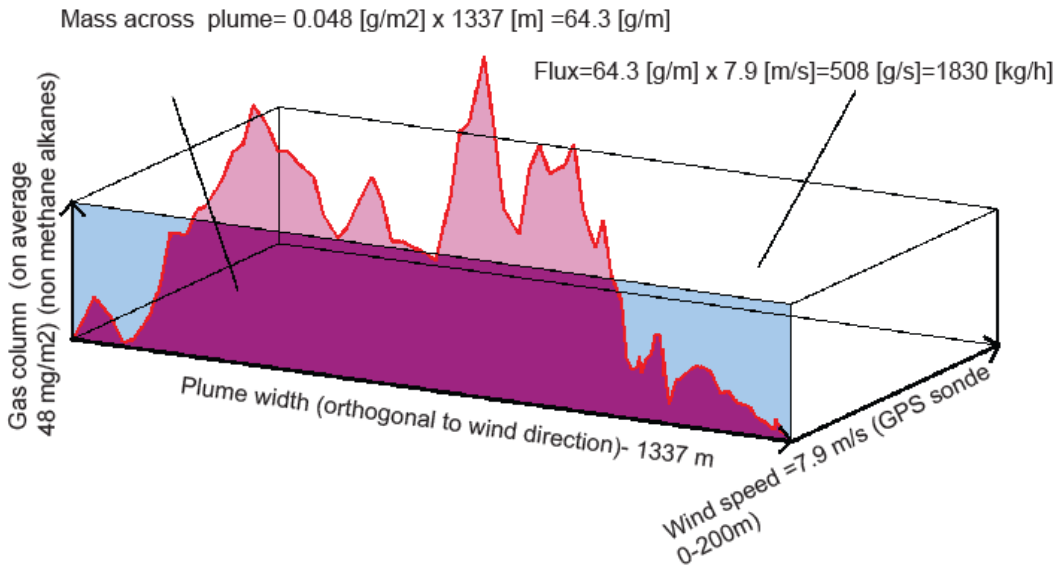

Figure 10 Illustration of the flux calculation in the SOF method for a measurement of alkanes conducted downwind of a refinery. The gas column of alkanes, retrieved from the spectra, is plotted versus distance. In the flux calculation the gas columns are integrated along the measurement transect, corresponding to the lilac area. This area, which is the integrated mass of the plume, corresponds to the same mass as an average column of 48 mg/m^2 integrated along the transect of 1337 m. The integrated mass is then multiplied with the wind speed yielding the flux in mass per seconds. Here an average wind speed from ground to 200 m was used corresponding to 7.9 m/s obtained from the GPS sonde in Figure 11.

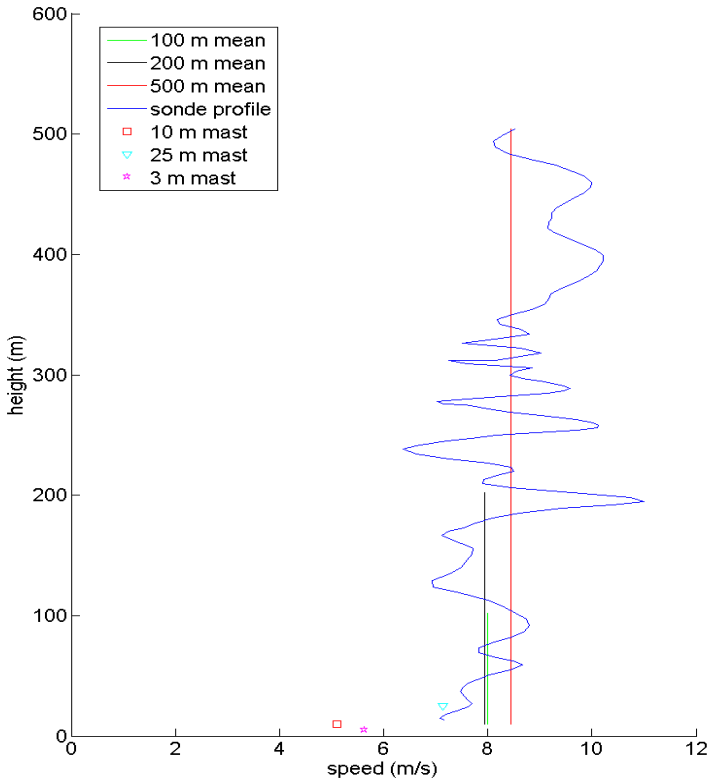

Figure 11 Wind profile measured with a GPS sonde less than ten minutes after the alkane transect shown in Figure 10 above. The wind speed versus height is shown for the balloon measurements in addition to the 0–500 and the 0–200 m average values, and values for several masts at the refinery.

To verify that a measured flux is originating from a specific area upwind of where the emission was detected, another measurement transect needs to be performed upwind of that area to make sure that the emission is not coming from another source further away. If no significant flux is detected on the upwind side, this measurement does not need to be repeated for every downwind transect. If a smaller flux is measured on the upwind side than on the downwind side, the emission from the area in between is the difference between these fluxes. In this case the upwind transect needs to be repeated with every downwind transect. This type of emission measurements is preferably avoided since it might increase the uncertainty. Upwind measurements were performed for all areas during the study, but they are not presented in the result chapter.

2.2 Mobile DOAS

2.2.1 General

Mobile DOAS (Differential Optical Absorption Spectroscopy) measurements of scattered solar light in zenith direction were carried out in parallel with the SOF measurements, from the same vehicle, in order to measure formaldehyde, NO_2 and SO_2. DOAS works in the ultraviolet (UV) and visible wavelength region while SOF works in the infrared region and hence there are large differences in spectroscopy and in the used spectrum evaluation methods. However, both methods measure vertical columns which are integrated along measurement transects and multiplied by the wind to obtain the flux. The principle of flux-measurements using Mobile DOAS is hence the same as for SOF, section 2.1.3, although it is not necessary to compensate for any slant angle observations since the telescope is always pointing towards zenith. The DOAS system also works under cloudy conditions in contrast to SOF, although the most precise measurements are conducted in clear sky.

The DOAS method was introduced in the 1970's [Platt 1979] and has since then become an increasingly important tool in atmospheric research and monitoring both with artificial light sources and in passive mode utilizing the scattered solar light. In recent time the multi axis DOAS method (scanning passive DOAS) has been applied in tropospheric research for instance measuring formaldehyde [Heckel 2005]. Passive DOAS spectroscopy from mobile platforms has also been quite extensively applied in volcanic gas monitoring [Galle et al., 2002] for SO_2 flux measurements and for mapping of formaldehyde flux measurements in megacities [Johansson 2009]. Mobile DOAS has only been used to a limited extent for measurements of industries; Rivera et al. [2009c] did SO_2 measurements on a power plant in Spain for validation purposes. They also made measurements at an industrial conglomerate in Tula in Mexico [Rivera 2009d] and measurements of SO_2, NO_2 and HCHO during the TexAQS 2006 campaign [Rivera 2009a, 2009b]. There are also groups in both China and Spain working with mobile mini DOAS.

2.2.2. Details of the method

The Mobile DOAS system used in this project, shown in Figure 12 and Figure 13, has been developed for airborne surveillance of SO_2 in ship plumes [Mellqvist 2008a] but has for this project been modified to also measure HCHO and NO_2. It consists of a UV spectrometer (ANDOR Shamrock 303i spectrometer, 303 mm focal length, 300 µm slit) equipped with a CCD (charge-coupled device) detector (Newton DU920N-BU2, 1024 by 255 pixels, thermoelectrically cooled -70^{o}C). The spectrometer has wavelength coverage of 309 to 351 nm and a spectral resolution of 0.63 nm (1800 grooves/mm holographic grating). The

spectrometer is connected to a quartz telescope (20 mrad field of view, diameter 7.5 cm) via an optical fiber (liquid guide, diameter 3 mm). An optical band pass filter (Hoya) is used to prevent stray light in the spectrometer by blocking wavelengths longer than 380 nm.

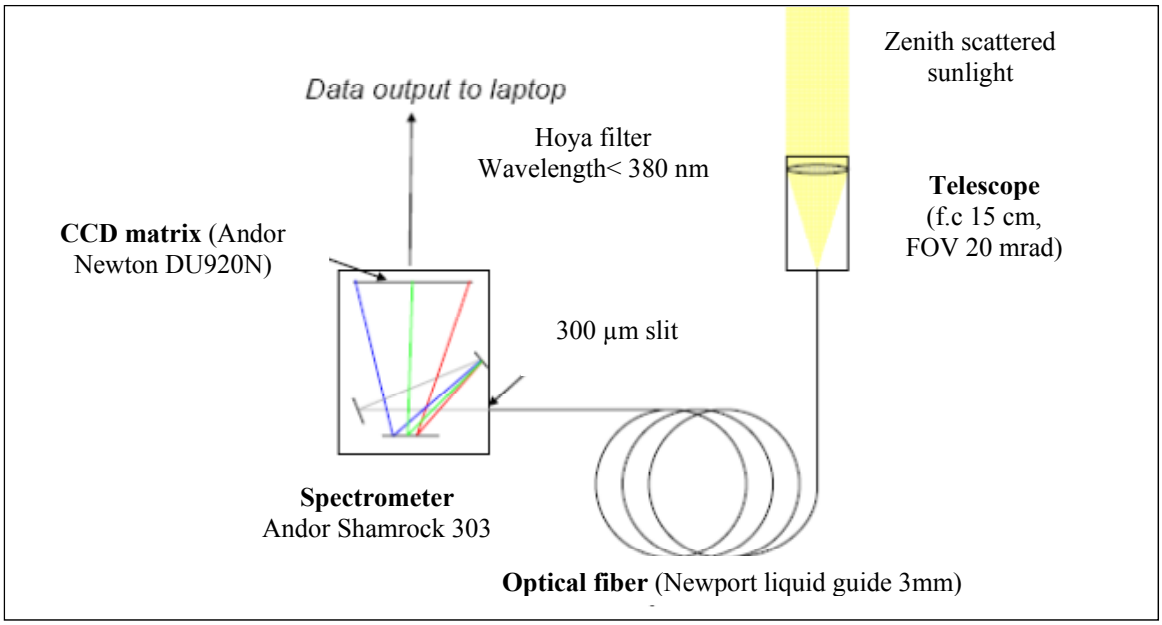

Figure 12 Overview of the Mobile DOAS system used. Scattered solar light is transmitted through a telescope, and an optical fiber to a UV/visible spectrometer. From the measured spectra the amount of HCHO, NO_2 and SO_2 in the solar light can be retrieved.

The DOAS system measures ultraviolet spectra in the 308–352 nm spectral region from which total columns of HCHO, NO_2 and SO_2 can be retrieved, Figure 14. HCHO and NO_2 are retrieved between 324 to 350 nm, together with the interfering species O_3, O_4 and SO_2. SO_2 and O_3 is then retrieved between 310 to 324 nm together with the NO_2 and HCHO columns obtained from the previous retrieval at 324–350 nm, Figure 15.

In the spectral evaluation the recorded spectra along the measurement transect are first normalized against a reference spectrum recorded upwind the industry of interest. In this way most of the absorption features of the atmospheric background and the inherent structure of the sun is eliminated. Ideally the reference spectrum is expected not to include any concentration above ambient of the trace species of interest, however in urban and industrial areas this is difficult to achieve, and therefore our measurement in this case will produce the difference in vertical columns between the reference spectrum and all measured spectra across the plume for every measurement series. The normalized spectra are further high pass filtered according the algorithms proposed by Platt and Perner [1979], and then calibration spectra are scaled to the measured ones by multivariate fitting. Here we have used a software package denoted QDOAS [Van Roozendael 2001] developed at the Belgian Institute for Space Aeronomy (BIRA/IASB) in Brussels.

The calibration spectra used here for the various gases are obtained from the following: HCHO [Cantrell 1990], NO_2 [Vandaele 1998], SO_2 [Bogumil 2003], O_3 [Burrows 1999] and O_4 [Hermans 1999]. In addition to these calibration spectra it is also necessary to fit a so called Ring spectrum, correcting for spectral structures arising from inelastic atmospheric scattering [Fish 1995]. The Ring spectra used have been synthesized with a component of the QDOAS software, which uses a high resolution solar spectrum to calculate the spectrum of Raman scattered light from atmospheric nitrogen and oxygen, convolves this spectrum and

the high resolution solar spectrum with the instrument lineshape and calculate the ratio between them. One problem with the acquired spectra is the fact that the wavelength scale of the spectrometer was variable with shifts in the wavelength scale for the individual spectra. Even though these shifts were minute, within 0.02 nm, they still cause large residuals when normalizing the spectra to the reference spectrum. To overcome this we have used the QDOAS program, to characterize the wavelength calibration of the spectra by comparing the positions of the solar absorption lines with a high-resolved solar spectrum. This improved the results quite considerably. An example of a fit can be seen in Figure 14 in which a calibration spectrum of formaldehyde has been fitted to the measured differential absorbance. This differential spectrum corresponds to a high pass filtered atmospheric spectrum with the features of ozone, NO_2 and spectrum of inelastic atmospheric scattering removed. This spectrum was measured south west of the HSC and corresponds to 3.8 10^{16} molecules/cm^2 as can be seen in Figure 14.

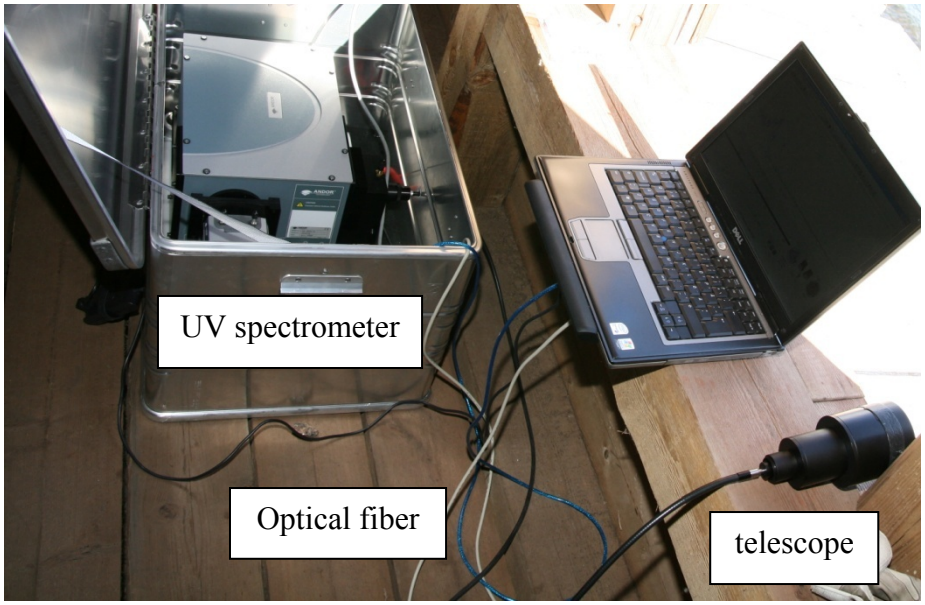

Figure 13 The Mobile DOAS system consisting of a UV spectrometer, optical fiber and UV telescope.

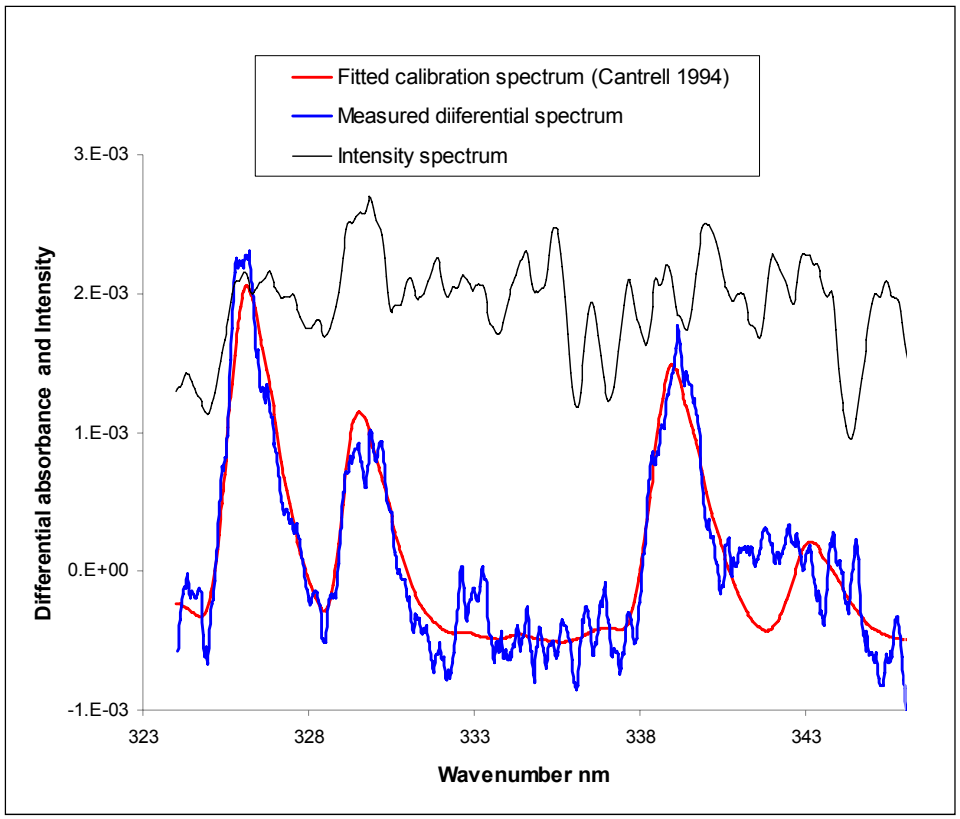

Figure 14 Ultraviolet spectrum (Intensity counts versus wavelength) measured south west of HSC by the Mobile DOAS system on May 20 2009, 10:40, adapted from Mellqvist 2010. From this spectrum a formaldehyde column of 3.8 10^{16} molecules/cm^2 was derived by fitting a calibration spectrum to the measured high pass filtered absorbance (after subtraction of ozone, NO_2 and inelastic atmospheric scattering).

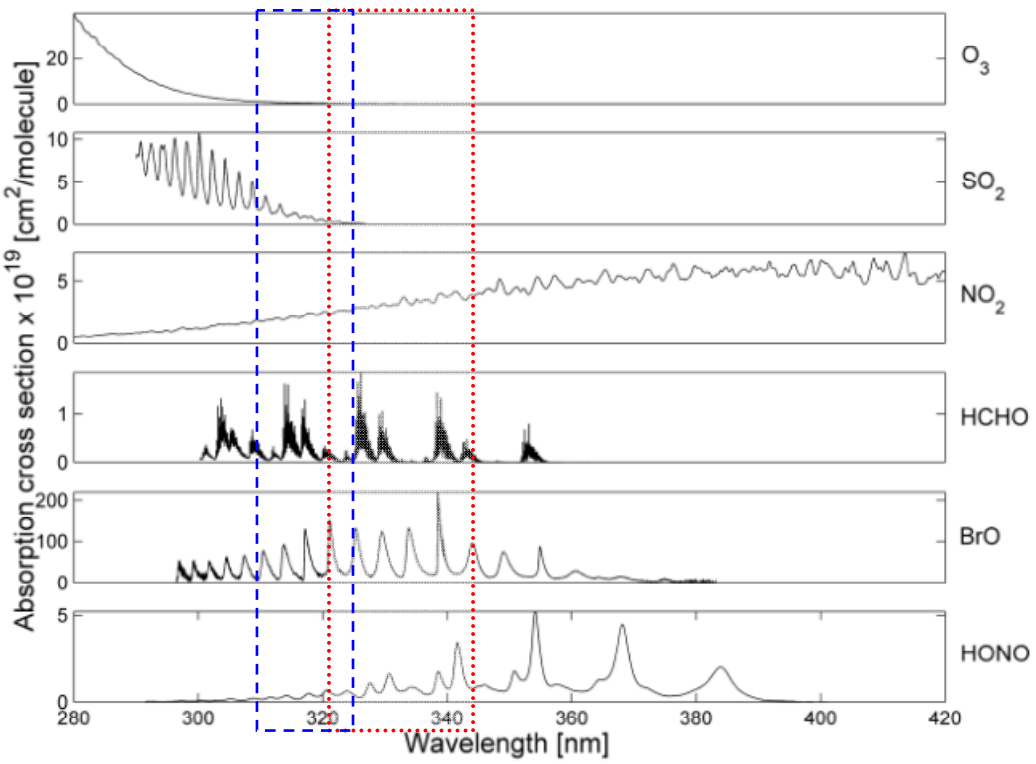

Figure 15 Absorption features of formaldehyde and some other interfering species of relevance are shown. The two wavelength regions applied for the retrieval of HCHO (red) and NO_2 (red) and SO_2 (blue), respectively, indicated by the colored rectangles. The above species were retrieved simultaneously, together with oxygen dimer (O_4) and a zenith sky spectrum and a so called ring spectrum.

2.3. Mobile extractive FTIR and tracer correlation

In addition to the SOF and Mobile DOAS measurements, Chalmers University operated a Mobile extractive FTIR (MeFTIR) system, measuring ground concentrations of mainly ethene, propene, alkanes, methane, NH_3, CO, CO_2, and CH_4. In contrast to the line integrating methods SOF and DOAS, MeFTIR measures the concentration in one mobile point. This provides additional information on the vertical distribution of plumes detected by the SOF system, comparing the vertical columns with the point concentration at the ground.

The extractive FTIR system contains a spectrometer of the same type used for the SOF system, Bruker IRCube, but utilizes an internal glow bar as an infrared radiation source instead of the sun, and transmits this light through a measurement cell. The spectrometer was connected to an optical multi-pass cell (Infrared Analysis Inc.) operated at 40 m path-length, and the transmitted light was detected simultaneously with an InSb-detector (indium antimonide) in the 2.5–5.5 µm (1800–4000 cm^{-1}) region and a MCT (mercury cadmium telluride) detector in the 8.3–14.3 µm (700–1200 cm^{-1}) region . Temperature and pressure averages in the cell were integrated over the cycle of each spectrum. Atmospheric air was continuously pumped with high flow through the optical cell from the outside, taking the air in from the roof of the van through a Teflon tube. A high flow pump was used to ensure that the gas volume in the cell was fully replaced within a few seconds. Spectra were subsequently recorded with an integration time of typically 10 seconds. A GPS-receiver was used to register the position of the van every second.

The concentration in the spectra was analyzed online, fitting a set of calibration spectra based on the Hitran2000 infrared database (updated to the 2007 edition) [Rothman et al. 2003] and the PNL database [Sharpe 2004] in a least-squares fitting routine [Griffith 1996]. Since the MeFTIR system was an add-on and not included in the project only a few examples are shown here.

The MeFTIR system is used in the emission plume together with tracer gas releases at the emission source, in order to quantify the emission, so called tracer correlation approach. This way, emissions for a total tank filling cycle or ship loading procedure can be determined. The method has also been deployed for flare efficiency analysis and methane emissions [Babilotte 2009; Börjesson 2009; Samuelsson 2005a; Galle 2001]. The tracer correlation approach is described in a recent optical remote sensing handbook by the US EPA (EPA ORS Handbook, 2011).

In order to assess the emission of methane from the various sites, tracer gas was released in vicinity of the sources. When released to the atmosphere the tracer is dispersed in the same way as the emitted methane, given good mixing conditions, and the cross plume integrated concentration ratio of methane to tracer gives the methane emission rate from the site:

$$Emission_{CH4} = Q_{tracer} \cdot \frac{\int_{Plume\ end\ 1}^{Plume\ end\ 2} [CH4]dx}{\int_{Plume\ end\ 1}^{Plume\ end\ 2} [Tracer]dx} \cdot \frac{M_{CH4}}{M_{Tracer}} \qquad \text{(Eq. 2)}$$

where Q_{tracer} is the release rate of the tracer gas, C denotes the cross plume integrated concentrations above background (mixing ratio), M denotes the molar masses, and x corresponds to distance cross the plume. Repeated plume integrations during typically a one to three hour period results in an average emission and variability estimate for that time frame (including source variability and method uncertainties).

The tracer was released from commercial gas bottles (Tri-Gas), using two-stage flow regulators. The amount of released gas was weighed on a precision scale, and the total time of gas release was registered.
In order to minimize the error due to tracer misplacement compared to the actual methane release pattern, the plume should be integrated far downwind to allow for good mixing of the two plumes. In general a downwind distance of about 5 times the radius of the emitting part of is used.

Post-processing of all data are done, integrating the methane and tracer concentrations in the cross plume transects (according to Eq. 2). In connection to the measurement an upwind site transect should be made to certify that no interfering sources are present (e.g. show that the upwind concentration is the same as the background concentration at the plume edges). It should also be certified that the natural presence of tracer in the cross plume transect is negligible compared to when the tracer release is active.

Figure 16 The MeFTIR instrument used in parallel with the SOF system during the campaign. The gas is extracted into the White-cell where it is analysed by infrared absorption measurements. The residence time in the gas cell, and hence the measurements time resolution, is a few seconds.

Figure 17 Tracer releases of N_2O from a car upwind of a well and mobile compressor station in Fort Worth.

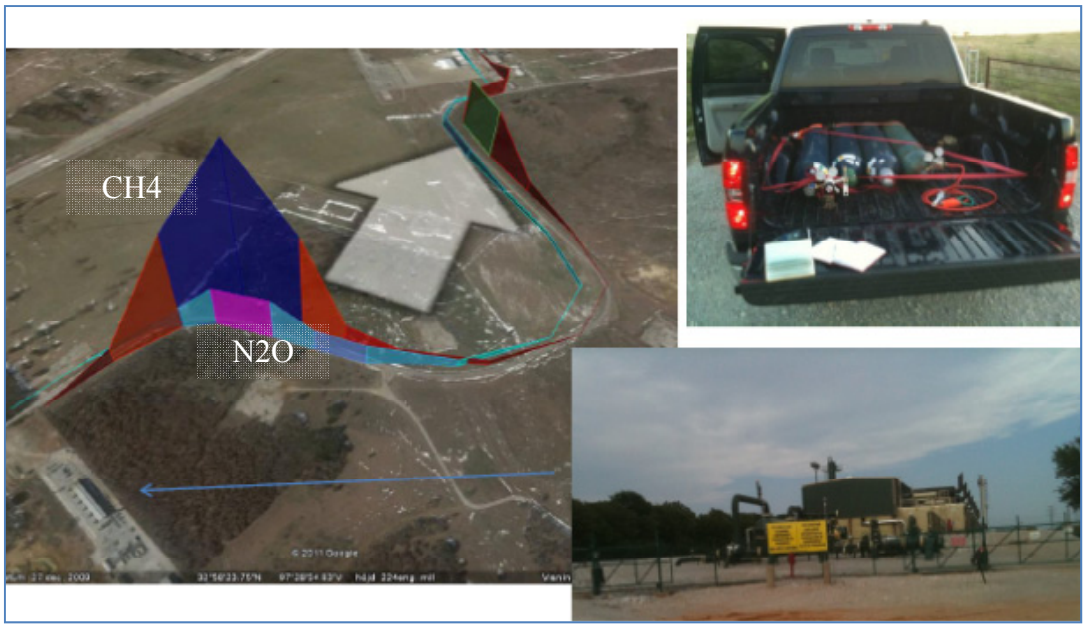

Figure 18 Example of a tracer correlation measurements at a compressor and well pad facility at , 1.8 km SSE of the CAM75 site close to the Kenneth Copeland airfield. The methane (red to blue) and tracer gas (pink to cyan) is shown downwind.

2.4 Thermal FTIR

In contrast to the earlier described SOF measurements where the solar infrared absorption by molecules in the plume is measured, passive thermal FTIR spectroscopy utilizes the infrared energy in the warm exhaust plumes themselves. This method can be applied any hour of the day, since no external IR source (sun) is required, and by means of a viewing telescope objects can be surveyed at a distance pin pointing several different sources within a short time frame. As with SOF and FTIR in general, the method is non-intrusive and measures several compounds simultaneously in time. Figure 19 shows the thermal FTIR instrument (Bruker Optics EM27) mounted on a tripod. This is in fact the same spectrometer as used for the SOF measurements, but reassembled with a telescope in front and a visual aiming scope on top. Figure 20 shows the set-up and observed thermal signal at a flare measurement in Mont Belvieu, Texas. The infrared telescope has a field of view of 10 mrad, thus giving a probing cone of 10 m at a range of 1000 m. For further technical details of the FTIR spectrometer, see the SOF section.

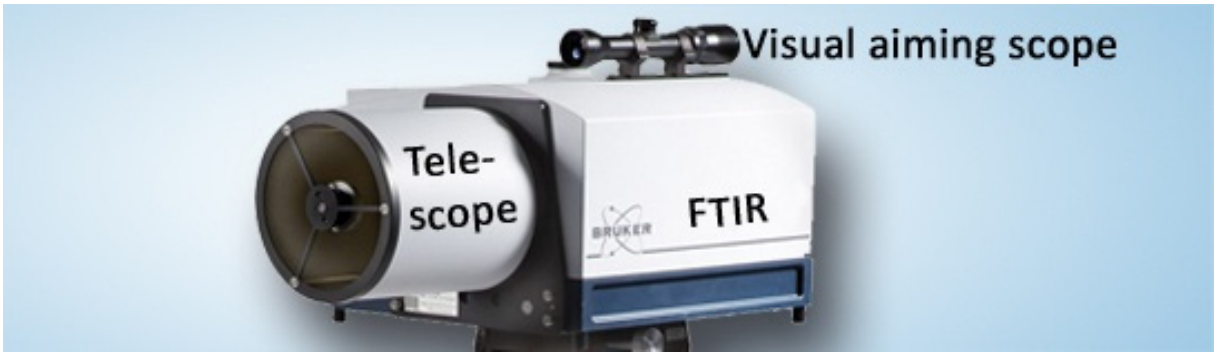

Figure 19 The passive thermal emission FTIR (Bruker Optics EM27), assembled with a infrared telescope and visual aiming scope, all mounted on a tripod.

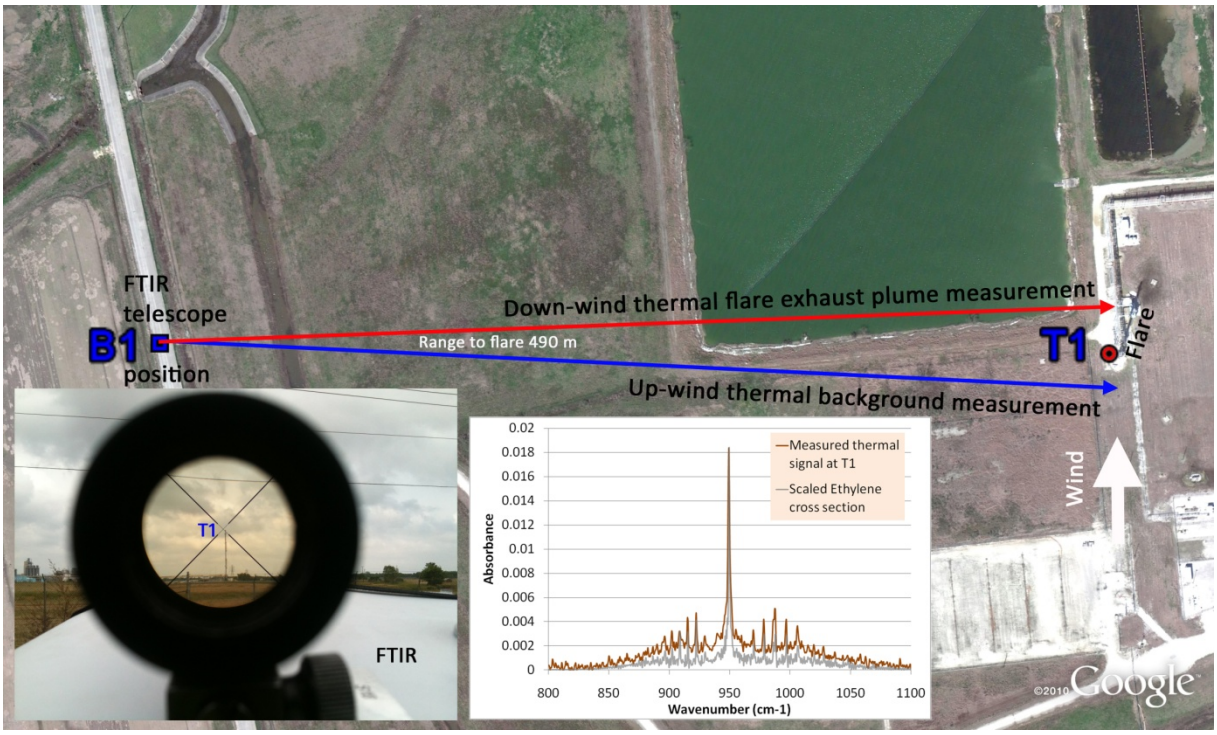

Figure 20 Set-up of the thermal FTIR measurements at flare T1 in Mont Belvieu. The blue square indicates the base position (B) of the infrared telescope, whereas the red circle (T) indicates the corresponding thermal emission survey object. Down left a photo through the visual aiming scope of the FTIR is enclosed. The thermal background of the atmosphere measured immediately up-wind the flare is subtracted from the down-wind plume measurement. The resulting thermal emission signal is shown in the enclosed graph, showing evident ethene presence (compare with the ethene cross section from the Pacific Northwest National Laboratory infrared data base in grey).

By subtracting the atmospheric background immediately up-wind the source from the thermal signal in the down-wind plume, the presence of ethene, propene and other compounds in the exhaust can be established. Ethene and propene was measured with a mercury cadmium telluride (MCT) detector in the 10 µm wavelength region. Figure 21 shows the thermal signal measured in a flare exhaust plume on top of the corresponding atmospheric background signal.

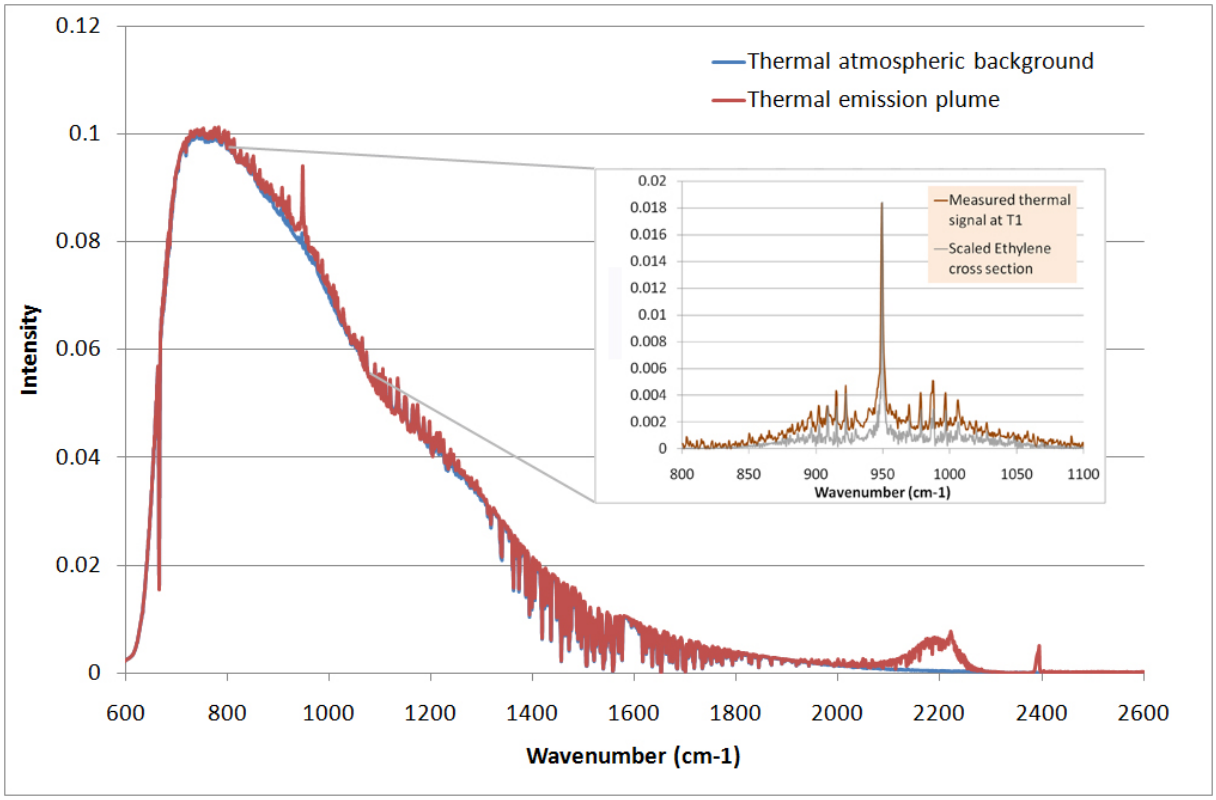

Figure 21 Thermal signal measured in the flare exhaust plume on top of the corresponding atmospheric background signal. The enclosed graph shows the thermal signal with the atmospheric background subtracted, along with the scaled cross section fingerprint of ethene.

In order to go further in the analysis and obtain quantitative measures, several issues have to be addressed. This process is, for example, thoroughly described in a report to the TCEQ (URS Corporation, 2004). The analysis includes establishment of the plume temperature, which can be done by observing the emission strength among different lines along the emission band. Furthermore, the absolute radiance response of the thermal instrument has to be calibrated against a black body source (perfectly infrared energy emitting body) at various temperatures.
In the present project black body calibration was done with an internal source in the spectrometer, and the thermal response was established over the 283 K to 358 K range (10 deg. C – 85 deg. C). Quantitative analysis of the thermal measurements is not within the scope of this report. Instead the passive FTIR method was used to show presence of alkenes in various flares and stacks, in areas known from quantitative SOF measurements to have substantial alkene emissions. Nevertheless, the thermal emission data set could be further processed to also retrieve quantitative data.

2.5. Canister sampling

Canisters were supplied by the University of Houston. These canisters were 1 L uniquely labeled 2-valve electro-polished stainless steel canisters (Fäth, Eschau-Hobbach, Germany). These canisters have demonstrated effective and stable ambient air storage in various intercomparisons [Slemr, 2002; Plass-Dülmer et al., 2006; Rappenglück et al., 2006] and have been used both in airborne missions [e.g. Winkler et al., 2002; Methven et al., 2006; Arnold et al., 2007] as in air quality studies [e.g. Winkler et al., 2002; Rappenglück et al., 2005] and emission studies [e.g. Slemr, 2002; Schürmann et al., 2007]. As an inlet a stainless steel

tubing (about 1 m) was connected to the pressurization metal bellow pump employing an inline PTFE membrane filter (pore size 0,45 µm; stainless steel filter holder). The samples were drawn from above the roof of the mobile van. The tubing is used to destroy ozone prior to entering the canister according to a method by Koppmann et al., [1995] and the filter to protect the pump and canisters from particles and aerosols. For sampling, a canister is attached downstream to the pump. The basic sampling arrangement for one 2-valve canister is shown in Figure 22. Due to the requirement of this project to sample duplicate canisters a T-union was installed behind the pressure gauge in the tubing connecting the pump and the canisters.

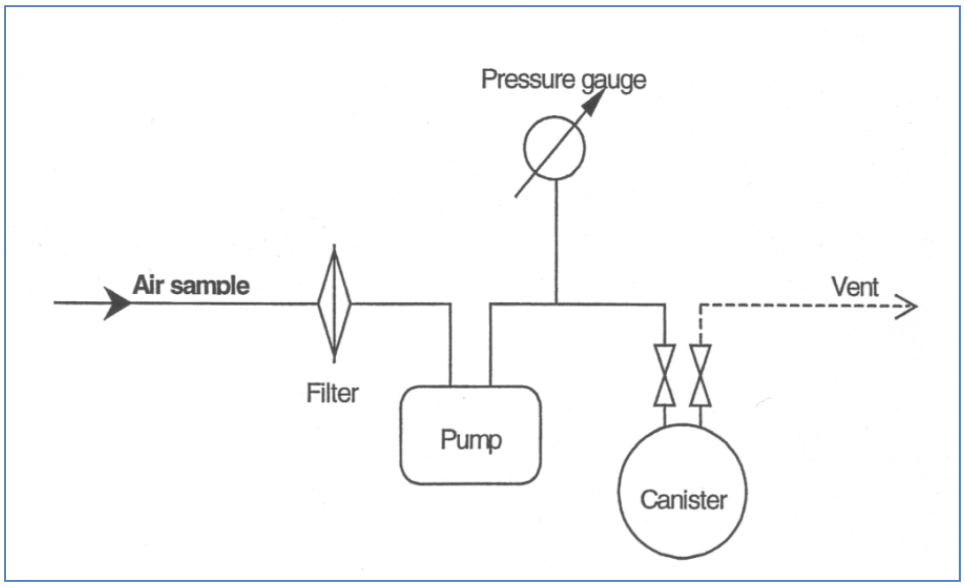

Figure 22 Sampling procedure for 2-valve canisters

The canister is flushed with ambient air 10 times the canister volume and repeatedly pressurized 3 times with ambient air up to 3/4 of the final pressure and released prior to the actual sampling by a final pressurization (about 2 bar). The actual sampling time is determined by the ambient pressure, the volume to be filled, and the desired final pressure. Since this project required that each canister sample was accompanied by one duplicate canister drawing the same sample (i.e. through the same sampling line) the total canister volume to be filled was 2 L leading to a sampling time of approximately 2 min. The pressurization steps are done manually and are controlled via a pressure gauge connected to the pump. After sampling, valves were closed and plugged. Also, the sample tubing was plugged. Canisters were stored in air conditioned rooms and protected against direct insolation. Canisters samples were shipped overnight in insulated boxes. The samples were analyzed within two weeks after sampling. Altogether 34 ambient air canister samples were collected. All samples were accompanied by duplicates. For 4 samples results of three canisters taken concurrently for each sampling were reported.

3. Wind Measurements

Accurate wind measurements are crucial to calculating fluxes from the measured concentration columns. For this purpose radiosondes with built-in GPS receivers are launched with helium balloons to track the wind as the balloon follows it. From the data sent back by the radiosonde, a wind profile i.e. wind speed and direction as a function of height, can be reconstructed. Examples of two wind profiles obtained from radiosonde launches during the campaign can be seen in Figure 23. One was launched in Baytown and the other in Orange.

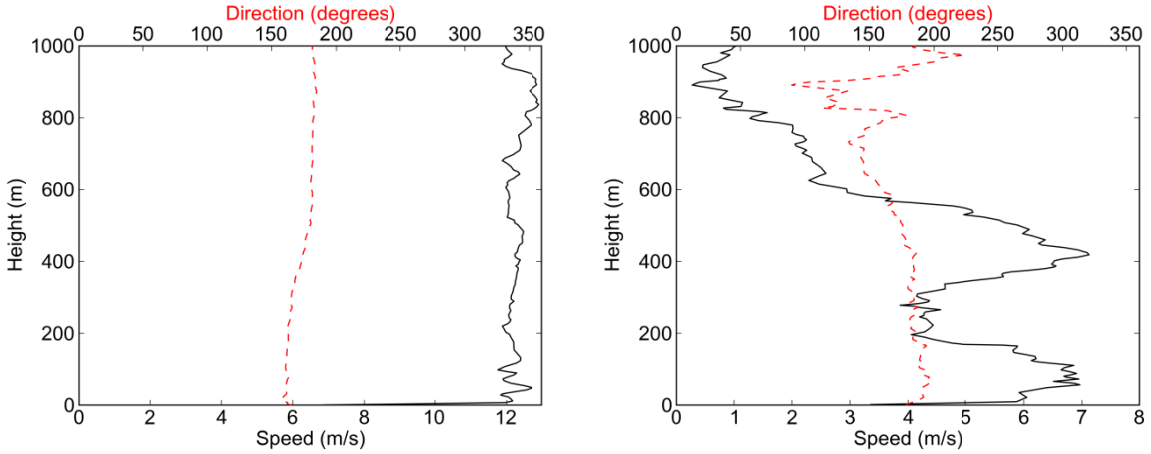

Figure 23 Wind profiles measured with radiosondes. The left profile is from a sonde launched from Baytown at 15:46 on April 23. The right profile is from a sonde launched from Orange, located west of Beaumont/Port Arthur at 17:24 on May 17.

The wind profiles are averaged over the height interval in which the plume is assumed to be distributed to obtain a mean plume speed. Since we lack specific information about the height distribution of the plumes, the plume is assumed to be well mixed in the interval from 0 to 500 m. Given a reasonable distance downwind of the source, this assumption is well satisfied. Depending on the perceived distance from the source and height of the source this assumption is sometimes modified and a different height interval employed. In practice this usually makes a little difference since the wind profiles do not vary substantially above the first 50 meters or so.

Wind profiles have been used directly for flux calculations only in a few instances, primarily Texas City on April 17. The primary wind source for flux calculations are continuous wind measurements made from masts located in the approximate vicinity of the measurements. To compensate for wind masts generally recording lower wind speeds, due to being close to the ground, and to assure that the wind measured by the masts is a good proxy for the wind higher up, the wind data from the masts at the time of nearby radiosonde launches have been compared to 0–500 m wind profile averages from those launches.

Wind data from measurements by 10 m high masts at four CAMS sites in the Ship Channel Area were used for flux calculations and to assess the temporal and spatial variation in wind. The data from the masts were compared to all sonde profiles in the Ship Channel during the campaign (8) at the times of their launches. A multiplicative factor was established for each mast to obtain the best fit it to the sonde profiles. Comparisons between these masts and the sonde profiles is shown in Figure 24 and Figure 25 and summarized in Table 3.

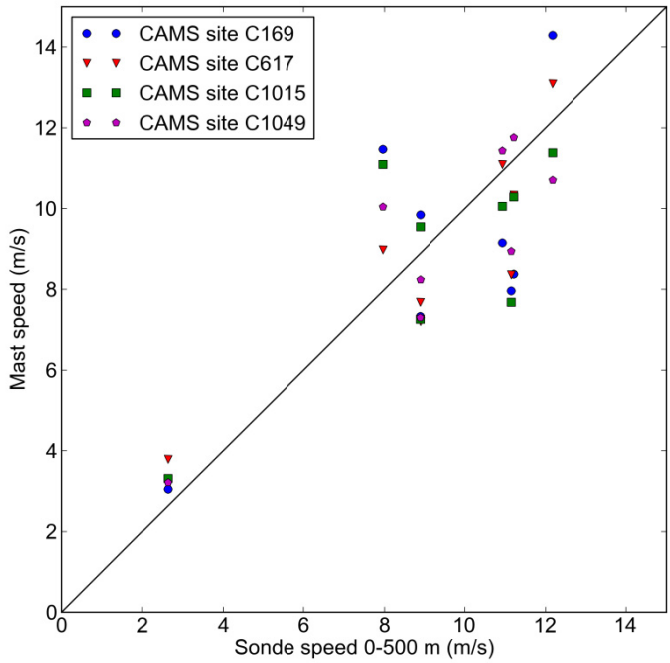

Figure 24 Comparison between wind speed from scaled 10 m high masts at CAMS sites and 0–500 m averages of radiosonde profiles in Houston Ship Channel.

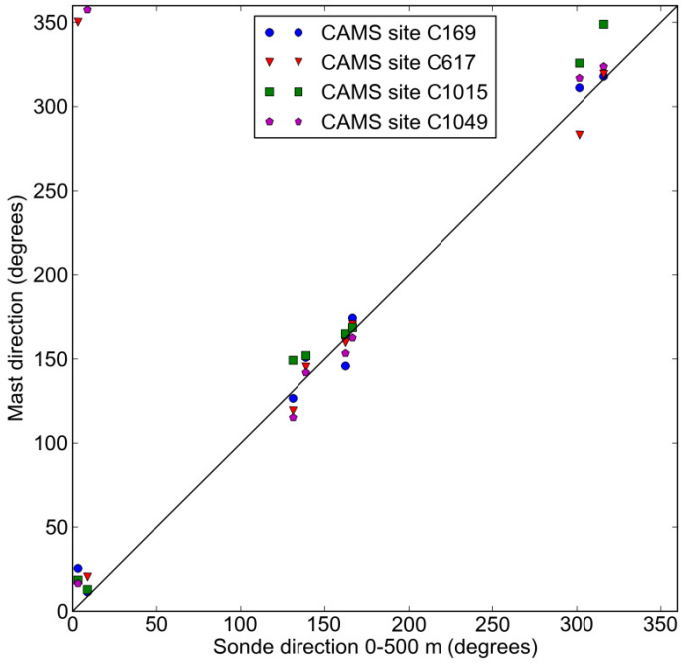

Figure 25 Comparison between wind direction from scaled 10 m high masts at CAMS sites and 0–500 m averages of radiosonde profiles in Houston Ship Channel.

As shown in Table 3, the error in wind speed when using the mast winds as proxies for 0–500 m averages varies between 16 and 24 % and the error in direction can be up to 14±10°.

Table 3 Statistical differences between 0 to 500 m averages of wind data from sondes launched in Houston Ship Channel and simultaneous TCEQ CAMS mast measurements.

Wind measurement	**Relative difference in speed compared to radiosonde 0-500 m (Relative error)**	**Difference in direction compared to radiosonde 0-500 m**
CAMS site C169	±24 %	4±11°
CAMS site C617	±20 %	-3±10°
CAMS site C1015	±22 %	14±10°
CAMS site C1049	±16 %	0±11°

The same procedure was used for the Beaumont/Port Arthur area. For this area wind data from 10 m high masts at three CAMS sites and data from a local radar profiler were used. The profiles from the radar profiler were averaged from 200 to 700 m since lower heights seemed to contain artifacts. Comparisons between these data sources and the sonde profiles measured in this area (14) shown in Figure 26 and Figure 27 and summarized in Table 4.

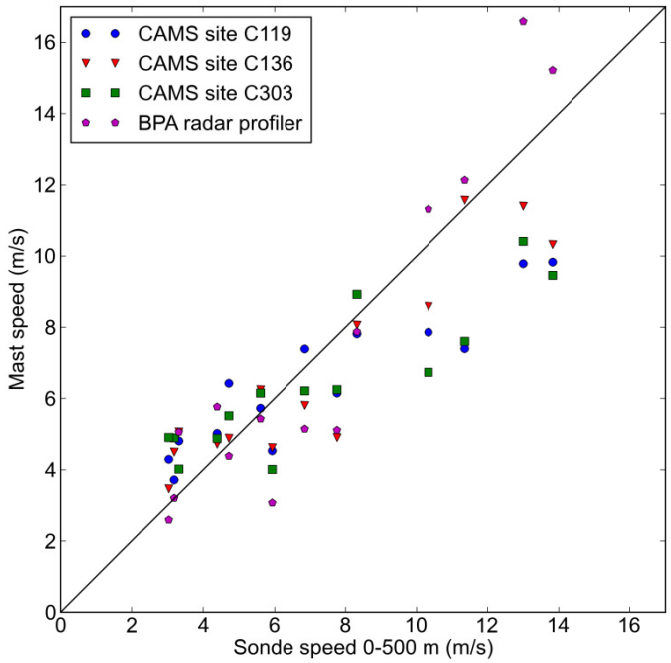

Figure 26 Comparison between wind speed from scaled 10 m high masts at CAMS sites and a radar wind profiler; and 0–500 m averages of radiosonde profiles in Beaumont/Port Arthur.

As shown in Table 4, the error in wind speed when using the mast winds as proxies for 0–500 m averages varies between 24 and 30 % and the error in direction can be up to -1±22°.

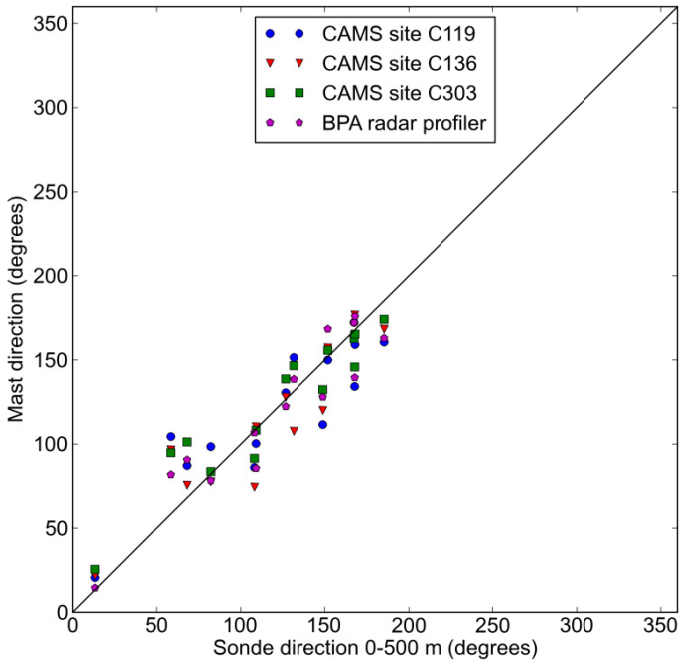

Figure 27 Comparison between wind direction from scaled 10 m high masts and a radar wind profiler; and 0–500 m averages of radiosonde profiles in Beaumont/Port Arthur.

Table 4 Statistical differences between 0 to 500 m averages of wind data from sondes launched in Beaumont/Port Arthur and simultaneous TCEQ CAMS mast and radar profiler measurements.

Wind measurement	**Relative difference in speed compared to radiosonde 0-500 m (Relative error)**	**Difference in direction compared to radiosonde 0-500 m**
CAMS site C119	±26 %	-1±22°
CAMS site C136	±24 %	-3±18°
CAMS site C303	±30 %	3±17°
BPA radar profiler	±26 %	-2±16°

4. Measurement uncertainty and quality assurance

4.1 SOF

4.1.1. Measurement uncertainty SOF and Mobile DOAS

The main uncertainty for the flux measurements in the SOF and Mobile DOAS measurements comes from the uncertainty in the wind field. From the wind speed data in Table 3 and Table 4, the 1σ spread relative to the 0–500 m GPS sonde wind is 16–30 % with highest uncertainty in Beaumont/Port Arthur. This error is seen as a measure of the uncertainty in wind speed when calculating fluxes from the measured concentration columns. The wind direction is also associated with an uncertainty, and this error actually depends on how orthogonal the plume is to the transect being conducted. When the plume transect is orthogonal to the wind direction an uncertainty in the wind direction affect the flux uncertainty much less than for more oblique transect angles. A 11–24º wind direction uncertainty (1σ) is estimated for the measurements, from the wind direction errors in Table 3 and Table 4, giving an average of 18 º. This implies a 6 % flux uncertainty at an orthogonal plume transect, and 9 % on average for the transect angle of 75º.

The absorption line parameters of the retrieved compounds are well established in published databases, stating an uncertainty of 3–3.5 % for the spectroscopic part for the VOCs [Sharpe 2004]. For the UV cross section the NO_2 is stated as 4 % [Van Daele 1998]. The cross section of HCHO has been evaluated by Gratien [2007] showing only a few percent difference between cross section measurements by several groups, in the spectral region we have been using. To the error we have also added a retrieval uncertainty of 10–20 %. This is the combined effect of instrumentation and retrieval stability on the total columns for a plume transect [Mellqvist 2009a]. The high value for propene is due to the fact that mechanical artifact caused spectral artifacts for this species. Also affecting the uncertainty is the error in the SOF alkane mass retrieval due to interference of various compounds in the plume mixture (6 %). The composite flux measurement uncertainty for the SOF measurements, obtained as the square root sum of the quadratic errors for the parameters described above, is around 24 % for the retrieved alkane mass, see Table 5.

Table 5 Uncertainty estimation of the flux measurements (the variability of the sources not taken into account).

	Wind Speed [a)]	**Wind Direct** [b)]	**Spectroscopy (cross sections)** [c)]	**Retrieval error** [d)]	**Composite flux measurement uncertainty** [e)]
Alkanes	16–30 %	6–9 %	3.5 %	12 %	21–34 %
Ethene	16–30 %	6–9 %	3.5 %	10 %	20–33 %
Propene	16–30 %	6–9 %	3.5 %	20 %	27–37 %
HCHO	16–30 %	6–9 %	3 %	10 %	20–33 %
SO2	16–30 %	6–9 %	2.8 %	10 %	20–33 %
NO2	16–30 %	6–9 %	4 %	10 %	20–33 %

a) Comparing mast wind averages with the 0–500 m GPS sonde averages, the max data spreads 16–30 % (1σ, 30 %)
b) The 1σ deviation among the wind data compared to the 0–500 m sonde is 18º. For a plume transect orthogonal to the wind direction, which is always the aim, this would give a 6 % error. For a measurement in 75º angle the error is 9 %.
c) Includes systematic and random errors in the cross section database.
d) The combined effects of instrumentation and retrieval stability on the retrieved total columns during the course of a plume transect and error of the SOF alkane mass retrieval. Estimated for SOF.
e) The composite square root sum of squares uncertainty

4.1.2 Validation and comparisons

The performance of the SOF method has been tested by comparing it to other methods and tracer gas release experiments. In one experiment, tracer gas (SF_6) was released from a 17 m high mast on a wide parking lot. The emission rate was then quantified by SOF measurements 50–100 m downwind the source, yielding a 10 % accuracy for these measurements when averaging 5–10 transects [Kihlman 2005b].

More difficult measurement geometries have also been tested by conducting tracer gas releases of SF_6 from the top of crude oil tanks. For instance, in an experiment at Nynas refinery in Sweden tracer gas was released from a crude oil tank. In this case, for close by measurements in the disturbed wind field at a downwind distance of about 5 tank heights, the overestimation was 30 %, applying wind data from a high mast [Kihlman 2005a; Samuelsson 2005b].

The SOF method has also been compared against other methods. In another experiment at the Nynas refinery a fan was mounted outside the ventilation pipe, sucking out a controlled VOC flow from the tank. The pipe flow was measured using a so called pitot pipe and the concentration was analyzed by FID (Flame ionization detector) which made it possible to calculate the VOC emission rate, which was 12 kg/h. In parallel, SOF measurements were carried out at a distance corresponding to a few tank heights, yielding an emission rate of 9 kg/h, a 26 % underestimation in this case. Similar measurements from a joint ventilation pipe from several Bitumen cisterns yielded a FID value of 7 kg/h and only 1 % higher emission from the SOF measurements [Samuelsson 2005b].

During the TexAQS 2006 the SOF method was used in parallel to airborne measurements of ethene fluxes from a petrochemical industrial area in Mont Belvieu [De Gouw 2009]. The agreement was here within 50 % and in this case most of the uncertainties were in the airborne measurements. The SOF method has not been directly compared to the laser based DIAL method (Differential Absorption LIDAR) [Walmsley 1998] which is commonly used for VOC measurements. Nevertheless, measurements at the same plant in Sweden (Preem refinery) yield very similar results when measuring at different years. Differences have been seen for bitumen refineries however [Samuelsson 2005b]. Rivera et al. [2009] did Mobile DOAS measurements of SO_2 on a power plant in Spain and the average determined flux with the DOAS came within 7 % of the values monitored at the plant measurements. All in all the experiment described above is consistent with an uncertainty budget of 20–30 %.

4.1.3. Quality assurance

A formalized QA/QC protocol has not yet been adopted for the SOF method or for Mobile DOAS. However, the spectroscopic column concentration measurements is basically the same as a long path FTIR measurement through the atmosphere corresponding to an effective path length of about 5 km for atmospheric background constituents. For such measurements, there is an EPA guidance document (FTIR Open-Path Monitoring Guidance Document," EPA-600/R-96/040, April 1996). The SOF method and some QA work is also described in a recent optical remote sensing handbook by the US EPA (EPA ORS Handbook, 2011). In addition the US-EPA has developed a test method (OTM 10, Optical Remote Sensing for Emission Characterization from Non-Point Sources), [Thoma 2009] for fugitive emission of methane from landfills. This method is based on measuring the gas flux by integrating the mass across

the plume and then multiplying with the wind speed. The mass is here measured by long path FTIR or tuneable diode lasers. The OTM 10 is hence quite similar to the SOF method, since it uses long path FTIR but more importantly since it determines the flux in the same principal manner. The spectral retrieval code used in the SOF method (QESOF) [Kihlman 2005a] relies on principles adopted by the NDACC community (Network for the detection of atmospheric composition change. www.ndsc.ncep.noaa.gov), which is a global scientific community in which precise solar FTIR measurements are conducted to investigate the gas composition changes of the atmosphere. Chalmers University is a partner of this community and has operated a solar FTIR in Norway since 1994. The QESOF code has been evaluated against several published codes developed within NDACC with good agreement, better than 3 %.

Even though a formalized QA/QC protocol is missing there are several QA procedures carried out prior to conducting the SOF measurements. This includes checking the instrumental spectral response (usually done by measuring solar spectra and investigating the width and line position of these) and investigating that the instruments measures in the same manner, independent of the direction of the instrument relative to the sun. Usually the instrument is aligned to have the same light response in all directions.

The FTIR instrument, used in SOF, is not calibrated prior to measurements but one instead relies on calibration data from the scientific literature. This is appropriate as long as the instrument is well aligned, and whether the alignment has been sufficient can actually be checked afterwards by investigating the widths and shape of the absorption lines in the measured solar spectra.
Noteworthy is the fact that the spectra are stored in a computer and that the spectral analysis is conducted afterwards which makes it possible to conduct quality control on the data. From this analysis the individual statistical error is obtained for each measurement. Quality control is also conducted by removing "bad" spectra".

For open path DOAS standardization work is carried out which is very similar to this application from a spectroscopic point of view. For instance the US EPA has tested several long path instruments within their environmental technology verification program with good results.

The spectral evaluation used in this study is similar to many other studies since we rely on a software package widely used by the DOAS community (QDOAS) and we use published calibration reference data. The most important issue when it comes to quality assurance is to investigate the lineshape of the spectrometer and the wavelength calibration. During the campaign this was done by regular measurement with a low pressure Hg calibration lamp. The wavelength calibration was also corrected afterwards by comparing the measured spectra to a solar spectrum, and then shifting them accordingly to the difference.
The quality of the data can be checked by investigating the spectral fitting parameters and in this way remove bad data.

4.2 MeFTIR

The FTIR instrument, used by the MeFTIR, is not calibrated prior to measurements but one instead relies on calibration data from the scientific literature. This is appropriate as long as the instrument is well aligned, and whether the alignment has been sufficient can actually be checked afterwards by investigating the widths and shape of the absorption lines in the measured spectra. In terms of overall absolute accuracy for the tracer correlation

measurements carried out by MeFTIR, including errors due to errors in database absorption cross sections and spectral concentration retrieval, tracer release rate and interfering tracer sources, plume integration and tracer release mismatch, an accuracy of 18 % could be expected at normal conditions [Samuelsson, 2005a]. Studies in the literature where area distributed releases of two or more tracer gases have been used for cross-retrieval of the released tracer amounts, show accuracy levels (residual sum of squares) of 14 % (Lamb, 1995) respectively 11–21 % [Mellqvist, 1999]. The collocation between the methane and tracer release along the wind direction is the single-most important parameter for the emission quantification accuracy, given that the full plumes are integrated in the cross wind direction. This collocation decides the time for vertical mixing of the respectively plume from the release to the measurement transect, so that any mismatch in the tracer release would give raise to a somewhat different dispersion. In this study co-locating the tracer with the source was not possible given that site access is restricted.

The amount of tracer released was determined from the flow. Here a reading of 1 lit/min on the flow tube corresponded 0.96 kg/h determined from weighing the gas cylinders.

4.3 Canisters

VOC analysis sampling and measurement performed is based on developments by [Veillerot et al. 1998]. The UH system has been described in [Leuchner and Rappenglück 2010]. Briefly, a Perkin-Elmer VOC-system consisting of a Clarus 500 gas chromatograph with heart cut device and equipped with two flame ionization detectors and two columns (Alumina PLOT column and BP-1) for multi-dimensional gas chromatography is used. Every hour VOCs are sampled for 40 min and pre-concentrated on a cold trap which contains carboneous sorbents and subsequently desorbed by a Turbomatrix 650 Automatic Thermal Desorber. Water is removed through a Nafion® dryer. In case of analysis of canister contents the inlets of the online system will be switched to an auto-sampler (Merlin MicroScience Canister Sampler MMS-CS-VOC-16). It can hold up to 16 canisters. This auto sampler is controlled by the GC software to take sequential samples from all canisters and inject them into the analytical cycle. The set of canisters includes up to 13 ambient air samples, one humidified zero air, one humidified NPL standard, and one humidified NCAR standard. Prior to the canister analysis the performance of GC/FID system is checked in its online path using zero air, and the NPL and NCAR standards.
The VOC GC system was calibrated using a 30 component EU Directive ozone precursor mixture provided by the UK National Physical Laboratory (NPL). This mixture contains VOC in mixing ratios of about 4 ppbv and has been found to be very stable over long time periods. Typical stability is less than 0.2 % per annum [Grenfell et al., 2010]. The certificate is valid for two years from the date of issue, which was June 08, 2010. Uncertainties are stated to be below 2 % (95 % confidence limit). For identification purposes a 72 VOC standard in the range of 0.13–10.98 ppbv (stated uncertainty below 5 %) provided by the National Center for Atmospheric Research (NCAR) was used. This standard allows optimum identification and has been successfully used in recent intercomparisons [Rappenglück et al., 2006]. Both standards do not need any dilution and thus minimize errors and uncertainties arising from dilution methods. Instrument response was correlated with concentration for each hydrocarbon species in the standard based on peak areas. Precision for the VOC measurements were within the range as stated in the QAPP.

Table 6 Results of blank runs through the hydrocarbon sampling system.

	Can#	75	4	62	4	4	21
NMHC [ppbv]	Date	5/19/2011	5/24/2011	5/30/2011	6/3/2011	6/21/2011	6/23/2011
ethane		ND	ND	ND	ND	ND	ND
ethylene		ND	ND	ND	ND	ND	ND
propane		ND	ND	ND	ND	ND	ND
propylene		ND	ND	ND	ND	ND	ND
i-butane		ND	ND	ND	ND	ND	ND
n-butane		ND	ND	ND	ND	ND	ND
acetylene		ND	ND	ND	ND	ND	ND
t-2-butene		ND	ND	ND	ND	ND	ND
1-butene		ND	ND	ND	ND	ND	0.01
i-butene		ND	ND	ND	0.01	0.02	0.02
c-2-butene		ND	ND	ND	ND	ND	ND
cyc-pentane		ND	ND	ND	ND	ND	ND
i-pentane		ND	ND	ND	ND	ND	ND
n-pentane		ND	ND	ND	ND	ND	ND
1,3-butadiene		ND	ND	ND	ND	ND	ND
cyc-pentene/2-me-2-butene		ND	ND	ND	ND	ND	ND
t-2-pentene		ND	ND	ND	ND	ND	ND
3-me-1-butene		ND	ND	ND	ND	ND	ND
2-me-1-butene		ND	ND	ND	ND	ND	ND
1-pentene		ND	ND	ND	ND	ND	ND
c-2-pentene		ND	ND	ND	ND	ND	ND
2,2-dime-butane		ND	ND	ND	ND	ND	ND
2,3-dime-butane		ND	ND	ND	ND	ND	ND
2-me-pentane		ND	ND	ND	ND	ND	ND
3-me-pentane		ND	ND	ND	ND	ND	ND
isoprene		ND	ND	ND	ND	ND	ND
n-hexane		ND	ND	ND	ND	ND	ND
c-3-hexene		ND	ND	ND	ND	ND	ND
t-2-hexene		ND	ND	0.02	ND	ND	ND
c-2-hexene		ND	ND	ND	ND	ND	ND
me-cyc-pentane		ND	ND	ND	ND	ND	ND
2,4-dime-pentane		ND	ND	ND	ND	ND	ND
benzene		ND	ND	ND	ND	ND	ND
cyc-hexane		ND	ND	ND	ND	ND	ND
2-me-hexane		ND	ND	ND	ND	ND	ND
2,3 dime-pentane		ND	ND	ND	ND	ND	ND
3-me-hexane		ND	ND	ND	ND	ND	ND
2,2,4-trime-pentane		ND	ND	ND	0.02	ND	ND
n-heptane		ND	ND	ND	ND	ND	ND
me-cyc-hexane		ND	ND	ND	ND	ND	ND
2,3,4-trime-pentane		ND	ND	ND	ND	ND	ND
toluene		ND	ND	ND	ND	ND	ND
2-me-heptane		ND	ND	ND	ND	ND	ND
4-me-heptane		ND	ND	ND	ND	ND	ND
3-me-heptane		ND	ND	ND	ND	ND	ND
n-octane		ND	ND	ND	0.02	ND	ND
et-benzene		ND	ND	ND	ND	ND	ND
m,p-xylene		ND	ND	0.10	ND	ND	ND
styrene		ND	ND	0.04	ND	ND	ND
o-xylene		ND	ND	0.08	ND	ND	ND
n-nonane		ND	ND	ND	0.06	ND	ND
i-prop-benzene		ND	ND	0.09	ND	ND	ND
n-prop-benzene		ND	ND	0.05	ND	ND	ND
3-et-toluene		ND	ND	0.03	ND	ND	ND
4-et-toluene		ND	ND	ND	ND	ND	ND
1,3,5-trime-benzene		ND	ND	ND	ND	ND	ND
2-et-toluene		ND	ND	ND	ND	ND	ND
1,2,4-trime-benzene/tert-but-benzene		ND	ND	ND	ND	0.02	ND
1,2,3-trime-benzene		ND	ND	ND	ND	ND	ND

ND: not detected

Blank values of the GC system were done prior each analysis sequence. Compound specific blank values were subtracted from the findings in ambient air samples. Canisters were cleaned by connecting in series and flushed with humidified zero air. The last can in the series was filled with humidified zero air and analyzed. After subtracting compound specific GC blank values from the canister blank data the cleaning batch did not show more than 0.2 ppbV of a single target analyte. Heat was not provided. The detection limit was 10 pptv for most target compounds. Detection limit for ethene and acetylene was 20 pptv.

In accordance with the QAPP six blank runs through the hydrocarbon sampling system were performed. Table 6 shows the results:

The 34 field measurements were always accompanied by at least one duplicate canister to assess between canister variability. All the results are listed in the appendix and show reasonable agreement among the canisters.
Due to the requirement of this project to sample duplicate canisters a T-union was installed behind the pressure gauge in the tubing connecting the pump and the canisters. This arrangement allowed that canisters would take the sample through the same sampling path and during the same time period. However, this arrangement had some drawbacks compared with the usual UH procedure:

1) flushing time for two canisters is longer than for one canister due to the larger volume to be flushed
2) pressure gauge indicates pressurization, even in case one canister was not adequately opened

Issue (2) does not occur when only one canister is being sampled. However issue (2) may occur with more than one canister hooked up to the sampling system, if either (i) valves of one can cannot be fully opened or (ii) onsite personnel mix up inflow or outflow valves. The latter one in particular occurred at the beginning of the field campaign, but was remedied quickly by adding appropriate procedures to the Standard Operating Procedures.
However, in any case issue (2) occurred at least one canister was filled appropriately as indicated by the pressure gauge. The result of this canister sample was used in further data analysis. However, for these rare cases no duplicate information was available.

One canister (can#55) was selected to be analyzed at a NELAP-certified laboratory as well as with the UH system.

Table 7 shows reasonable agreement among the two laboratories. In the appendix the results of the companion canisters (cans#22 and 57) which were taken together with can#55 at Baytown are listed.

Table 7 Results of Analysis of can#55 by UH and by Test America, Austin (NELAP certified laboratory). Test America employed EPA TO15.

NMHC [ppbv]	UH	NELAP	NELAP-MDL
ethane	2.22	2.44	0.07
ethylene	1.41	1.74	0.06
propane	2.26	2.02	0.04
propylene	14.87	12.50	0.02
i-butane	0.28	0.20*	0.05
n-butane	0.35	0.30*	0.03
acetylene	0.18	0.19*	0.06
t-2-butene	0.05	ND	0.05
1-butene	0.35	0.31*	0.02
i-butene	0.15	NR	NR
c-2-butene	ND	ND	0.04
cyc-pentane	ND	ND	0.05
i-pentane	0.27	0.29*	0.06
n-pentane	0.13	0.10*	0.05
1,3-butadiene	ND	ND	0.02
cyc-pentene/2-me-2-butene	ND	ND	0.10
t-2-pentene	ND	ND	0.05
3-me-1-butene	ND	ND	0.05
2-me-1-butene	ND	ND	0.03
1-pentene	ND	ND	0.03
c-2-pentene	ND	ND	0.04
2,2-dime-butane	0.02	ND	0.02
2,3-dime-butane	0.03	ND	0.05
2-me-pentane	0.09	0.12*	0.04
3-me-pentane	0.15	0.09*	0.04
isoprene	ND	0.06*	0.05
n-hexane	0.44	0.32*	0.05
c-3-hexene	ND	NR	NR
t-2-hexene	ND	ND	0.04
c-2-hexene	ND	ND	0.06
me-cyc-pentane	ND	0.05*	0.04
2,4-dime-pentane	0.03	ND	0.03
benzene	0.08	0.14*	0.03
cyc-hexane	0.06	0.05*	0.03
2-me-hexane	0.02	0.03*	0.02
2,3 dime-pentane	ND	ND	0.04
3-me-hexane	0.02	0.07*	0.03
2,2,4-trime-pentane	ND	ND	0.03
n-heptane	0.02	0.03*	0.03
me-cyc-hexane	0.04	0.04*	0.03
2,3,4-trime-pentane	ND	ND	0.03
toluene	0.22	0.29*	0.03
2-me-heptane	ND	ND	0.03
4-me-heptane	ND	NR	NR
3-me-heptane	ND	ND	0.03
n-octane	0.01	ND	0.04
et-benzene	0.11	0.21*	0.04
m,p-xylene	0.08	0.12*	0.08
styrene	0.02	ND	0.06
o-xylene	0.01	ND	0.04
n-nonane	0.03	ND	0.04
i-prop-benzene	ND	ND	0.05
n-prop-benzene	ND	ND	0.06
3-et-toluene/m-et-toluene	ND	ND	0.02
4-et-toluene/p-et-toluene	ND	ND	0.02
1,3,5-trime-benzene	ND	ND	0.07
2-et-toluene/o-et-toluene	ND	ND	0.07
1,2,4-trime-benzene/tert-but-benzene	0.01	ND	0.02
1,2,3-trime-benzene	ND	ND	0.07

**Data of limited reliability*

ND: not detected (UH: data below 10 pptv; NELAP: data below MDL)
NR: not reported
MDL: Measurement Detection Limit

5. Results of refinery and petrochemical measurements in SE Texas

Results obtained from SOF, Mobile DOAS, Mobile extractive FTIR and thermal FTIR are presented for Texas City, Mont Belvieu and HSC, Port Arthur, Beaumont and Longview. Local time (CDT) is given through the whole report.

5.1 Texas City

During the intensive campaign only one day, April 17, with clear weather was spent doing measurements in Texas City. Apart from that some Mobile DOAS measurements were performed on the cloudy days June 14, 20 and 26, giving more statistics for the SO_2 emissions. During the low intensity campaign additional alkane SOF measurement were made on June 9, 10 and 18. All measurements were conducted along State Highway 346/Texas Ave or 5th Ave S in southerly to southeasterly winds.

5.1.1 Alkanes

The alkane spatial distribution of the alkane plume coming from Texas City did generally not lend itself to a repeatable subdivision into smaller plumes. Hence the entire Texas City industrial complex was treated as a single emission source of alkanes. A total of 11 alkane traverses were performed giving a mean emission of 2111 kg/h with a standard deviation of 673 kg/h.

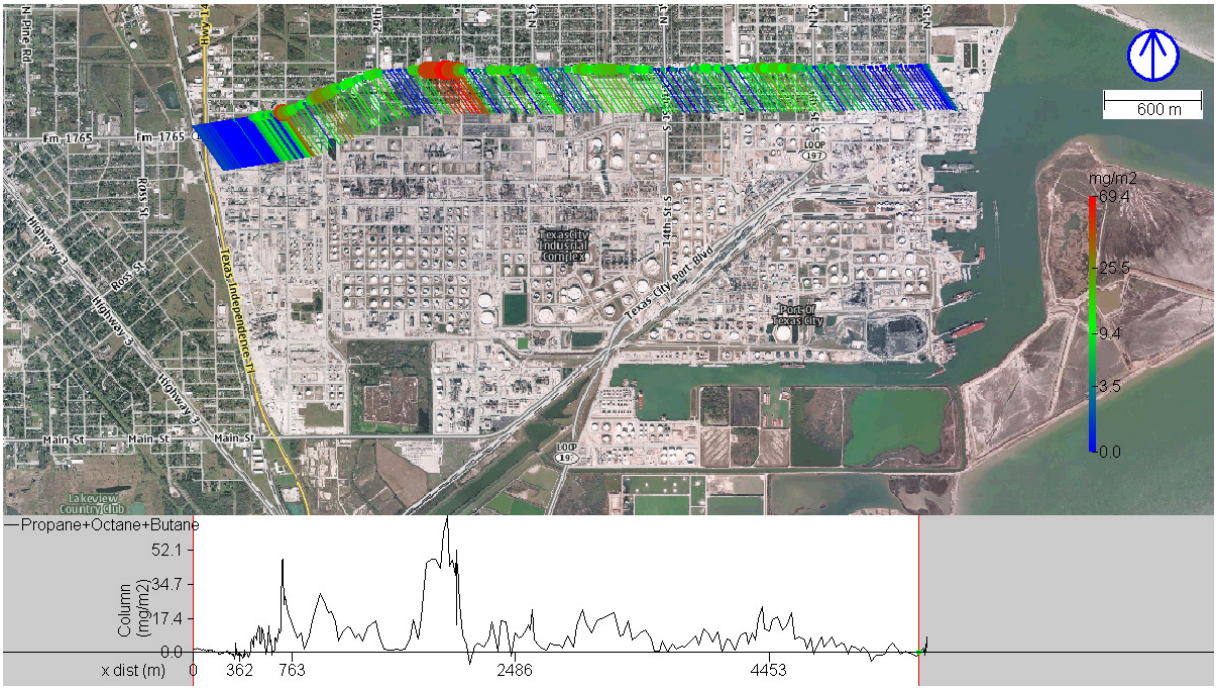

Figure 28 SOF measurement of alkanes north of Texas City on April 17, 2011, 14:32–14:45. Each measured spectrum is represented with a point, which color and size indicate the evaluated integrated vertical alkane column. The VOC column by distance driven through the plume is also shown in the lower part of the figure. A line from each point indicates the direction from which the wind is blowing.

Table 8 Summary of alkane emission transects from Texas City. N is the number of measurements, Start and Stop are start and stop times in HHMMSS, Mean and SD are the average and standard deviation of the calculated fluxes and WS and WD are wind speed and wind direction.

Region	Day	N	Start	Stop	Mean (kg/h)	SD (kg/h)	WS (m/s)	Range WD (deg)	
TC									
	110417	5	143207	182242	1903.9	233.5	10.7	146	146
	110610	1	104517	110143	3038.2		6.4	163	163
	110618	1	144517	150201	3832.9		11.0	196	196
Total		**7**	**104517**	**182242**	**2341.5**	**804.7**	**10.1**	**146**	**196**

5.1.2 Alkenes

During the one day alkenes were measured in Texas City an ethene plume was consistently detected from the westernmost part of the industrial complex. Altogether this plume was captured in 9 traverses. The average ethene emission was 97 kg/h and the standard deviation was 47 kg/h. The plume from this source is clearly seen in Figure 29. In the same traverses two other ethene sources were detected from central and eastern parts of the complex. Emissions from these sources averaged 47 kg/h and 33 kg/h. These measurements are summarized in Table 9. An average of 56 kg/h of propene was also detected from the central part as shown in Table 10.

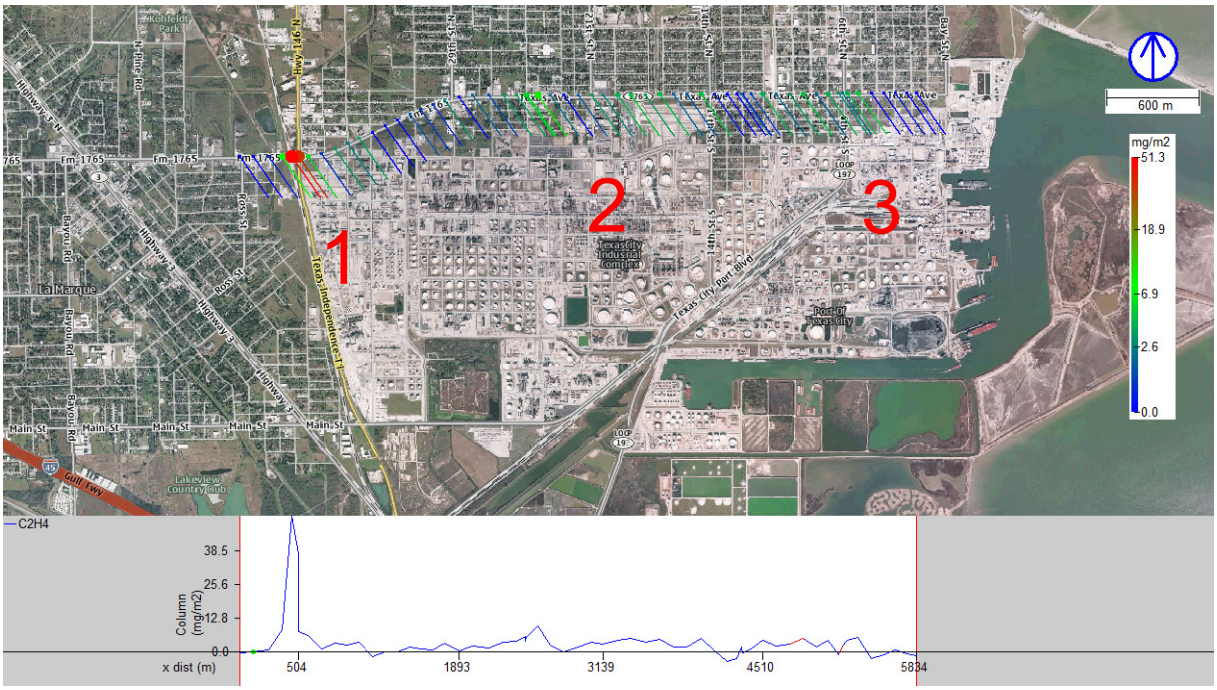

Figure 29 SOF measurement of ethene north of Texas City on April 17, 2011, 15:25–15:35. The three consistently appearing plumes are marked with 1 and 2. The third area is to the east of 2. Each measured spectrum is represented with a point, which color and size indicate the evaluated integrated vertical ethene column. The ethene column by distance driven through the plume is also shown in the lower part of the figure. A line from each point indicates the direction from which the wind is blowing.

Table 9 Summary of ethene emission transects from the sources found in Texas City.

Region	Day	N	Start	Stop	Mean (kg/h)	SD (kg/h)	WS (m/s)	Range WD (deg)	
TC 1	110417	9	145929	171045	96.6	42.5	10.7	146	146
TC 2	110417	9	150259	172601	47.2	16.0	10.7	146	146
TC 3	110417	7	150454	165316	33.0	14.1	10.7	146	146

Table 10 Summary of propene emission transects from the single source found in Texas City.

Region	Day	N	Start	Stop	Mean (kg/h)	SD (kg/h)	WS (m/s)	Range WD (deg)	
TC 2	110417	5	153013	172610	55.9	9.2	10.7	146	146

5.1.3 Formaldehyde (HCHO)

Formaldehyde emissions were also only possible to evaluate from measurements on the day with clear sky. Three sources of formaldehyde were detected on this day. One was significantly more distinct than the other and was detected in all 16 traverses while the other two was only detected in 14 and 9 traverses respectively. The average emissions of the three sources (when detected) were 25 kg/h, 10 kg/h and 15 kg/h respectively with standard deviations of 14 kg/h, 7 kg/h and 10 kg/h respectively.

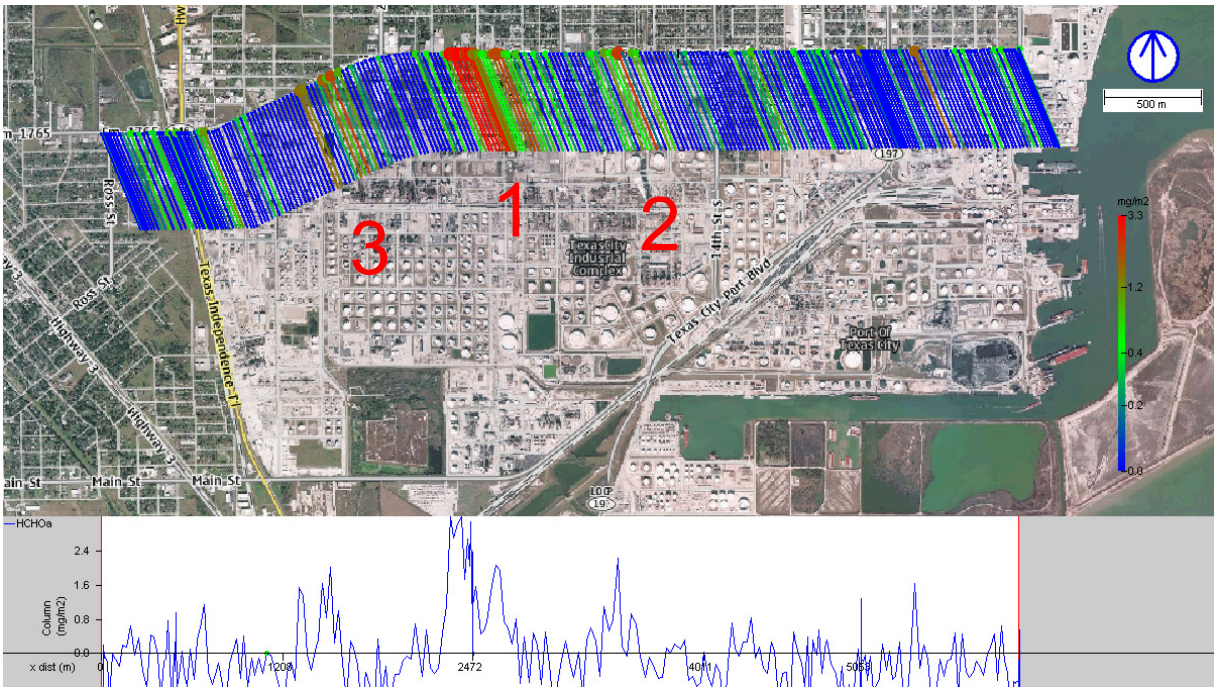

Figure 30 Mobile DOAS measurement of formaldehyde north of Texas City on April 17, 2011, 16:35–16:45. The three plumes identified are marked with 1, 2 and 3. Each measured spectrum is represented with a point, which color and size indicate the evaluated integrated vertical formaldehyde column. The formaldehyde column by distance driven through the plume is also shown in the lower part of the figure. A line from each point indicates the direction from which the wind is blowing.

Table 11 Summary of formaldehyde emission transects from the three sources found in Texas City.

Region	Day	N	Start	Stop	Mean (kg/h)	SD (kg/h)	WS (m/s)	Range WD (deg)	
TC1	110417	16	143835	181908	25.4	13.7	10.7	146	146
TC2	110417	14	144036	181809	9.5	6.7	10.7	146	146
TC3	110417	9	153231	180430	14.8	10.0	10.7	146	146

5.1.4 Sulfur dioxide (SO_2)

The SO_2 emissions from Texas City were generally divisible into three sources, one western, one central and one eastern source. The central was by far the largest and broadest and most likely consisted of several sources located close enough to be inseparable at our measurement distance. A total of 26 traverses were conducted showing average emissions of 234 kg/h, 951 kg/h and 100 kg/h with standard deviations of 134 kg/h, 394 kg/h and 98 kg/h for the western, central and eastern source respectively. This excludes one major upset emission from the central area 18:17 on August 17 measuring more than 6000 kg/h.

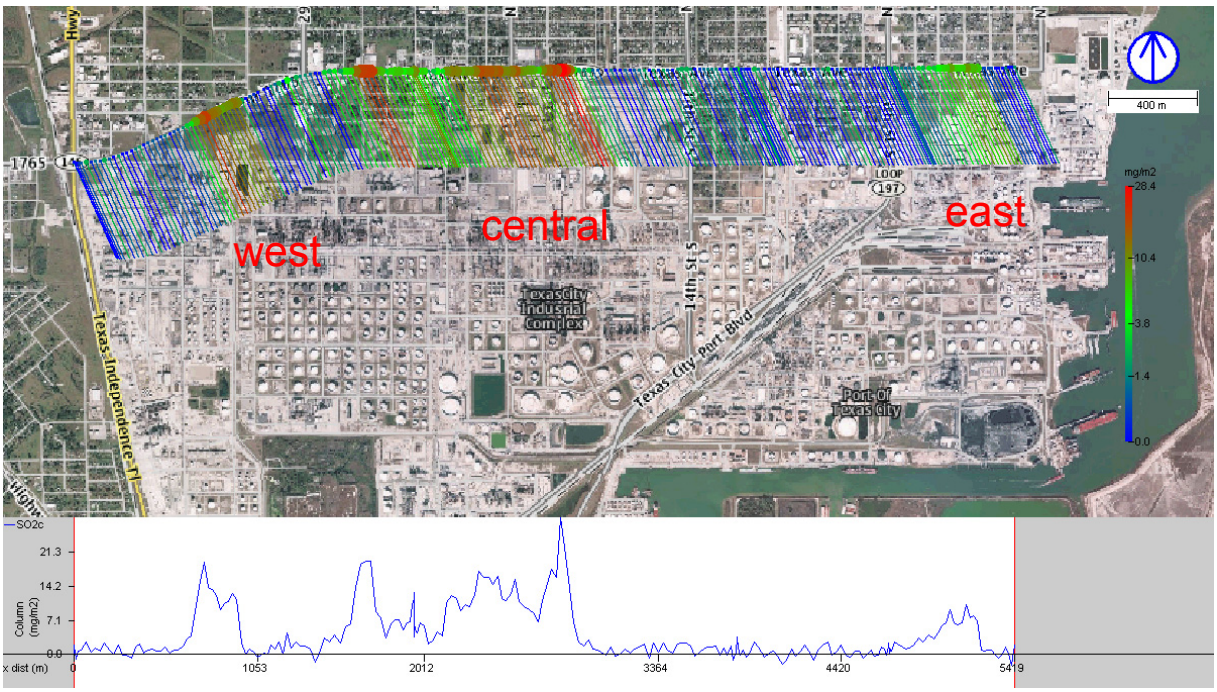

Figure 31 Mobile DOAS measurement of SO_2 north of Texas City on April 17, 2011, 15:25–15:34. The plumes identified are marked with west, central and east. Each measured spectrum is represented with a point, which color and size indicate the evaluated integrated vertical SO_2 column. The SO_2 column by distance driven through the plume is also shown in the lower part of the figure. A line from each point indicates the direction from which the wind is blowing.

Table 12 Summary of SO_2 emission transects from the three sources/areas in Texas City.

Region	Day	N	Start	Stop	Mean (kg/h)	SD (kg/h)	WS (m/s)	Range WD (deg)	
TCwest									
	110414	1	165611	165734	141.2		9.4	170	170
	110417	16	143653	182031	222.7	140.2	10.7	146	146
	110420	4	110927	131025	358.1	125.8	10.9	169	189
	110426	5	135019	151801	188.9	75.6	12.1	159	171
Total		**26**	**110927**	**182031**	**233.9**	**133.8**	**10.9**	**146**	**189**
TCcent									
	110414	1	165101	165456	654.2		9.3	170	170
	110417	15	143824	180656	743.7	223.0	10.7	146	146
	110420	4	111142	131726	1610.5	130.1	10.8	169	191
	110426	5	134702	151448	1108.9	311.7	12.1	161	171
Total		**25**	**111142**	**180656**	**951.8**	**394.4**	**10.9**	**146**	**191**
TCeast									
	110414	1	164739	164846	134.6		9.0	170	170
	110417	15	144251	181524	55.7	36.7	10.7	146	146
	110420	5	111803	132350	255.1	122.9	10.5	167	199
	110426	5	134431	150956	68.4	30.1	12.0	163	171
Total		**26**	**111803**	**181524**	**99.5**	**97.7**	**10.8**	**146**	**199**

5.1.5 Nitrogen dioxide (NO_2)

NO_2 emissions were also only possible to evaluate on April 17. The plume profile was generally similar to that of SO_2 so the emissions could be divided in to the same areas. An example measurement of NO_2 from Texas City is shown in Figure 32. The average emissions measured from the three areas during the day was 212 kg/h, 226 kg/h and 53 kg/h respectively with standard deviations of 39 kg/h, 57 kg/h and 18 kg/h respectively.

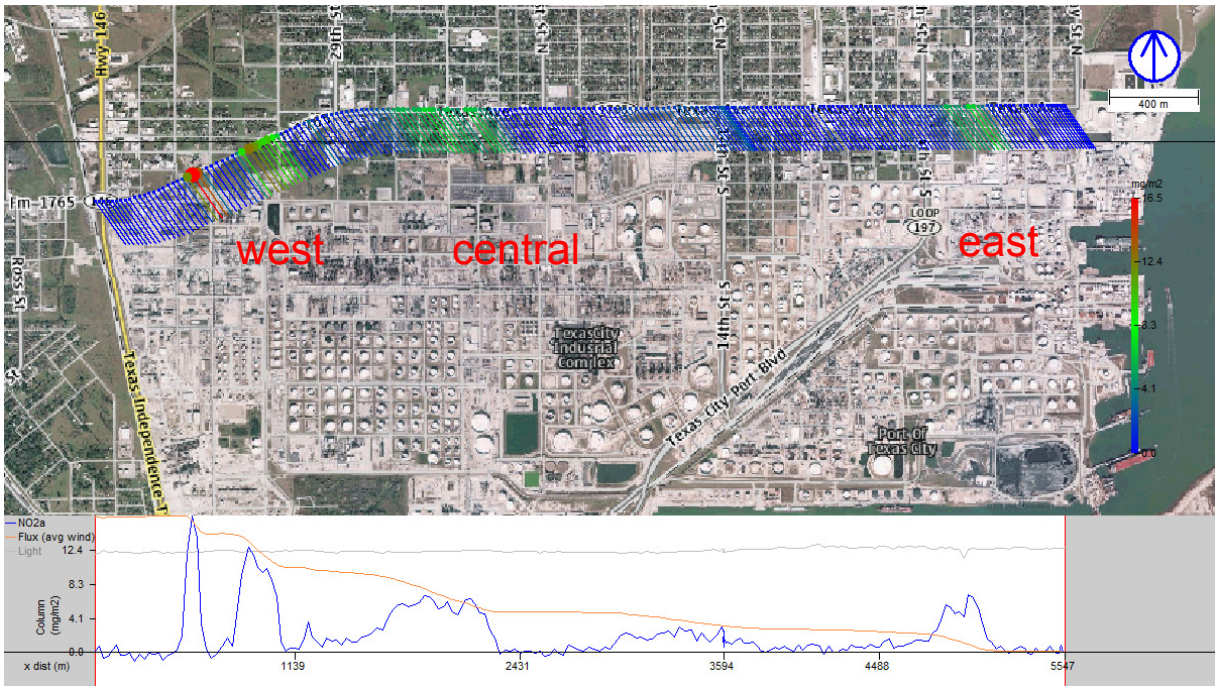

Figure 32 Mobile DOAS measurement of NO_2 north of Texas City on April 17, 2011, 14:46–14:54. The plumes identified are marked with west, central and east. Each measured spectrum is represented with a point, which color and size indicate the evaluated integrated vertical NO_2 column. The NO_2 column by distance driven through the plume is also shown in the lower part of the figure. A line from each point indicates the direction from which the wind is blowing.

Table 13 Summary of NO_2 emission transects from the three sources/areas in Texas City.

Region	Day	N	Start	Stop	Mean (kg/h)	SD (kg/h)	WS (m/s)	Range WD (deg)	
TCwest									
	110417	16	143607	182148	212.2	38.5	10.7	146	146
Total		**16**	**143607**	**182148**	**212.2**	**38.5**	**10.7**	**146**	**146**
TCcent									
	110417	16	143758	181936	226.4	56.8	10.6	131	146
Total		**16**	**143758**	**181936**	**226.4**	**56.8**	**10.6**	**131**	**146**
TCeast									
	110417	15	144153	181628	53.4	17.8	10.6	131	146
Total		**15**	**144153**	**181628**	**53.4**	**17.8**	**10.6**	**131**	**146**

5.2 Mont Belvieu

Chemical and petrochemical industries make up the bulk of the industries in Mont Belvieu and there are no refineries. No significant SO_2 emissions would be expected from this Area and neither this nor the 2009 campaign showed any. Measurements in Mont Belvieu were conducted on April 13, 15, 16, 27 and 28. There were also a few measurements done in the low intensity campaign on June 13.

5.2.1 Alkanes

The total alkane emissions from Mont Belvieu are best captured in transects along the I10 in northerly winds. Only two such measurement transects were performed, both on April 27. One of them is shown in Figure 33. The results of these measurements are summarized in Table 14. On April 15, one measurement was made from 146 and I10 south of Mont Belvieu. Alkane channel emissions on these three measurements were 1320 kg/h with a standard deviation of 280 kg/h.

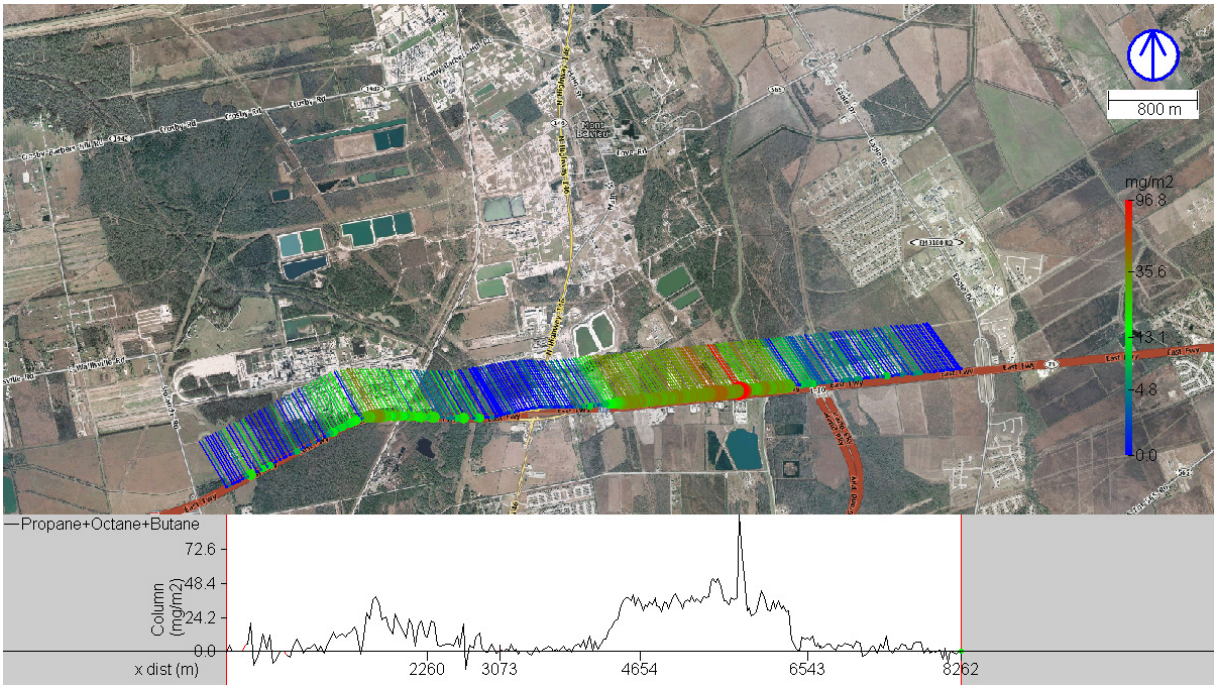

Figure 33 SOF measurement of alkanes south of Mont Belvieu on April 27, 2011, 18:10–18:25. Each measured spectrum is represented with a point, which color and size indicate the evaluated integrated vertical alkane column. The VOC column by distance driven through the plume is also shown in the lower part of the figure. A line from each point indicates the direction from which the wind is blowing.

Table 14 Summary of alkane emission transects on the south side of Mont Belvieu.

Region	Day	N	Start	Stop	Mean (kg/h)	SD (kg/h)	WS (m/s)	Range WD (deg)	
MB									
	110415	1	141419	141817	1598.6		10.7	328	328
	110427	2	181043	183952	1179.5	163.6	10.6	323	328
Total		**3**	**141419**	**183916**	**1319.2**	**280.4**	**9.5**	**328**	**336**

In westerly winds it is also possible to capture most of the alkane emissions from Mont Belvieu with transects along Highway 146. There are, however, some facilities on the east side of this road whose emissions will not be captured in these transects. This type of transects were performed on April 16 and 27. Figure 34 shows one of these transects. The results of these measurements are summarized in Table 15. The average emissions were 1567 kg/h with a standard deviation of 661 kg/h. The significantly higher average for this type of transect as well as the high standard deviation is mainly caused by one transect on April 27 which shows a total emission of around 2900 kg/h.

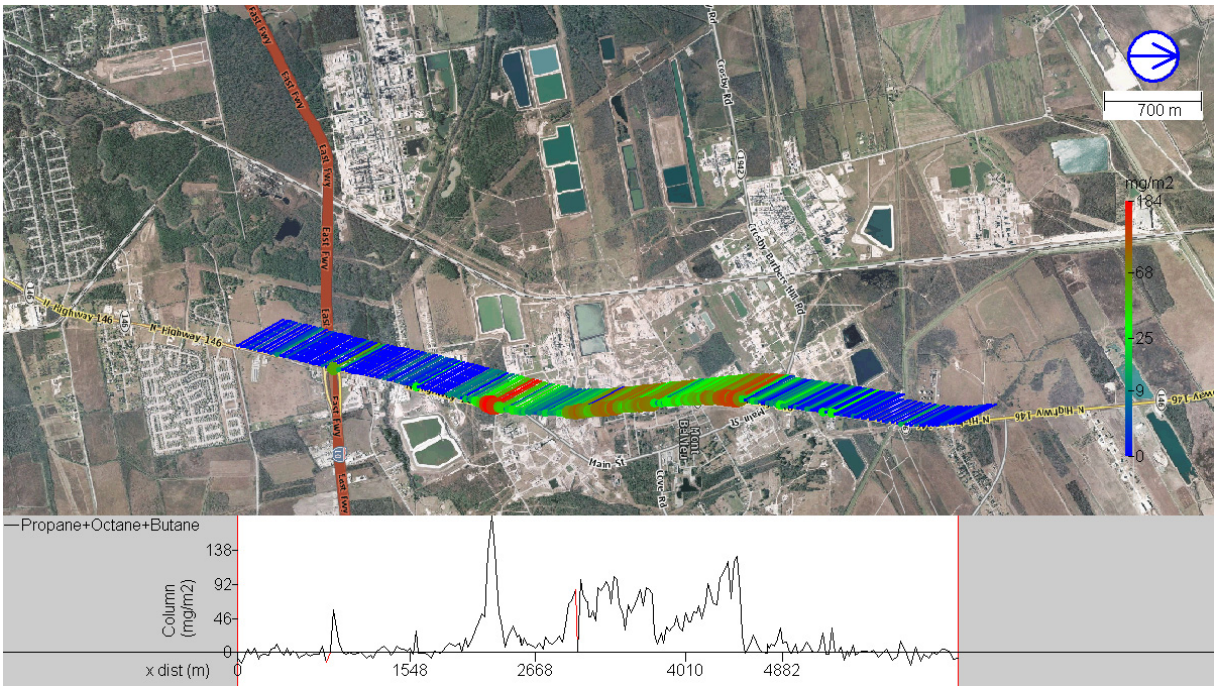

Figure 34 SOF measurement of alkanes east of Mont Belvieu on April 27, 2011, 17:49–18:00. Each measured spectrum is represented with a point, which color and size indicate the evaluated integrated vertical alkane column. The VOC column by distance driven through the plume is also shown in the lower part of the figure. A line from each point indicates the direction from which the wind is blowing.

Table 15 Summary of alkane emission transects on the east side of Mont Belvieu.

Region	Day	N	Start	Stop	Mean (kg/h)	SD (kg/h)	WS (m/s)	Range WD (deg)	
MB									
	110427	3	171139	180058	2028.4	893.0	10.4	315	330
	110416	1	171433	174322	1349.6	-	4.0	330	330
Total		**4**	**171139**	**180058**	**1858.7**	**804.3**	**8.8**	**315**	**330**

5.2.2 Alkenes

Alkene emissions were mainly detected from two areas in Mont Belvieu during this campaign. One of them was the northernmost industries along Hatcherville Road. A measurement of the ethene emissions from these facilities is shown in Figure 35. A summary of the ethene measurements from the northern part of Mont Belvieu is shown in Table 16. The average emission of ethene measured was 292 kg/h with a standard deviation of 102 kg/h. During these measurements the propene channel was noisy, see section 2.1.2 and hence measurements of this species is only available from one transect as seen in Table 17.

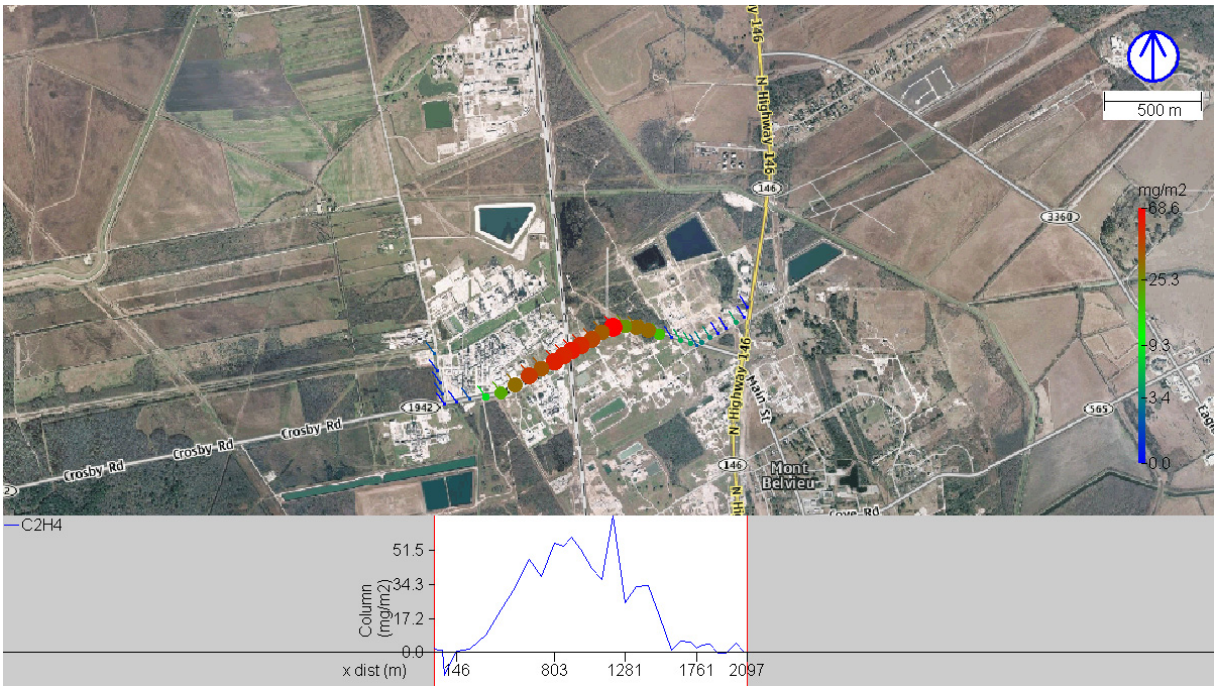

Figure 35 SOF measurement of ethene south of the northernmost industries in Mont Belvieu on April 16, 2011, 18:08–18:13. Each measured spectrum is represented with a point, which color and size indicate the evaluated integrated vertical ethene column. The ethene column by distance driven through the plume is also shown in the lower part of the figure. A line from each point indicates the direction from which the wind is blowing.

Table 16 Summary of ethene emission transects from the north part of Mont Belvieu.

Region	Day	N	Start	Stop	Mean (kg/h)	SD (kg/h)	WS (m/s)	Range WD (deg)	
MBnorth									
	110413	3	150916	152714	351.1	109.1	8.6	156	160
	110415	2	150310	151430	300.9	156.5	11.1	314	321
	110416	4	174621	182743	242.8	69.7	3.4	1	359
Total		**9**	**150310**	**182743**	**291.8**	**102.0**	**6.8**	**156**	**359**

Table 17 Summary of the single reliable propene emission transect from the north part of Mont Belvieu.

Region	Day	N	Start	Stop	Mean (kg/h)	SD (kg/h)	WS (m/s)	Range WD (deg)	
MBnorth									
	110416	1	175027	175626	58.1		3.6	2	2

The other main source of ethene was the facility along I10. An ethene measurement transect south of this facility is shown in Figure 36. The measurements of ethene from this industry are summarized in Table 18. Here we can see that there is very large difference between the two days of measurement. The average ethene emission measured on April 28 was 50 kg/h while it was 304 kg/h on June 13. The total average emission was 177 kg/h with a standard deviation of 160 kg/h.

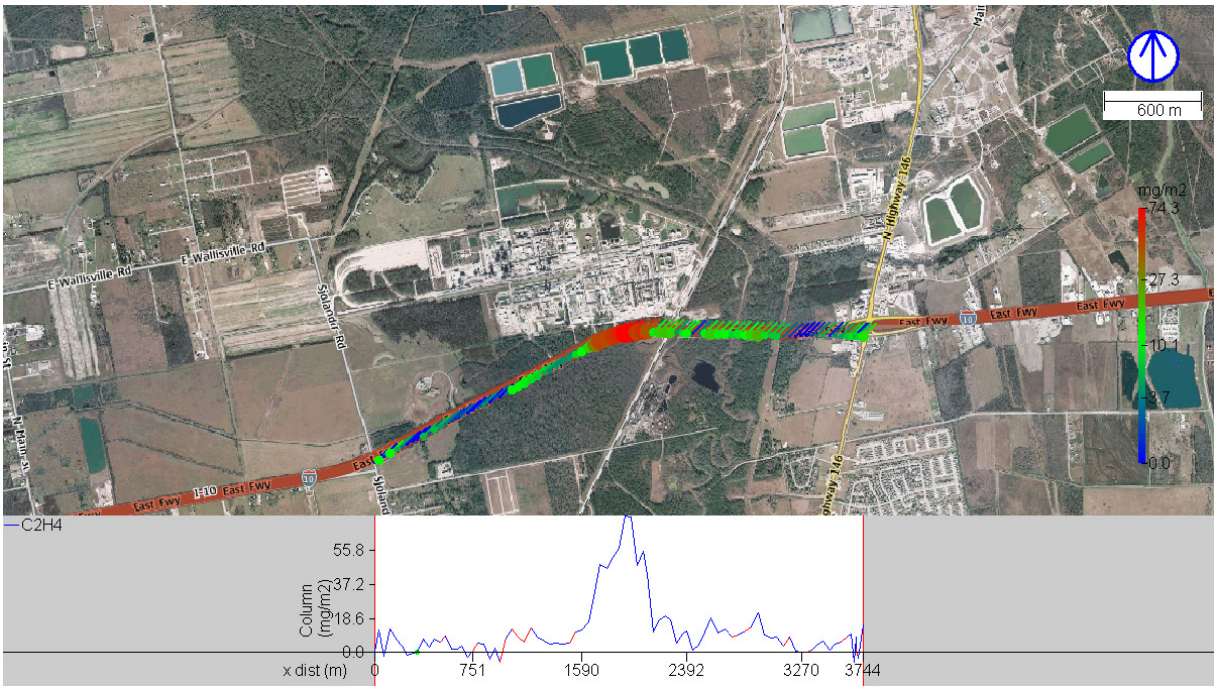

Figure 36 SOF measurement of ethene south of the southwestern facilities in Mont Belvieu on April 28, 2011, 18:17–18:24. Each measured spectrum is represented with a point, which color and size indicate the evaluated integrated vertical ethene column. The ethene column by distance driven through the plume is also shown in the lower part of the figure. A line from each point indicates the direction from which the wind is blowing.

Table 18 Summary of ethene emission transects from the southwestern part of Mont Belvieu.

Region	Day	N	Start	Stop	Mean (kg/h)	SD (kg/h)	WS (m/s)	Range WD (deg)	
MBsw									
	110428	2	175604	182302	175.7	78.5	3.9	10	14
	110613	2	153251	155338	453.7	160.5	8.4	157	159
	110614	2	112246	121431	128.9	10.9	6.4	213	225
Total		**6**	**112246**	**182302**	**252.8**	**176.3**	**6.2**	**10**	**225**

5.2.3 Formaldehyde (HCHO)

In Mont Belvieu there was a single source of formaldehyde that was repeatedly detected. This was from the northern facilities along Hatcherville Road. A measurement of the formaldehyde emissions from these facilities is shown in Figure 37. This emission source was detected on April 16 and 27. All measurements are summarized in Table 19. The average formaldehyde emission measured was 19.5 kg/h with a standard deviation of 5.5 kg/h.

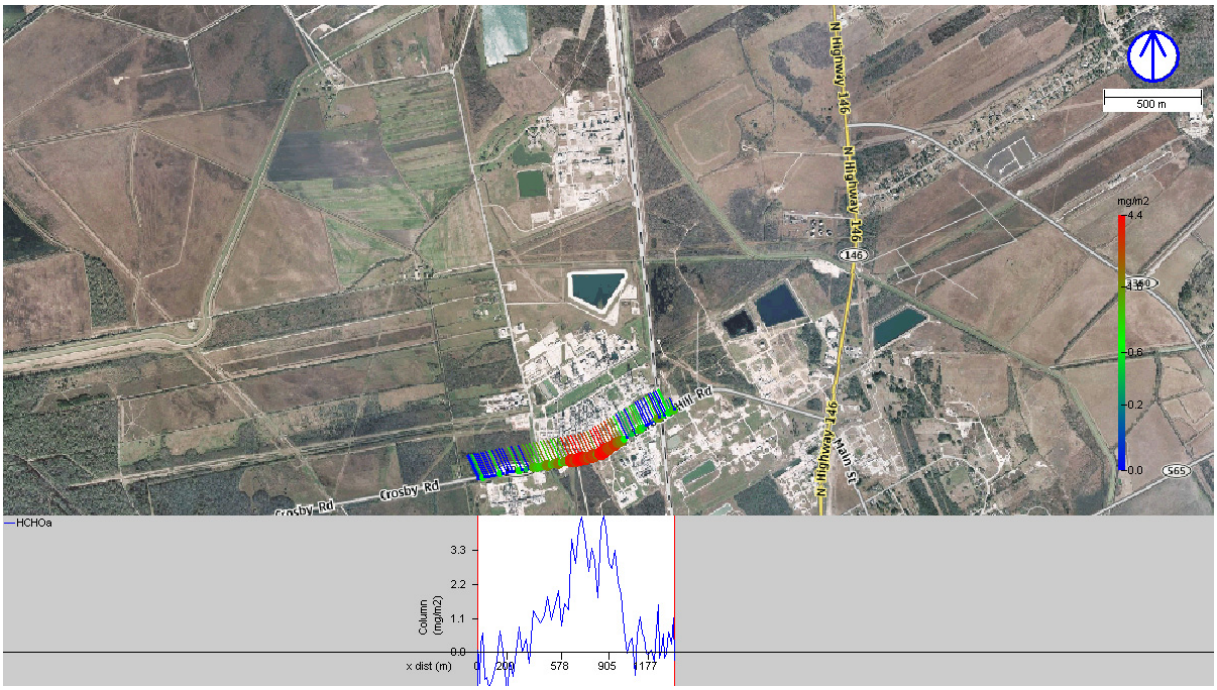

Figure 37 Mobile DOAS measurement of formaldehyde south of the northern facilities in Mont Belvieu on April 16, 2011, 17:57–18:00. Each measured spectrum is represented with a point, which color and size indicate the evaluated integrated vertical formaldehyde column. The formaldehyde column by distance driven through the plume is also shown in the lower part of the figure. A line from each point indicates the direction from which the wind is blowing.

Table 19 Summary of formaldehyde emission transects from the north part of Mont Belvieu.

Region	Day	N	Start	Stop	Mean (kg/h)	SD (kg/h)	WS (m/s)	Range WD (deg)	
MBnorth									
	110416	4	175434	182054	18.8	5.1	3.5	0	355
	110427	2	172948	175327	20.8	8.3	10.1	314	331
Total		**6**	**172948**	**182054**	**19.5**	**5.5**	**5.7**	**314**	**335**

5.2.4 Sulfur dioxide (SO_2)

No sulfur dioxide was detected in Mont Belvieu.

5.2.5 Nitrogen dioxide (NO_2)

Measurements of NO_2 from the northern facilities in Mont Belvieu were made on April 16 and 27, giving an average emission of 145 kg/h, as shown in Table 20. One of these measurements is visualized in Figure 38. On April 28, two measurements were made that captured the NO_2 emissions from all of Mont Belvieu. These measurement, averaging at 305 kg/h are also shown in Table 20.

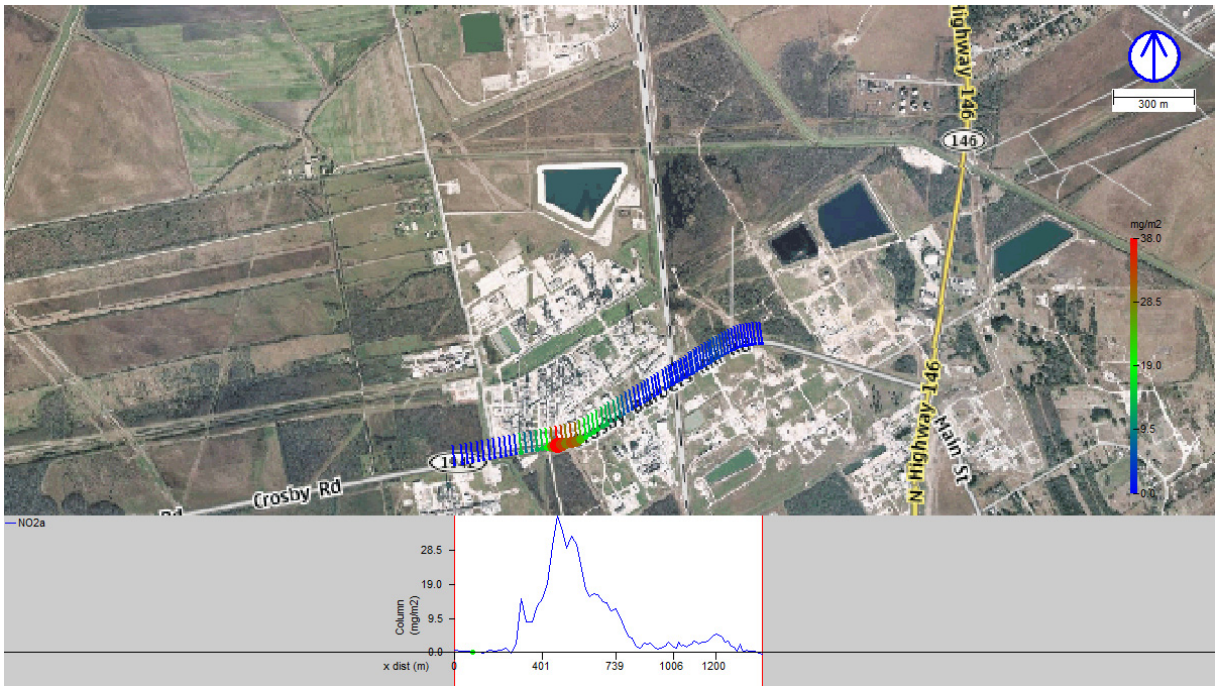

Figure 38 Mobile DOAS measurement of NO_2 south of the northern facilities in Mont Belvieu on April 16, 2011, 17:57–18:00. Each measured spectrum is represented with a point, which color and size indicate the evaluated integrated vertical NO_2 column. The NO_2 column by distance driven through the plume is also shown in the lower part of the figure. A line from each point indicates the direction from which the wind is blowing.

Table 20 Summary of NO_2 emission transects from Mont Belvieu.

Region	Day	N	Start	Stop	Mean (kg/h)	SD (kg/h)	WS (m/s)	Range WD (deg)	
MBnorth									
	110416	4	175436	182112	126.5	17.2	3.5	0	354
	110427	3	171531	175533	170.5	58.7	10.4	314	332
Total		**7**	**171531**	**182112**	**145.4**	**43.0**	**6.4**	**0**	**354**
MB all									
	110428	2	175235	182629	304.7	29.1	3.9	9	14
Total		**2**	**175235**	**182629**	**304.7**	**29.1**	**3.9**	**9**	**14**

5.3 Houston Ship Channel

Houston Ship Channel was surveyed with SOF in 2006 and 2009. To make it possible to compare the results from the different campaigns the same division of the channel into sectors has been used. This division is illustrated in Figure 39.

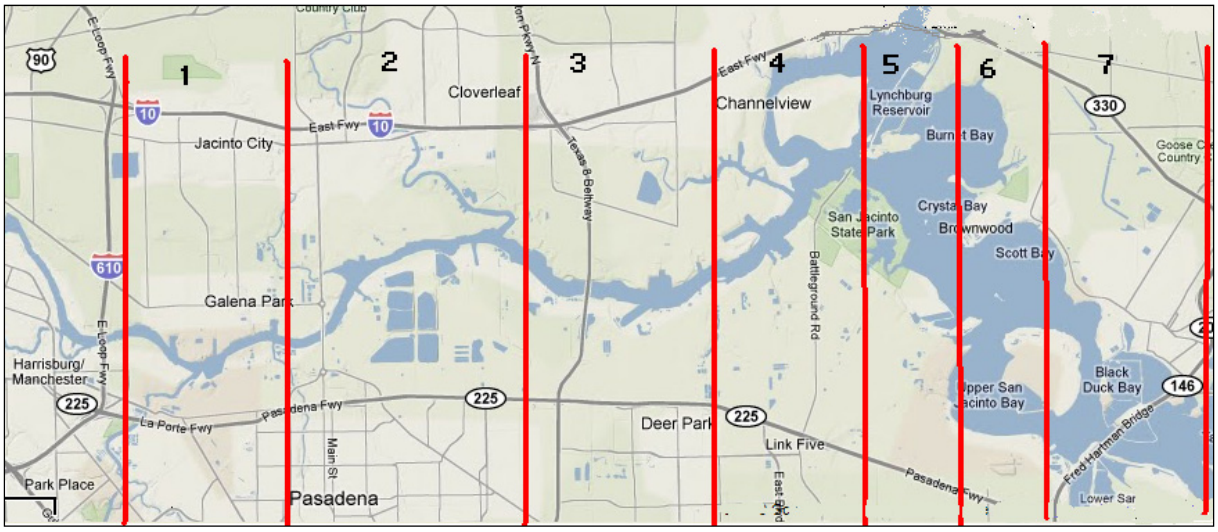

Figure 39 SOF sectors in the Houston ship channel into which the emissions were divided for analysis. The sectors are named: 1. Allen Genoa Rd, 2. Jefferson Rd (Davison in Mellqvist 2007), 3. Deer Park, 4. Battleground Rd, 5. Miller Cutoff Rd, 6. Sens Rd, 7. Baytown.

Most measurements in the Ship Channel were performed in northerly winds along Highway 225 but other types of measurement transects were made for specific sectors, most notably for Baytown. Dividing the plume into these sectors is not always an easy task and the difficulty increases the more the wind deviates from straight northerly. For this reason part of the plume from one sector may at some times be wrongly assigned to a neighboring sector.

5.3.1 Alkanes

A typical alkane traverse covering the entire Ship Channel along Highway 225 in northwesterly winds is shown in Figure 40. The emission measurements are summarized in Table 21, for each of the sectors as well as for the entire Ship Channel. Some of the sectors were only covered by measurements on a single day, April 15, while others, most notably Baytown, were covered on multiple days. The measurements of the full Ship Channel on April 27 were made along Highway 146 in southwesterly winds and could not be divided into sectors. Hence the set of transects used for sector emissions and the set used for the entire Ship Channel only partially overlap. Because of this the sum of the average emission for the sectors does not exactly match the average emission of the entire Ship Channel. The average alkane emission measured from the Ship Channel was 11 569 kg/h with a standard deviation of 2598 kg/h.

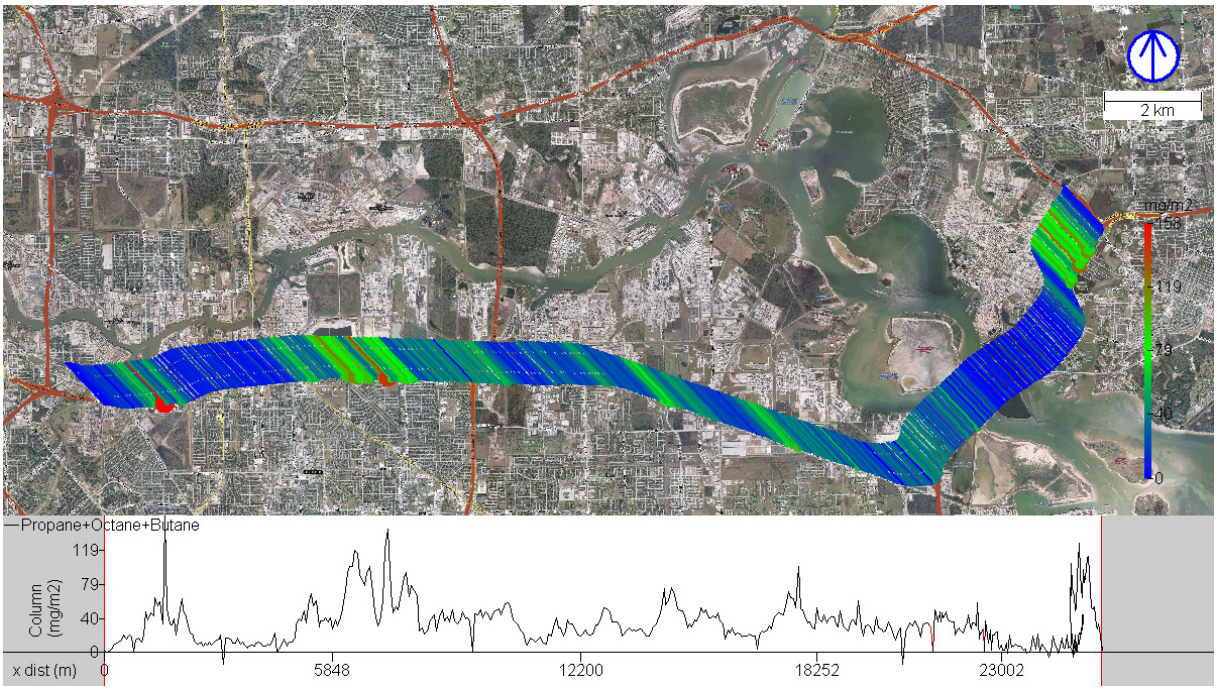

Figure 40 SOF measurement of alkanes south of the Houston Ship Channel on April 15, 2011, 17:30–17:51. Each measured spectrum is represented with a point, which color and size indicate the evaluated integrated vertical alkane column. The VOC column by distance driven through the plume is also shown in the lower part of the figure. A line from each point indicates the direction from which the wind is blowing.

Table 21 Summary of alkane emission transects in Houston Ship Channel.

Region	Day	N	Start	Stop	Mean (kg/h)	SD (kg/h)	WS (m/s)	Range WD (deg)	
HSC 1									
	110415	6	114923	183718	1491.9	476.3	10.7	317	334
	110427	3	115321	144710	1723.0	870.0	10.6	314	323
Total		**9**	**114923**	**183718**	**1568.9**	**586.8**	**10.6**	**314**	**334**
HSC 2									
	110415	6	115806	183351	3961.9	1029.0	10.8	318	331
	110427	1	144710	145242	5306.1		11.6	322	322
Total		**7**	**115806**	**183351**	**4154.0**	**1067.9**	**10.9**	**318**	**331**
HSC 3									
	110413	1	141017	141403	2526.4		7.9	176	176
	110415	6	120700	182853	1995.1	461.0	10.5	320	330
	110427	1	145242	150349	3715.2		11.4	322	322
	110614	1	175340	175843	3485.6		8.9	181	181
Total		**9**	**120700**	**182853**	**2410.9**	**788.1**	**10.1**	**176**	**330**
HSC 4									
	110415	3	135408	182510	1057.5	569.6	10.3	321	327
Total		**3**	**135408**	**182510**	**1057.5**	**569.6**	**10.3**	**321**	**327**
HSC 5									
	110415	3	135615	182255	955.7	355.1	10.1	322	329
Total		**3**	**135615**	**182255**	**955.7**	**355.1**	**10.1**	**322**	**329**
HSC 6									
	110415	3	135816	182109	894.3	107.0	10.1	322	331
Total		**3**	**135816**	**182109**	**894.3**	**107.0**	**10.1**	**322**	**331**
HSC 7									
	110413	4	141817	172655	1494.0	362.7	9.0	153	167
	110415	3	140153	181747	2074.4	812.1	10.3	326	332
	110420	2	144242	150234	1494.1	128.2	8.0	151	153
	110423	3	141236	162404	1179.2	391.3	11.3	161	174
	110427	2	154332	163844	2926.5	24.7	10.9	296	303
	110611	1	160608	161723	1902.3		7.8	151	151
	110614	1	174832	175340	1734.7		10.5	166	166
	110419	2	130437	131642	1630.8	0.0	10.2	177	177
Total		**18**	**130437**	**181747**	**1748.7**	**620.4**	**9.8**	**151**	**332**
HSC all									
	110415	3	134238	183721	12867.6	2678.1	11.0	321	325
	110427	2	154332	163841	9621.8	108.2	10.3	293	302
Total		**5**	**134238**	**183721**	**11569.3**	**2598.0**	**10.7**	**293**	**325**

5.3.2 Alkenes

Alkenes were measured in the Ship Channel on April 16 and 28 and were mainly detected coming from three areas in the Ship Channel, from Jefferson Road (Sector 2), from Deer Park (Sector 3) and from the area around Sector 4 and 5. This is clearly exemplified in the full ethene transect shown in Figure 41. Ethene was also detected from Baytown. The ethene and

propene emission transects are summarized for each of these sectors in Table 22 and Table 23 respectively. The average ethene emissions for Sector 2, Sector 3, Sector 4+5+6 and Sector 7 were 133 kg/h, 165 kg/h, 246 kg/h and 69 kg/h respectively with standard deviations of 103 kg/h, 90 kg/h, 95 kg/h and 22 kg/h respectively. The average propene emissions for Sector 2, Sector 3 and Sector 4+5 were 76 kg/h, 149 kg/h and 241 kg/h respectively with standard deviations of 59 kg/h, 50 kg/h and 283 kg/h respectively as shown in Table 23. Only one measurement of propene from Sector 7 was obtained, showing a flux of 97 kg/h. The propene emissions in sector 4+5 were highly variable with one extraordinarily large emission of 872 kg/h on April 28 as shown in Figure 42.

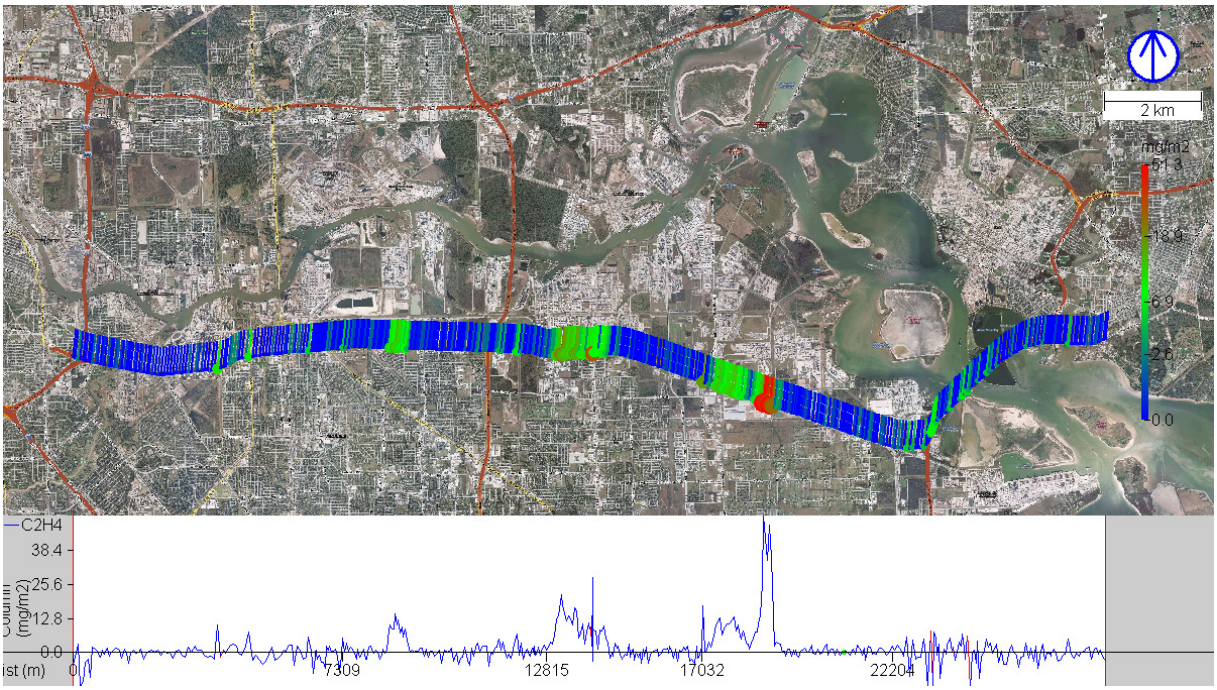

Figure 41 SOF measurement of ethene south of the Houston Ship Channel on April 28, 2011, 13:31–14:14. Each measured spectrum is represented with a point, which color and size indicate the evaluated integrated vertical ethene column. The ethene column by distance driven through the plume is also shown in the lower part of the figure. A line from each point indicates the direction from which the wind is blowing.

Table 22 Summary of ethene emission transects in Houston Ship Channel.

Region	Day	N	Start	Stop	Mean (kg/h)	SD (kg/h)	WS (m/s)	Range WD (deg)	
HSC 2									
	110416	7	113911	154809	181.3	124.3	6.6	5	346
	110417	2	104916	120826	122.8	76.5	9.7	119	153
	110428	5	105721	163802	68.9	26.3	4.3	4	35
Total		**14**	**104916**	**163802**	**132.8**	**103.2**	**6.2**	**4**	**346**
HSC 3									
	110416	4	95101	154134	82.7	26.7	6.1	11	359
	110428	5	110640	165224	230.0	60.2	4.4	9	39
Total		**9**	**95101**	**165224**	**164.5**	**90.0**	**5.2**	**9**	**359**
HSC 456									
	110416	6	95550	153357	234.5	98.3	7.0	1	358
	110428	4	112112	165751	264.1	100.7	4.5	7	28
Total		**10**	**95550**	**165751**	**246.3**	**94.8**	**6.0**	**1**	**358**
HSC7									
	110416	3	133710	144649	58.0	7.1	4.1	7	33
	110428	1	142306	142931	100.5		4.1	347	347
Total		**4**	**133710**	**144649**	**68.6**	**22.0**	**4.1**	**7**	**347**

Table 23 Summary of propene emission transects in Houston Ship Channel.

Region	Day	N	Start	Stop	Mean (kg/h)	SD (kg/h)	WS (m/s)	Range WD (deg)	
HSC 2									
	110416	4	94501	154658	111.0	78.0	6.4	4	360
	110428	5	105858	163541	48.1	13.2	4.3	3	35
Total		**9**	**94501**	**163541**	**76.0**	**58.9**	**5.2**	**3**	**360**
HSC 3									
	110416	2	94916	154006	140.5	67.9	6.2	339	359
	110428	1	164451	165102	166.6		3.9	20	20
Total		**3**	**94916**	**165102**	**149.2**	**50.3**	**5.4**	**20**	**359**
HSC 45									
	110416	2	95828	153220	122.3	47.1	6.2	341	357
	110428	5	112402	165948	288.7	331.5	4.4	3	33
Total		**7**	**95828**	**165948**	**241.2**	**283.3**	**4.9**	**3**	**357**
HSC 7									
	110416	1	144208	144826	96.7		4.2	13	13
Total		**1**	**144208**	**144826**	**96.7**		**4.2**	**13**	**13**

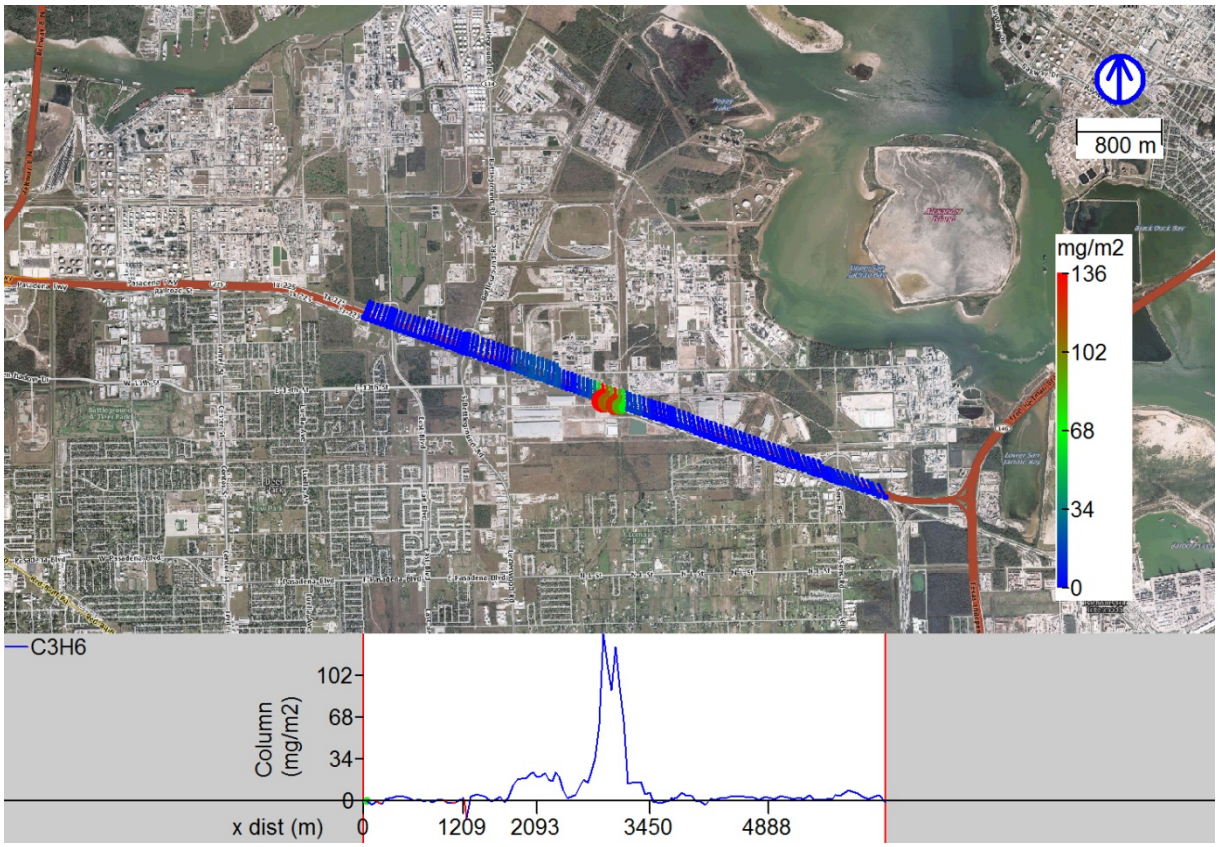

Figure 42 SOF measurement of propene form Area 4+5 on April 28, 2011, 13:58–14:02. Each measured spectrum is represented with a point, which color and size indicate the evaluated integrated vertical propene column. The propene column by distance driven through the plume is also shown in the lower part of the figure. A line from each point indicates the direction from which the wind is blowing.

5.3.3 Formaldehyde (HCHO)

Two distinct sources of formaldehyde were repeatedly detected with the Mobile DOAS measurements in the Ship Channel. One was in the western part of the Ship Channel, close to Jefferson Road. This source was also detected in the 2009 campaign and was the largest formaldehyde source found in that campaign. A measurement transect on the south side of this source is shown in Figure 43. The other source detected was in the eastern part of the Ship Channel, close to Strang Road nearby the western bridgehead of the Fred Hartman Bridge. This source had not been detected in the 2009 campaign. Figure 44 shows a measurement of the formaldehyde emissions from this source.

A summary of the measured formaldehyde emissions from these sources is given in Table 24. The average measured formaldehyde emissions from these sources were 39 kg/h and 30 kg/h respectively with standard deviations of 36 kg/h and 32 kg/h respectively. The high standard deviations reflect how highly variable these sources are.

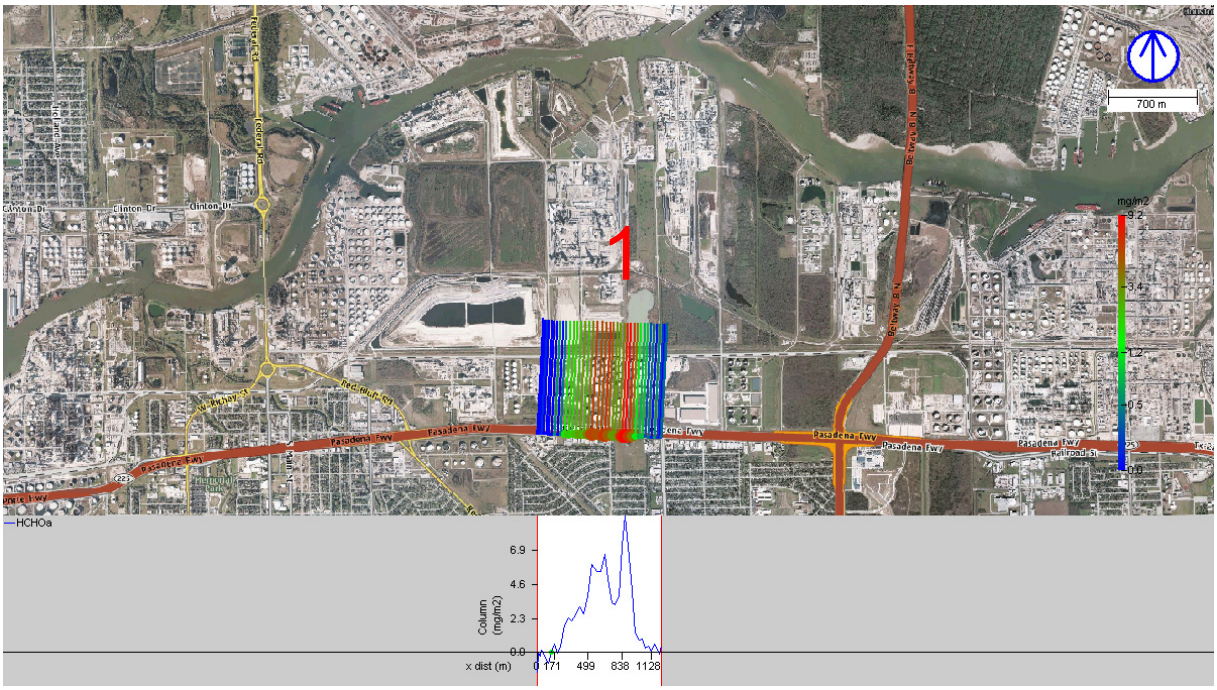

Figure 43 Mobile DOAS measurement of formaldehyde south of the source close to Jefferson Road on April 16, 2011, 12:40–12:42. Each measured spectrum is represented with a point, which color and size indicate the evaluated integrated vertical formaldehyde column. The formaldehyde column by distance driven through the plume is also shown in the lower part of the figure. A line from each point indicates the direction from which the wind is blowing.

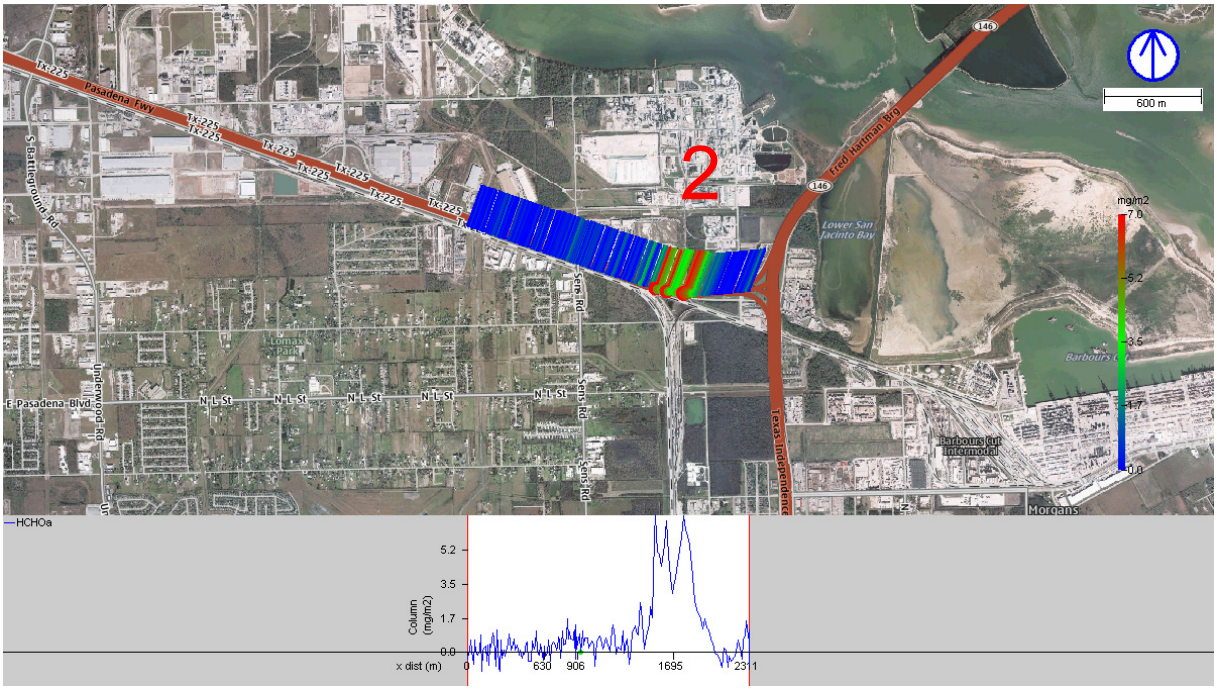

Figure 44 Mobile DOAS measurement of formaldehyde south of the source close to Strang Road on April 28, 2011, 11:31–11:37. Each measured spectrum is represented with a point, which color and size indicate the evaluated integrated vertical formaldehyde column. The formaldehyde column by distance driven through the plume is also shown in the lower part of the figure. A line from each point indicates the direction from which the wind is blowing.

Table 24 Summary of formaldehyde emission transects from the two sources found in Houston Ship Channel.

Region	Day	N	Start	Stop	Mean (kg/h)	SD (kg/h)	WS (m/s)	Range WD (deg)	
HSC 1									
	110415	1	130403	130558	24.0		10.3	325	325
	110416	7	94616	162944	45.7	38.8	6.9	4	359
	110428	4	105904	163507	14.6	7.3	4.6	17	35
Total		**12**	**94616**	**163507**	**33.6**	**32.7**	**6.4**	**4**	**359**
HSC 2									
	110415	1	181955	182115	76.8		9.8	322	322
	110416	2	133734	150709	18.8	0.7	4.5	38	323
	110428	3	113437	143103	22.8	14.5	5.0	15	34
Total		**6**	**113437**	**182115**	**30.5**	**24.6**	**5.6**	**15**	**323**

5.3.4 Sulfur dioxide (SO_2)

There are four areas in Houston Ship Channel showing significant SO_2 emissions. In relation to the sectors in Figure 39 the first one is to the west of Sector 1, referred to as Sector 0, the second one includes areas on both sides of the border between Sector 1 and 2, the third one is the combination of Sector 3 and 4 and the fourth one is Sector 7, Baytown.
A measurement transect covering all of these areas is displayed in Figure 45. All the measurements of the SO_2 are summarized in Table 25. The average emissions for these areas were 678 kg/h, 389 kg/h, 869 kg/h and 424 kg/h respectively with standard deviations of 336 kg/h, 244 kg/h, 294 kg/h and 159 kg/h.

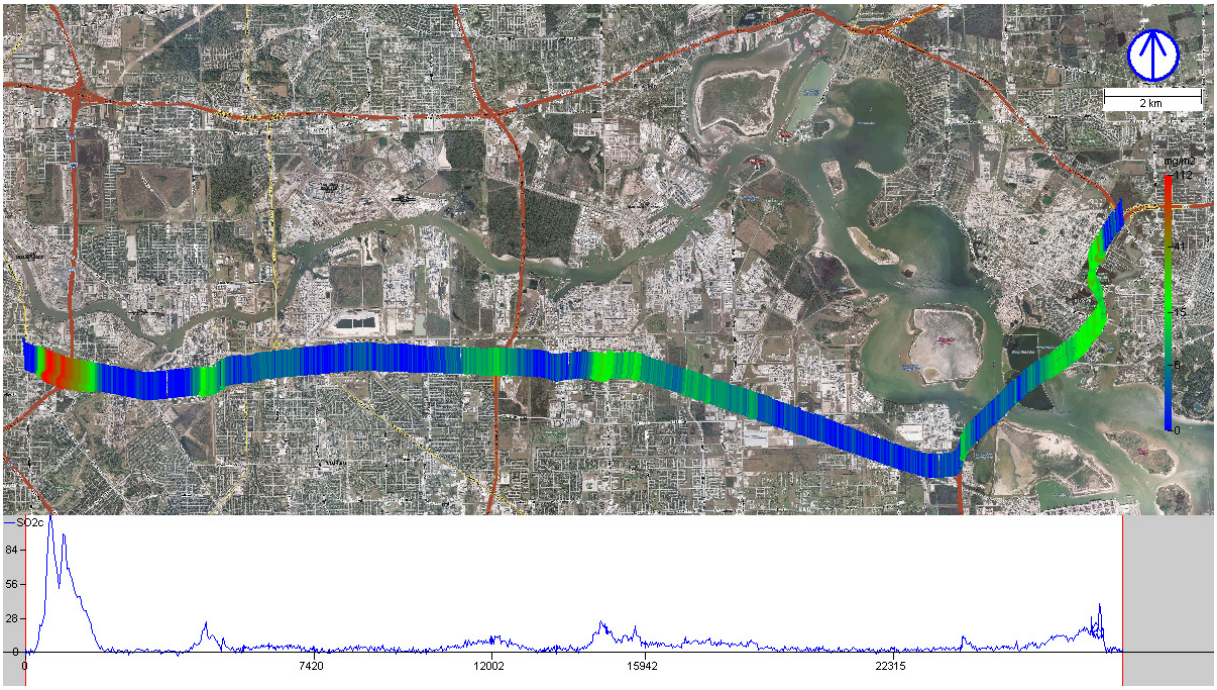

Figure 45 Mobile DOAS measurement of SO_2 south of Houston Ship Channel on April 16, 2011, 16:14–17:00. Each measured spectrum is represented with a point, which color and size indicate the evaluated integrated vertical SO_2 column. The SO_2 column by distance driven through the plume is also shown in the lower part of the figure. A line from each point indicates the direction from which the wind is blowing.

Table 25 Summary of SO_2 emission transects in Houston Ship Channel.

Region	Day	N	Start	Stop	Mean (kg/h)	SD (kg/h)	WS (m/s)	Range WD (deg)	
HSC 0									
	110415	3	134124	183757	555.4	285.3	11.3	316	332
	110416	8	91833	161746	567.4	165.6	5.9	9	353
	110428	3	124524	162525	678.8	138.1	4.8	15	42
	110422	1	155423	155618	370.2		10.7	174	174
	110427	3	114903	144443	519.7	263.3	10.3	315	323
Total		**18**	**91833**	**183757**	**565.1**	**190.2**	**7.6**	**9**	**353**
HSC 12									
	110415	3	130821	183440	446.9	62.1	10.7	316	333
	110416	7	93718	162513	299.7	143.0	5.9	8	357
	110428	4	105305	163231	205.3	82.3	4.5	9	33
	110420	1	171307	171830	258.9		7.1	162	162
	110422	1	155155	155316	315.6		11.0	173	173
	110427	2	115525	144653	687.2	571.5	10.6	315	323
Total		**18**	**93718**	**183440**	**344.9**	**222.7**	**7.3**	**8**	**357**
HSC 34									
	110415	4	121416	182631	709.0	308.2	10.9	316	328
	110416	5	95313	164734	666.2	245.5	5.7	11	359
	110417	1	115658	120509	1501.7		11.5	121	121
	110428	4	110545	165249	1069.9	72.6	4.6	19	37
	110420	1	170300	170834	752.4		7.4	154	154
	110419	1	115645	115951	1094.1		10.2	173	173
	110422	1	154459	154736	1033.1		11.0	171	171
	110427	2	154855	163305	701.4	222.8	10.0	294	301
Total		**19**	**95313**	**182631**	**854.2**	**298.6**	**7.9**	**11**	**359**
HSC 7									
	110416	5	133631	170009	632.1	301.8	6.6	326	358
	110417	1	115019	115500	784.8		10.6	145	145
	110428	4	113022	143044	405.9	31.4	4.7	15	333
	110420	5	144720	170044	726.7	211.6	9.2	148	155
	110419	2	120649	131458	521.3	99.1	11.7	166	167
	110422	2	152555	154217	600.4	24.5	11.8	158	162
	110427	3	153853	163612	368.2	101.3	10.9	302	302
	110423	3	141437	162544	519.3	66.9	12.5	163	171
Total		**25**	**113022**	**170044**	**564.3**	**205.9**	**9.0**	**15**	**358**

5.3.4 Nitrogen dioxide (NO_2)

The sectors in Figure 39 were also used for the NO_2 emissions, although sector 3 and 4 were combined since they were difficult to separate. An example measurement covering all sectors is shown in Figure 46. All measurements are summarized day by day in Table 26. The

average NO_2 emissions measured were 380 kg/h, 248 kg/h, 617 kg/h, 115 kg/h, 90 kg/h and 379 kg/h for sector 1, 2, 3+4, 5, 6 and 7 respectively with standard deviations of 179 kg/h, 84 kg/h, 246 kg/h, 41 kg/h, 52 kg/h and 70 kg/h respectively.

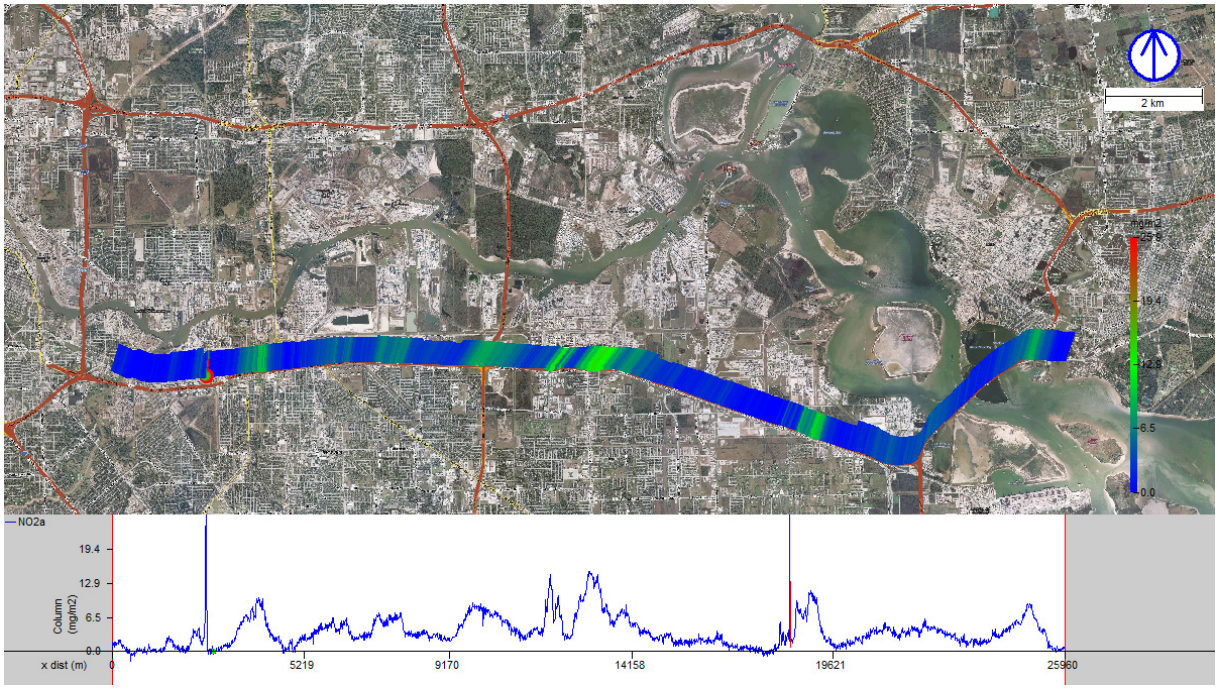

Figure 46 Mobile DOAS measurement of NO_2 south of Houston Ship Channel on April 18, 2011, 11:56–12:44. Each measured spectrum is represented with a point, which color and size indicate the evaluated integrated vertical NO_2 column. The NO_2 column by distance driven through the plume is also shown in the lower part of the figure. A line from each point indicates the direction from which the wind is blowing.

Table 26 Summary of NO_2 emission transects in Houston Ship Channel.

Region	Day	N	Start	Stop	Mean (kg/h)	SD (kg/h)	WS (m/s)	Range WD (deg)	
HSC 1									
	110416	9	91017	162332	317.3	94.5	5.7	9	354
	110428	4	105107	162851	307.9	145.1	4.6	10	39
	110427	3	115422	144754	666.1	148.0	10.1	307	323
Total		**16**	**91017**	**162851**	**380.3**	**178.9**	**6.3**	**9**	**354**
HSC 2									
	110416	7	94032	163438	251.5	73.3	5.9	10	359
	110428	4	105550	163636	197.2	35.5	4.4	11	35
	110427	1	144744	145221	424.4		9.3	308	308
Total		**12**	**94032**	**163636**	**247.8**	**84.0**	**5.7**	**10**	**359**
HSC 34									
	110416	5	95023	164811	574.1	145.3	5.7	11	359
	110428	4	110601	165511	670.7	355.8	4.6	18	38
Total		**9**	**95023**	**165511**	**617.0**	**246.2**	**5.2**	**11**	**359**
HSC 5									
	110416	6	100036	165101	94.9	37.8	6.0	7	358
	110428	4	120520	170028	145.7	25.3	4.1	10	350
Total		**10**	**100036**	**170028**	**115.2**	**41.2**	**5.2**	**7**	**358**
HSC 6									
	110416	3	100438	152038	63.1	35.5	6.4	330	358
	110428	2	140520	143318	130.8	53.5	3.9	328	358
Total		**5**	**100438**	**152038**	**90.2**	**52.2**	**5.4**	**328**	**358**
HSC 7									
	110416	5	133736	170047	367.0	75.7	6.6	14	357
	110428	2	140920	142903	350.8	17.0	3.9	10	346
	110427	2	154554	163600	438.3	81.2	10.9	301	302
Total		**9**	**133736**	**170047**	**379.2**	**70.0**	**6.9**	**10**	**357**

5.4 Beaumont/Port Arthur/Orange

The areas studied in the Beaumont/Port Arthur region are shown in Figure 47. In this region nor SOF nor Mobile DOAS has been used previously. There are numerous refineries and petrochemical industries as well as large storage depots. The areas for which results will be presented in this chapter are marked in blue and numbered in the map in Figure 47. Alkane emissions have also been detected from other smaller areas but this report focuses on the most significant sources. In the Alkenes section emissions are also reported from a facility in Orange, located north-east of Beaumont/Port Arthur.

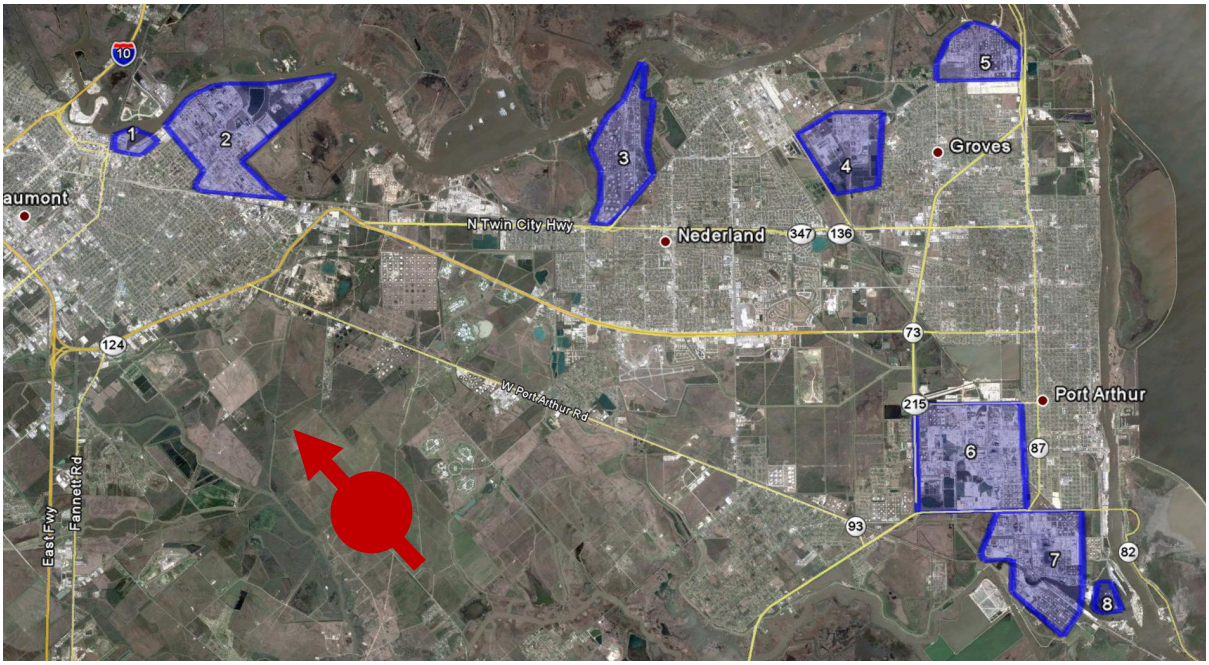

Figure 47 Industrial site areas studied in the Beaumont/Port Arthur region. Area 1, 2, 6, 7 and 8 correspond to refineries, area 3 to a storage facility and area 4 and 5 to petrochemical plants.

5.4.1 Alkanes

Alkane measurements were performed in Beaumont/Port Arthur on April 29, May 1, 3, 4 and 18. Northerly to easterly winds were used for the northern sites while southerly to easterly winds were used for the southern sites. A long measurement transect covering all the facilities along the Neches River is shown in Figure 48. Alkane measurements from all the areas in Beaumont/Port Arthur are summarized in Table 27. The average alkane emissions from Area 1, 2, 3, 5, 6 and 7 was 266 kg/h, 1758 kg/h, 1711 kg/h, 883 kg/h, 1588 kg/h and 548 kg/h respectively with standard deviations of 276 kg/h, 382 kg/h, 934 kg/h, 473 kg/h, 667kg/h and 215 kg/h respectively. For Area 4 emissions were more difficult to separate from the surrounding interfering sources given the wind direction on the day of measurement. One transect gave emissions of 657 kg/h.

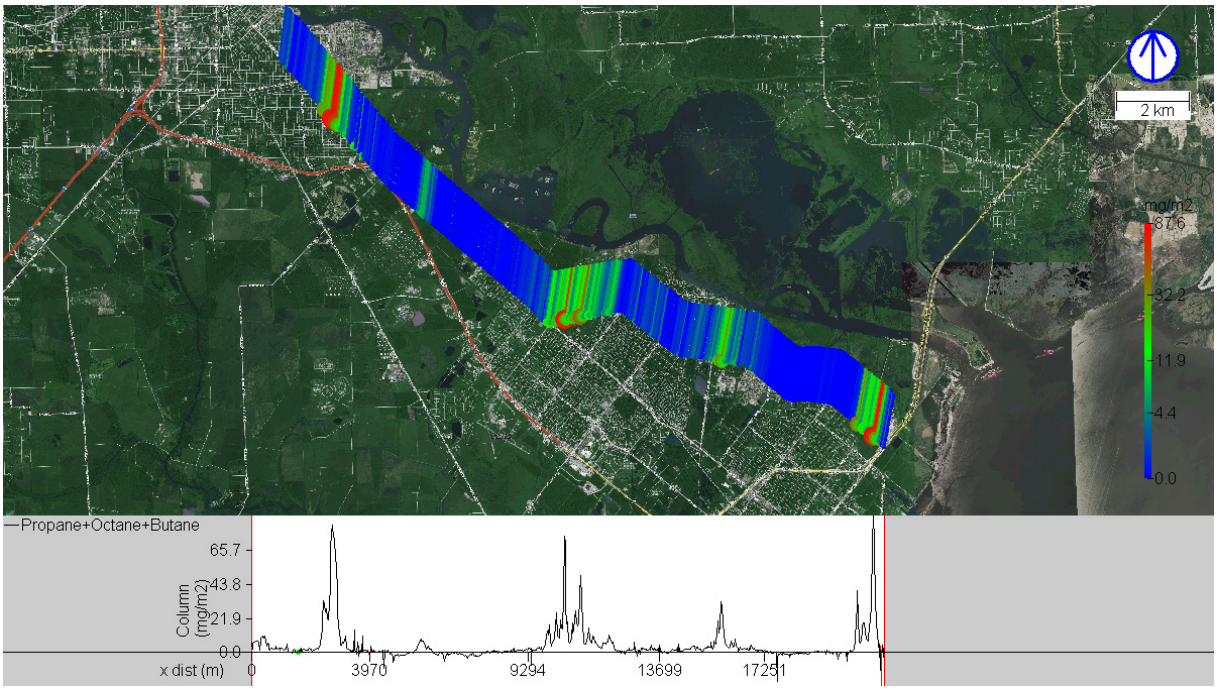

Figure 48 SOF measurement of alkanes covering area 1, 2, 3 and 5 in Beaumont/Port Arthur on May 3, 2011, 13:55–14:31. Each measured spectrum is represented with a point, which color and size indicate the evaluated integrated vertical alkane column. The VOC column by distance driven through the plume is also shown in the lower part of the figure. A line from each point indicates the direction from which the wind is blowing.

Table 27 Summary of alkane emission transects in Beaumont/Port Arthur (BPA).

Region	Day	N	Start	Stop	Mean (kg/h)	SD (kg/h)	WS (m/s)	Range WD (deg)	
BPA 1									
	110503	8	134244	170704	211.2	304.8	10.9	14	26
	110504	4	121259	135853	376.6	196.6	7.6	69	82
Total		**12**	**121259**	**170704**	**266.3**	**276.2**	**9.8**	**14**	**82**
BPA 2									
	110503	8	133735	171124	1606.6	274.6	11.0	13	27
	110504	4	120734	140456	2059.7	419.3	7.7	70	77
Total		**12**	**120734**	**171124**	**1757.6**	**381.7**	**9.9**	**13**	**77**
BPA 3									
	110503	5	140834	184853	1383.9	742.6	10.1	14	26
	110504	2	114531	143139	2529.0	1075.6	7.6	73	93
Total		**7**	**114531**	**184853**	**1711.1**	**934.2**	**9.3**	**14**	**93**
BPA 4									
	110504	1	94850	95139	657.4		6.3	83	83
Total		**1**	**94850**	**95139**	**657.4**		**6.3**	**83**	**83**
BPA 5									
	110503	6	142703	182000	617.8	305.3	9.6	23	26
	110504	4	90723	144639	1281.9	406.9	6.3	68	93
Total		**10**	**90723**	**182000**	**883.4**	**473.9**	**8.3**	**23**	**93**
BPA 6									
	110518	2	143437	150508	1821.5	1318.5	8.1	147	150
	110504	4	100505	113533	1471.4	327.7	6.2	80	84
Total		**6**	**100505**	**150508**	**1588.1**	**666.9**	**6.8**	**80**	**150**
BPA 7									
	110429	2	174626	184217	424.9	27.7	7.6	143	146
	110501	1	153636	154605	796.4		10.3	154	154
Total		**3**	**153636**	**184217**	**548.7**	**215.4**	**8.5**	**143**	**154**
Orange									
	110504	**2**	**150239**	**152604**	**1720.0**	**487.9**	**8.3**	**75**	**76**

5.4.2 Alkenes

Alkenes emissions were measured in the Beaumont/Port Arthur area on April 29, May 4, 5, 6 and 17. Southerly to easterly winds were used. Compared to the Houston area, relatively little ethene and propene was measured. The areas that had some ethene emissions were Area 4, 5, 6, 7 and a facility in Orange, west of Beaumont/Port Arthur. Ethene transects close to Area 4 and 5 are shown in Figure 50 and Figure 49 respectively. The ethene source in Orange was by far the largest according to the measurements. Figure 51 shows a transect on the north side of the facility in Orange in southerly winds. All the ethene measurements in Beaumont/Port Arthur are summarized in
Table 28. The average ethene emissions from Area 4, 5, 6, 7 and the Orange facility were 92 kg/h, 28 kg/h, 34 kg/h, 24 kg/h and 235 kg/h respectively with standard deviations of 26 kg/h, 16 kg/h, 12 kg/h, 13 kg/h and 112 kg/h respectively.

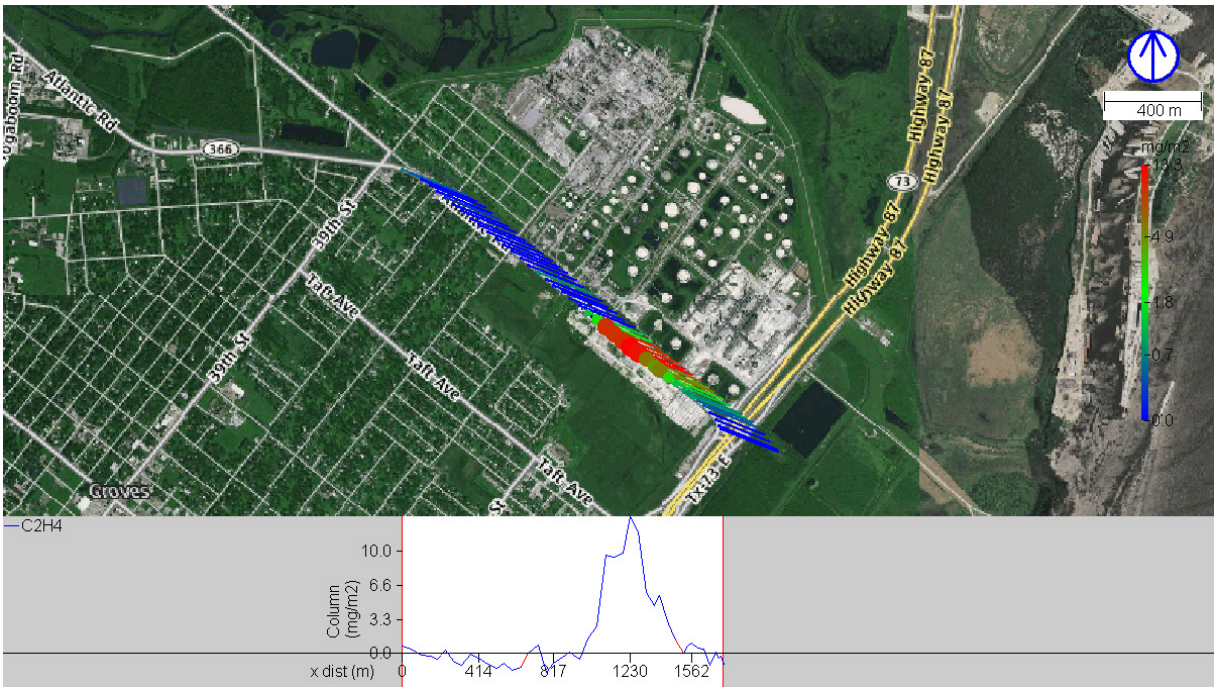

Figure 49 SOF measurement of ethene from area 5 in Port Arthur on May 4, 2011, 16:12–16:18. Each measured spectrum is represented with a point, which color and size indicate the evaluated integrated vertical ethene column. The ethene column by distance driven through the plume is also shown in the lower part of the figure. A line from each point indicates the direction from which the wind is blowing.

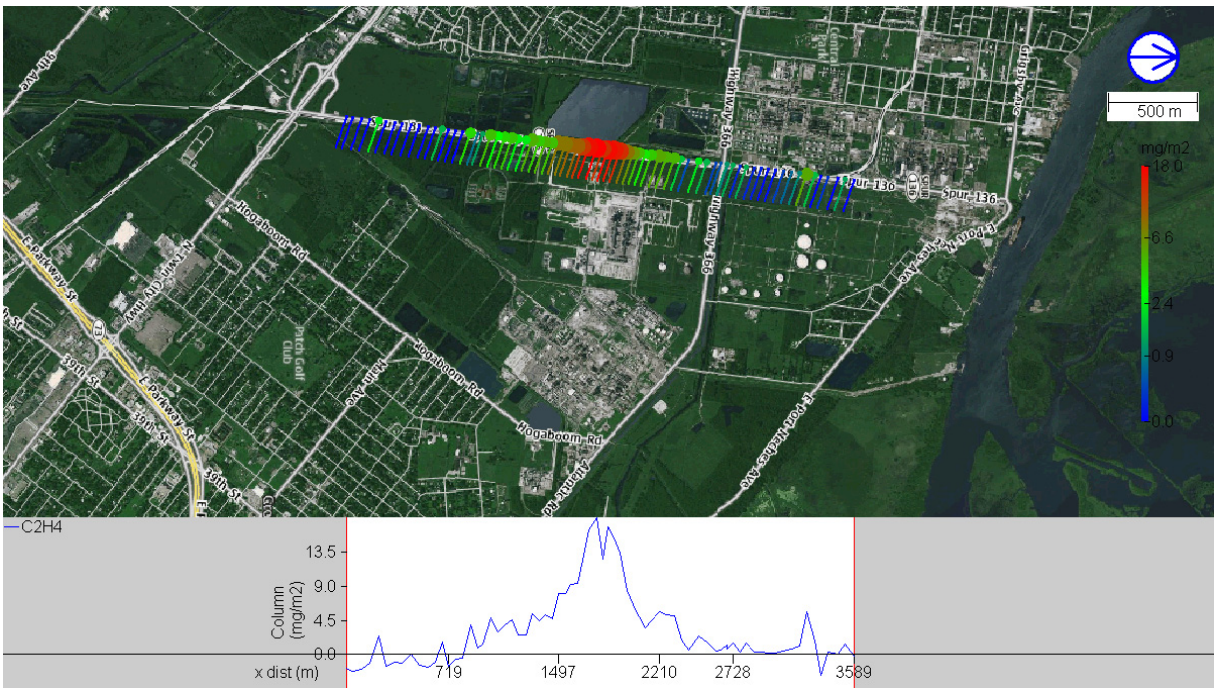

Figure 50 SOF measurement of ethene from area 4 in Port Arthur on May 4, 2011, 17:17–17:25. Each measured spectrum is represented with a point, which color and size indicate the evaluated integrated vertical ethene column. The ethene column by distance driven through the plume is also shown in the lower part of the figure. A line from each point indicates the direction from which the wind is blowing.

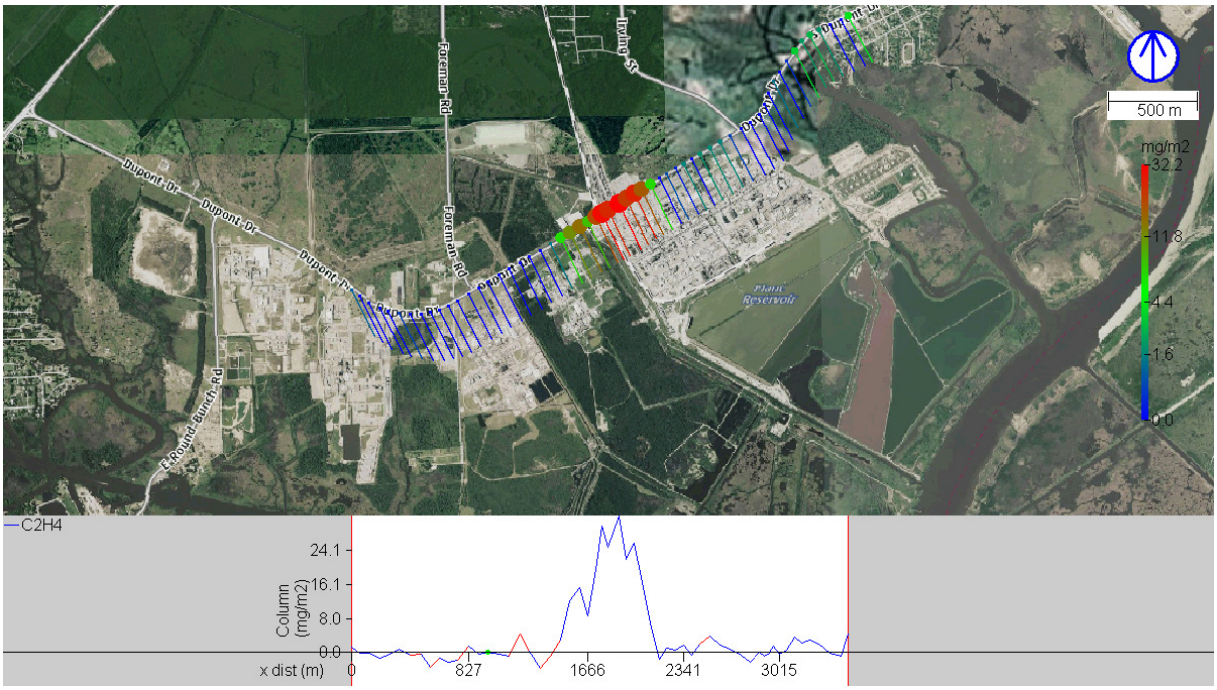

Figure 51 SOF measurement of ethene from facility in Orange on May 6, 2011, 15:00–15:07. Each measured spectrum is represented with a point, which color and size indicate the evaluated integrated vertical ethene column. The ethene column by distance driven through the plume is also shown in the lower part of the figure. A line from each point indicates the direction from which the wind is blowing.

Table 28 Summary of ethene emission transects in Beaumont/Port Arthur.

Region	Day	N	Start	Stop	Mean (kg/h)	SD (kg/h)	WS (m/s)	Range WD (deg)	
BPA 4									
	110429	3	95626	102757	81.7	3.1	7.4	96	98
	110504	2	171835	173356	119.3	34.2	5.1	87	88
	110505	1	143432	144420	71.6		5.9	149	149
Total		**6**	**95626**	**173356**	**92.5**	**26.1**	**6.4**	**87**	**149**
BPA 5									
	110429	1	94419	94911	37.0		7.5	99	99
	110504	6	155644	164834	26.2	16.6	5.3	89	106
Total		**7**	**94419**	**164834**	**27.8**	**15.7**	**5.6**	**89**	**106**
BPA 6									
	110429	3	110636	131218	26.0	6.1	8.7	136	139
	110506	1	135549	135918	48.7		3.2	132	132
	110517	3	122822	132902	37.1	12.4	6.6	120	127
Total		**7**	**110636**	**135918**	**34.0**	**11.7**	**7.0**	**120**	**139**
BPA 7									
	110429	2	111751	114128	35.3	2.3	8.2	136	136
	110506	1	95708	100520	11.1		4.0	151	151
	110517	1	121327	121605	13.5		7.4	119	119
Total		**4**	**95708**	**121605**	**23.8**	**13.4**	**7.0**	**119**	**151**
Orange									
	110506	5	150316	163753	256.0	111.4	5.7	160	184
	110517	1	181524	182807	132.6		5.8	171	171
Total		**6**	**150316**	**182807**	**235.4**	**111.6**	**5.7**	**160**	**184**

Only small quantities of propene was detected from from Area 4,6 and 7. The average propene emissions measured from these areas were 20 kg/h, 13 kg/h and 21 kg/h respectively as shown in Table 29.

Table 29 Summary of propene emission transects in Beaumont/Port Arthur.

Region	Day	N	Start	Stop	Mean (kg/h)	SD (kg/h)	WS (m/s)	Range WD (deg)	
BPA 4									
	110429	1	100907	101050	19.8		7.3	95	95
Total		**1**	**100907**	**101050**	**19.8**		**7.3**	**95**	**95**
BPA 6									
	110429	1	110649	110754	12.7		7.2	112	112
	110506	2	103517	111613	14.6	3.6	2.9	168	175
	110517	2	122915	125036	10.3	4.8	3.3	141	160
Total		**5**	**103517**	**125036**	**12.5**	**3.7**	**3.9**	**112**	**175**
BPA 7									
	110429	2	111751	114128	22.7	3.6	7.6	119	134
	110517	1	121411	121512	16.2		4.7	135	135
Total		**3**	**111751**	**121512**	**20.5**	**4.5**	**6.6**	**119**	**135**

From Area 5, the SOF measurements also detected significant emissions of 1,3-butadiene and isobutene. The spectral evaluation of these species is significantly more noisy than for ethene, but the large magnitude of the column concentrations, especially for 1,3-butadiene, still made the signal very clear. Figure 52 shows a measurement of 1,3-butadiene emissions from Area 5. All the measurements of 1,3-butadiene and isobutene from Area 5 are summarised in Table 30 and Table 31 respectively. The average 1,3-butadiene emission measured was 235 kg/h with a standard deviation of 145 kg/h, while the average isobutene emission was 48 kg/h with a standard deviation of 26 kg/h. It should be noted that the isobutene emissions measured on May 4 were not very large and this together with the noisy evaluation makes the error significantly larger for these measurements.

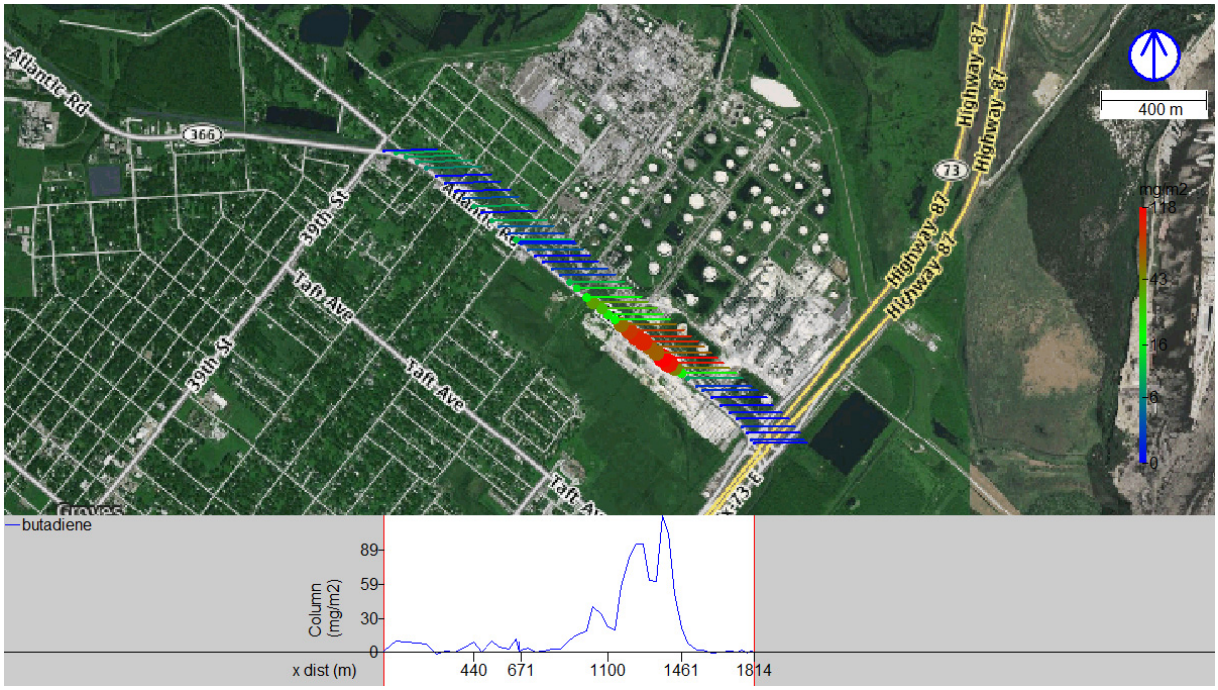

Figure 52 SOF measurement of 1,3-butadiene from area 5 in Port Arthur on May 4, 2011, 16:19–16:25. Each measured spectrum is represented with a point, which color and size indicate the evaluated integrated vertical 1,3-butadiene column. The 1,3-butadiene column by distance driven through the plume is also shown in the lower part of the figure. A line from each point indicates the direction from which the wind is blowing.

Table 30 Summary of 1,3-butadiene emission transects in Beaumont/Port Arthur.

Region	Day	N	Start	Stop	Mean (kg/h)	SD (kg/h)	WS (m/s)	Range WD (deg)	
BPA 5									
	110429	1	94543	94819	160.8	-	7.5	99	99
	110504	5	155656	164827	195.0	148.3	5.3	89	106
Total		6	94543	162241	189.3	133.4	5.6	89	106

Table 31 Summary of isobutene emission transects in Beaumont/Port Arthur.

Region	Day	N	Start	Stop	Mean (kg/h)	SD (kg/h)	WS (m/s)	Range WD (deg)	
BPA 5									
	110429	1	94530	94734	80.2	-	7.5	99	99
	110504	3	155656	164827	35.8	9.8	5.3	89	106
Total		6	94530	164827	43.2	20.1	5.6	89	106

5.4.3 Formaldehyde (HCHO)

Three distinct sources of formaldehyde were repeatedly detected in the Beaumont/Port Arthur area. Like most formaldehyde sources detected in the campaign, the emission rates were quite variable and not detectable at some times. The formaldehyde sources were located in Area 2, 4 and 5. Transects from all of these sources are shown in Figure 53, Figure 55 and Figure 54 respectively. All of the measurements detecting formaldehyde are summarized in Table 32. The average formaldehyde emissions from these sources were 26.6 kg/h, 8.8 kg/h and 10.4 kg/h with standard deviations of 9.0 kg/h, 5.9 kg/h and 2.5 kg/h.

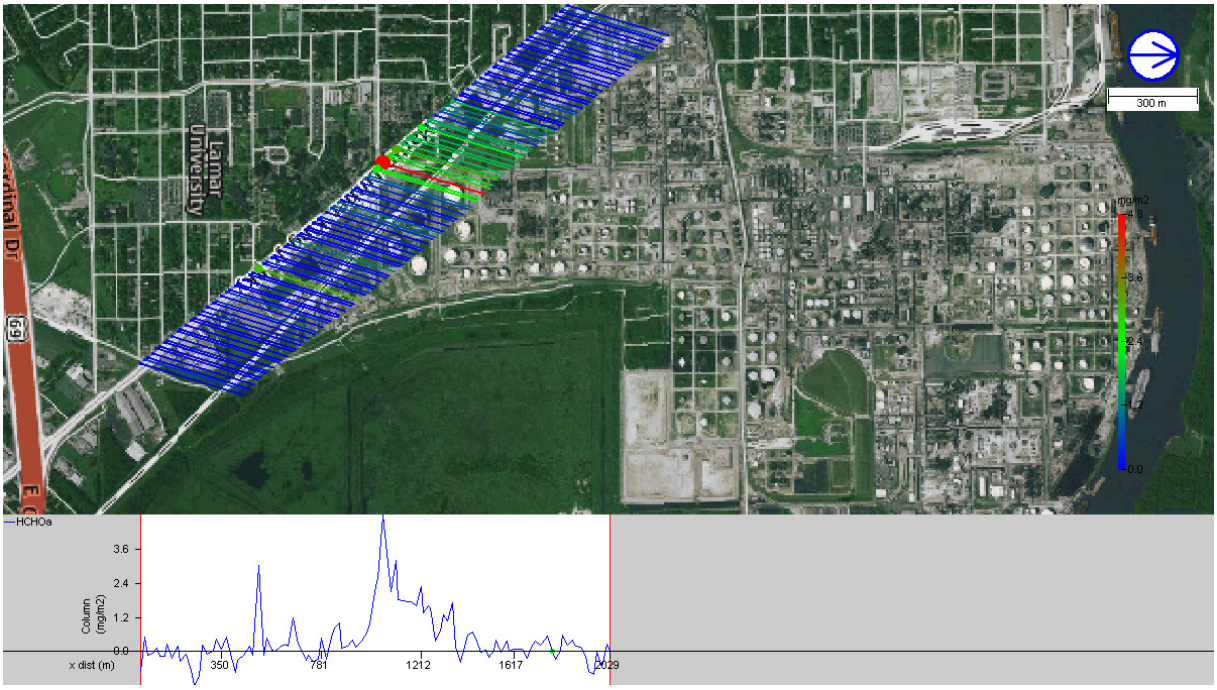

Figure 53 Mobile DOAS measurement of formaldehyde from area 2 in Beaumont on May 3, 2011, 16:25–16:28. Each measured spectrum is represented with a point, which color and size indicate the evaluated integrated vertical formaldehyde column. The formaldehyde column by distance driven through the plume is also shown in the lower part of the figure. A line from each point indicates the direction from which the wind is blowing.

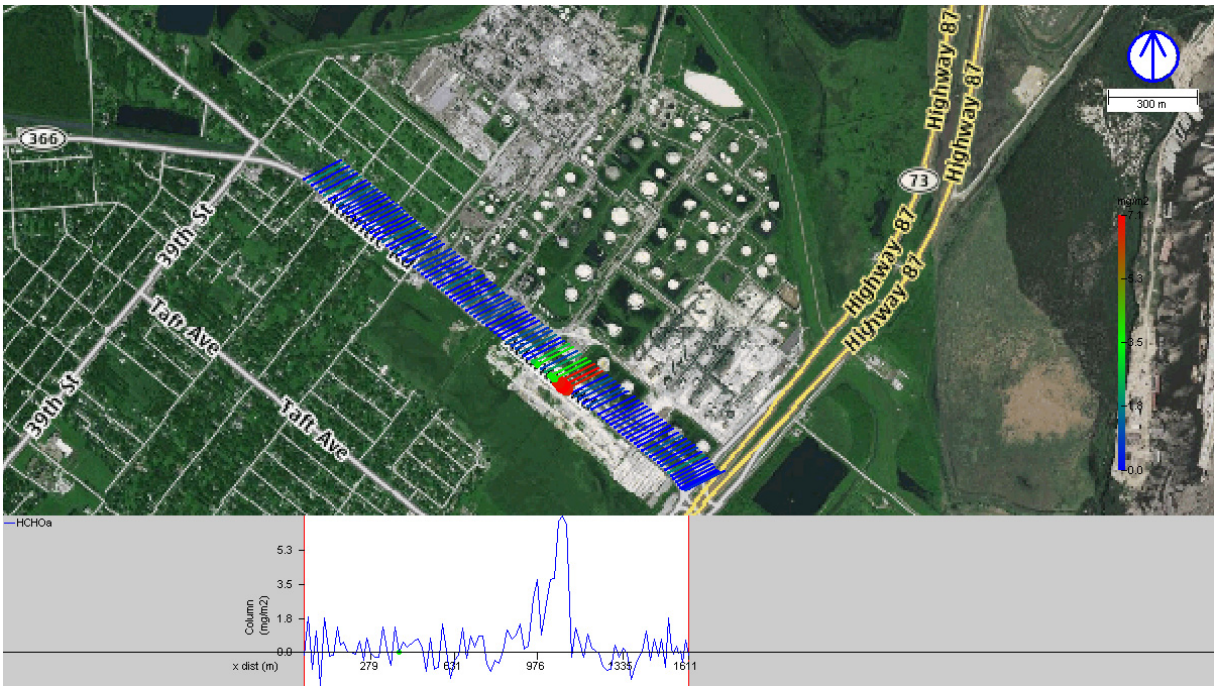

Figure 54 Mobile DOAS measurement of formaldehyde from area 5 in Port Arthur on May 4, 2011, 09:07–09:11. Each measured spectrum is represented with a point, which color and size indicate the evaluated integrated vertical formaldehyde column. The formaldehyde column by distance driven through the plume is also shown in the lower part of the figure. A line from each point indicates the direction from which the wind is blowing.

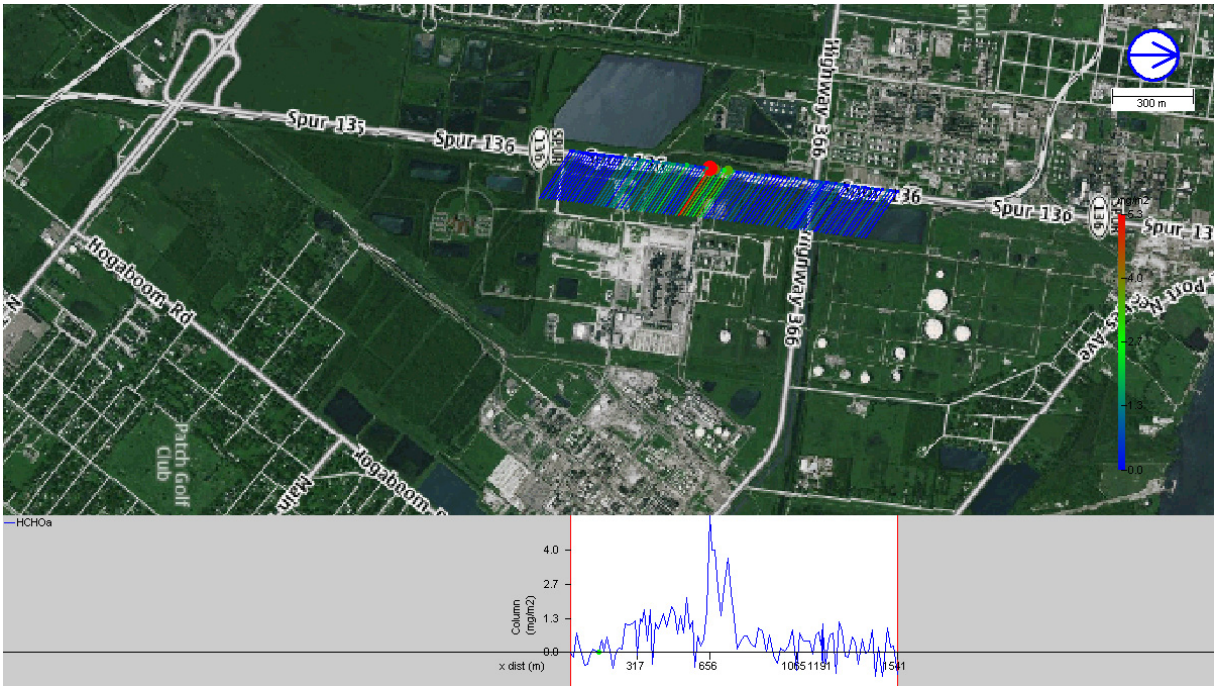

Figure 55 Mobile DOAS measurement of formaldehyde from area 4 in Port Arthur on May 4, 2011, 17:18–17:22. Each measured spectrum is represented with a point, which color and size indicate the evaluated integrated vertical formaldehyde column. The formaldehyde column by distance driven through the plume is also shown in the lower part of the figure. A line from each point indicates the direction from which the wind is blowing.

Table 32 Summary of formaldehyde emission transects in Beaumont/Port Arthur.

Region	Day	N	Start	Stop	Mean (kg/h)	SD (kg/h)	WS (m/s)	Range WD (deg)	
BPA 2									
	110503	5	133942	162712	19.9	9.4	7.8	7	20
Total		**5**	**133942**	**162712**	**19.9**	**9.4**	**7.8**	**7**	**20**
BPA 4									
	110503	2	172022	173344	8.6	4.5	5.6	87	88
Total		**2**	**172022**	**173344**	**8.6**	**4.5**	**5.6**	**87**	**88**
BPA 5									
	110503	1	151741	151759	1.8		2.8	39	39
	110504	5	90806	162348	27.5	9.3	7.7	71	82
Total		**6**	**90806**	**162348**	**23.3**	**13.4**	**6.9**	**39**	**82**

5.4.4 Sulfur dioxide (SO_2)

Sulfur dioxide was measured most days that the Mobile DOAS system was deployed in Beaumont/Port Arthur. These days were April 29 and May 1–6. A large number of measurements were performed on Area 7 and 8 since the weather often allowed measurements there when they could not be performed elsewhere. Figure 56 shows a measurement transect covering Area 2 while Figure 57 shows a measurement on the west side of Area 7 and 8. Table 32 summarizes the measurements from all the areas from which SO_2 was detected, which were Area 2, 5, 7 and 8. The average emissions from these areas were 282 kg/h, 71 kg/h, 354 kg/h and 904 kg/h respectively with standard deviations of 96 kg/h, 21.4 kg/h, 173 kg/h and 400 kg/h respectively.

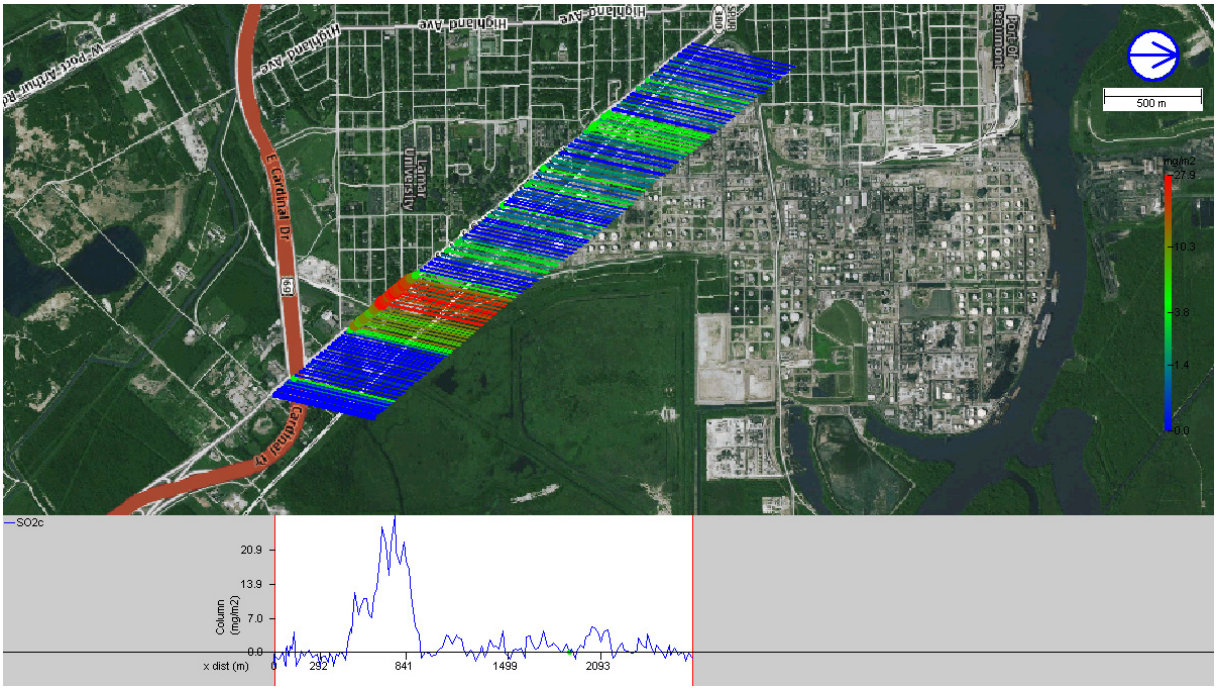

Figure 56 Mobile DOAS measurement of SO_2 from area 2 in Beaumont on May 3, 2011, 16:13–16:18. Each measured spectrum is represented with a point, which color and size indicate the evaluated integrated vertical SO_2 column. The SO_2 column by distance driven through the plume is also shown in the lower part of the figure. A line from each point indicates the direction from which the wind is blowing.

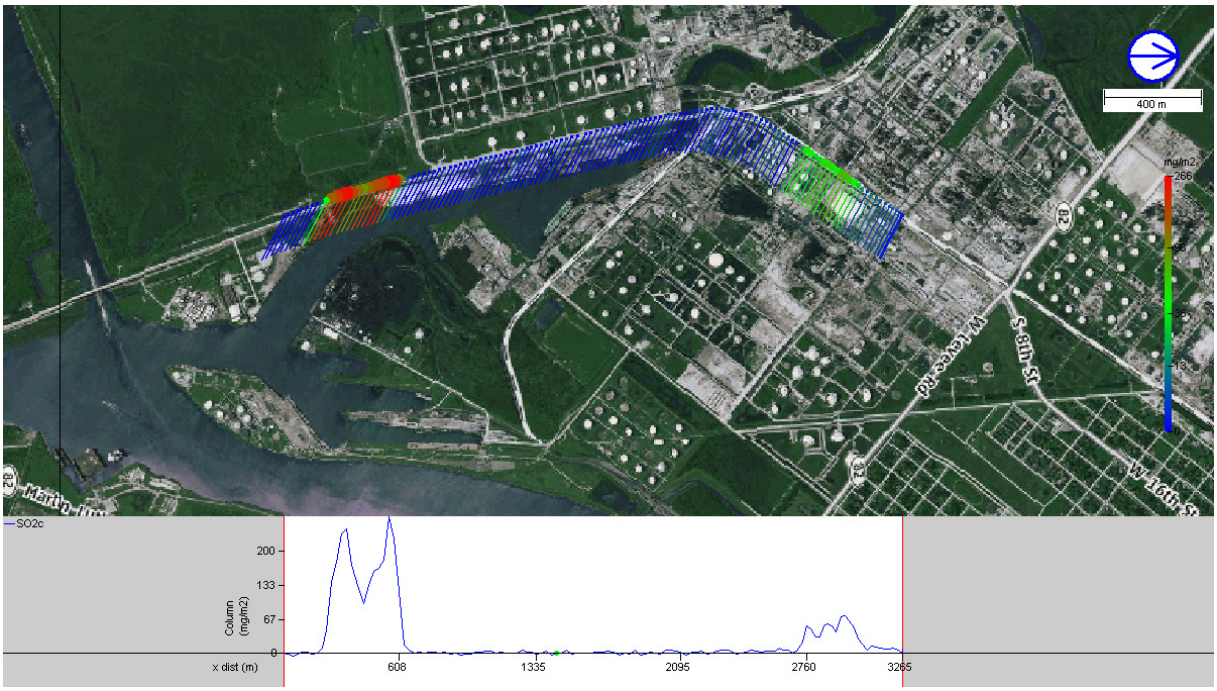

Figure 57 Mobile DOAS measurement of SO_2 from area 7 and 8 in Port Arthur on May 4, 2011, 18:07–18:11. Each measured spectrum is represented with a point, which color and size indicate the evaluated integrated vertical SO_2 column. The SO_2 column by distance driven through the plume is also shown in the lower part of the figure. A line from each point indicates the direction from which the wind is blowing.

Table 33 Summary of SO_2 emission transects in Beaumont/Port Arthur.

Region	Day	N	Start	Stop	Mean (kg/h)	SD (kg/h)	WS (m/s)	Range WD (deg)	
BPA 2									
	110504	1	120626	121450	450.0	-	8.2	79	79
	110505	1	114720	120326	264.9	-	5.2	107	107
	110503	7	133841	171051	260.9	83.2	10.5	8	24
Total		**9**	**114720**	**171051**	**282.4**	**95.7**	**9.7**	**8**	**107**
BPA 5									
	110504	1	171539	171738	93.9	-	5.5	124	124
	110503	2	151756	181001	59.7	11.7	9.6	11	22
Total		**3**	**151756**	**181001**	**71.1**	**21.4**	**8.2**	**11**	**124**
BPA 7									
	110429	2	111750	134238	329.6	158.1	7.8	124	126
	110504	2	180728	183803	449.0	117.2	4.6	105	117
	110506	1	131732	132113	685.8	-	3.2	131	131
	110501	13	124915	183227	317.2	164.5	9.0	140	169
Total		**18**	**111750**	**183803**	**353.7**	**173.3**	**8.1**	**105**	**169**
BPA 8									
	110429	4	112321	133839	1067.1	933.5	7.9	124	125
	110504	4	181040	183501	974.0	67.0	4.7	107	116
	110506	1	132106	132525	703.0	-	3.2	131	131
	110501	12	125019	183106	853.3	216.9	9.1	140	169
	110502	1	144127	144244	786.3	-	6.2	151	151
Total		**22**	**112321**	**183501**	**904.3**	**399.8**	**7.7**	**107**	**169**

5.4.5 Nitrogen dioxide (NO_2)

NO_2 emissions were repeatedly detected from all the major areas in Beaumont / Port Arthur except from Area 3, which is a tank park and would not be expected to emit NO_x. An example measurement is shown in Figure 58, covering area 1, 2, and 5. All NO_2 emission measurements in Beaumont / Port Arthur are summarized in Table 34. The average emissions measured from Area 1, 2, 4, 5, 6, 7 and 8 were 66 kg/h, 360 kg/h, 72 kg/h, 189 kg/h, 419 kg/h, 267 kg/h and 49 kg/h respectively with standard deviation of 20 kg/h, 75 kg/h, 3 kg/h, 56 kg/h, 234 kg/h, 88 kg/h and 18 kg/h respectively.

Table 34 Summary of NO_2 emission transects in Beaumont/Port Arthur.

Region	Day	N	Start	Stop	Mean (kg/h)	SD (kg/h)	WS (m/s)	Range WD (deg)	
BPA 1									
	110504	3	122340	135913	74.8	29.2	5.7	82	97
	110503	4	134233	170540	60.0	9.7	11.0	13	25
Total		**7**	**122340**	**170540**	**66.4**	**19.8**	**8.7**	**13**	**97**
BPA 2									
	110504	3	122713	140408	347.1	35.6	5.7	77	92
	110506	1	180051	180258	311.7		5.6	177	177
	110503	6	133827	170848	374.6	93.1	10.6	13	24
Total		**10**	**122713**	**180258**	**360.1**	**74.5**	**8.6**	**13**	**177**
BPA 4									
	110429	1	100916	101244	68.1		7.2	122	122
	110504	2	171903	173342	73.8	0.8	3.3	109	109
Total		**3**	**100916**	**173342**	**71.9**	**3.4**	**4.6**	**109**	**122**
BPA 5									
	110429	1	94126	95322	236.0		7.6	99	99
	110504	4	90716	161651	140.1	23.0	4.8	68	97
	110503	5	151615	182124	218.7	50.2	6.7	6	28
Total		**10**	**90716**	**182124**	**189.0**	**55.6**	**6.0**	**6**	**99**
BPA 6									
	110429	2	110441	135319	298.8	33.7	8.3	127	127
	110504	3	100323	180627	307.0	85.7	5.4	74	109
	110505	1	133421	133817	907.9		5.9	149	149
	110506	1	135156	140400	504.7		3.2	131	131
Total		**7**	**100323**	**180627**	**418.8**	**234.1**	**6.0**	**74**	**149**
BPA 7									
	110429	1	174554	175411	365.0		7.5	143	143
	110506	1	95707	100329	203.7		3.5	209	209
	110501	3	153907	173533	256.1	92.2	12.6	152	154
Total		**5**	**95707**	**175411**	**267.4**	**88.0**	**9.8**	**143**	**209**
BPA 8									
	110429	4	112052	133814	57.8	28.3	8.3	127	127
	110504	4	181024	183515	40.4	5.0	3.3	109	109
	110506	2	122842	132748	70.2	18.0	3.7	131	133
	110501	8	144916	182218	42.8	11.2	10.6	148	163
Total		**18**	**112052**	**183515**	**48.6**	**18.0**	**7.7**	**109**	**163**

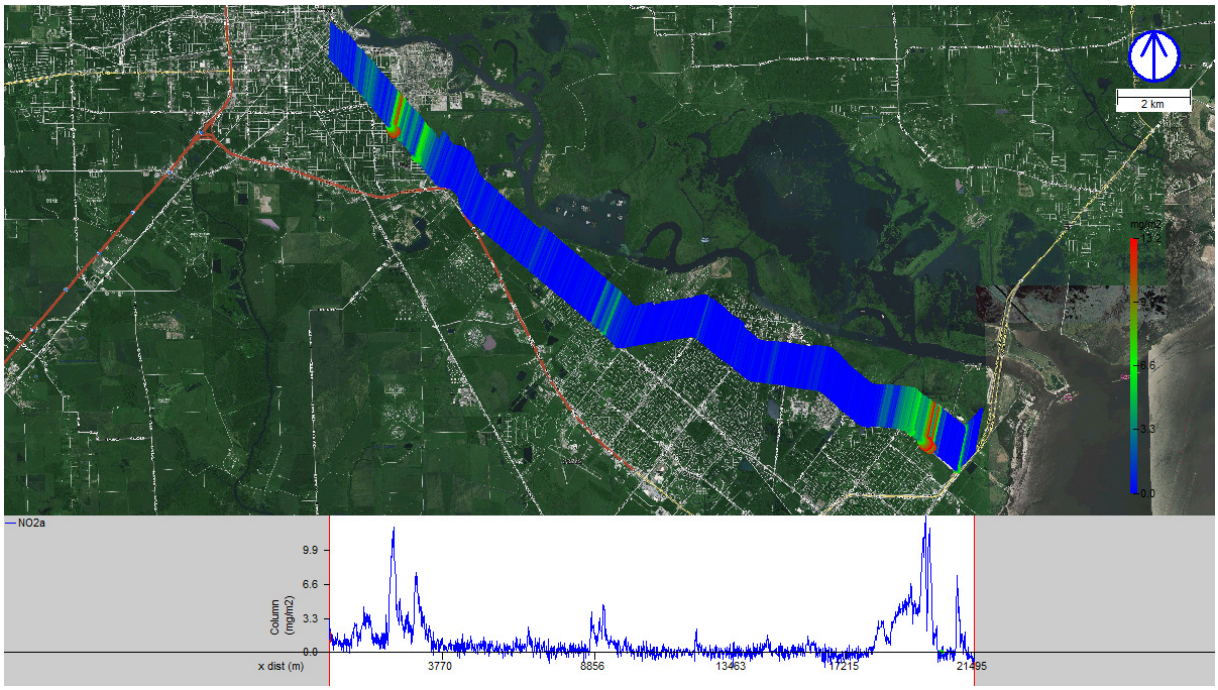

Figure 58 Mobile DOAS measurement of NO_2 covering area 1, 2 and 5 in Beaumont/Port Arthur on May 3, 2011, 15:16–15:50. Each measured spectrum is represented with a point, which color and size indicate the evaluated integrated vertical NO_2 column. The NO_2 column by distance driven through the plume is also shown in the lower part of the figure. A line from each point indicates the direction from which the wind is blowing.

5.5 Longview

The emissions of alkanes, ethene, propene and NO_2 from Longview were measured on the 7 May 2011. The measurements were done with clear sunny skies and a distinct southerly wind. Winds were measured by three radio sondes, with complimentary measurements aboard the vehicle and with information from the nearby airport.

5.5.1 Alkanes

Four plume transects averaged to an alkane emission of 841 kg/h for the Longview plant, with a standard deviation of 122 kg/h, see Table 35. One of the measurements is shown in Figure 59.

Table 35 Summary of alkane emission transects in Longview.

Region	Day	N	Start	Stop	Mean (kg/h)	SD (kg/h)	WS (m/s)	Range WD (deg)	
Longview									
	110507	4	165325	173702	841	122	8.3	183	196
Total		**4**	**165325**	**173702**	**841**	**122**	**8.3**	**183**	**196**

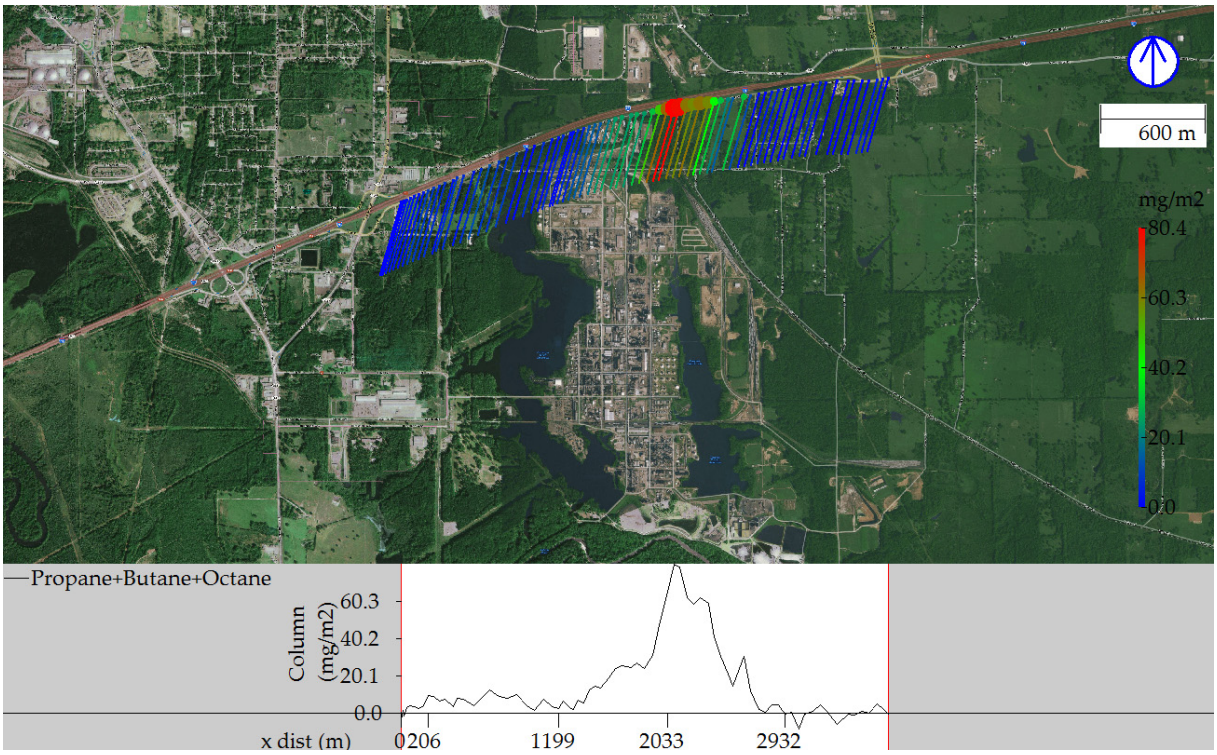

Figure 59 SOF measurement of the alkane emission from the Longview plant on the 7 May 2011, 16:53. Each measured spectrum is represented with a point, which color and size indicate the evaluated integrated vertical alkane column. The VOC column by distance driven through the plume is also shown in the lower part of the figure. A line from each point indicates the direction from which the wind is blowing.

5.5.2 Alkenes

Nine plume transects averaged to an ethene emission of 452 kg/h for the Longview plant, with a standard deviation of 191 kg/h, see Table 36. One of the measurements is shown in Figure 60. One emission transect really stood out, probably due to an upset. Leaving this one out would result in an average emission of 384±82 kg/h ethene.

Table 37 summarizes the propene measurements, showing an average emission of 282±59 kg/h, based on eight measurements. Figure 61 shows a propene measurement in Longview.

Table 36 Summary of ethene emission transects in Longview.

Region	Day	N	Start	Stop	Mean (kg/h)	SD (kg/h)	WS (m/s)	Range WD (deg)	
Longview	110507	9	150024	184834	452	191	8.3	183	196
Total		**9**	**150024**	**184834**	**452**	**191**	**8.3**	**183**	**196**

Table 37 Summary of propene emission transects in Longview.

Region	Day	N	Start	Stop	Mean (kg/h)	SD (kg/h)	WS (m/s)	Range WD (deg)	
Longview	110507	8	150024	184116	282	59	8.3	183	196
Total		**8**	**150024**	**184116**	**282**	**59**	**8.3**	**183**	**196**

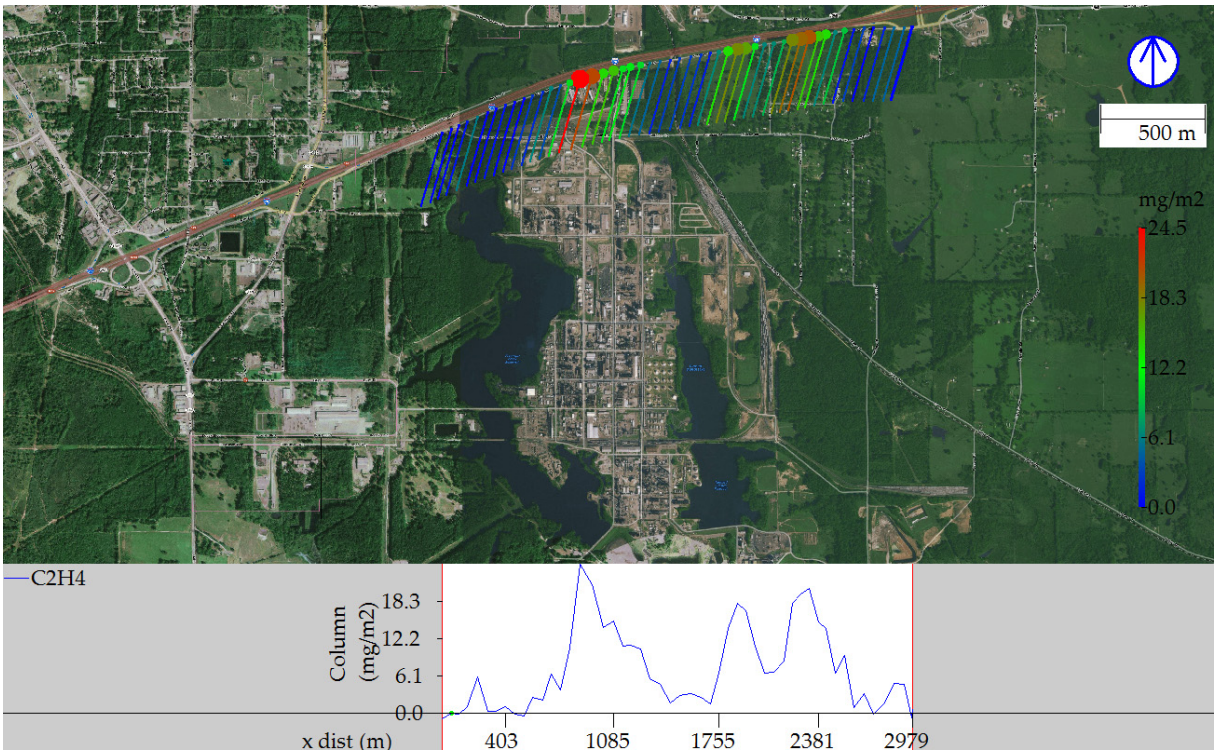

Figure 60 SOF measurement of the ethene emission from the Longview plant on the 7 May 2011, 15:12. Each measured spectrum is represented with a point, which color and size indicate the evaluated integrated vertical ethene column. The ethene column by distance driven through the plume is also shown in the lower part of the figure. A line from each point indicates the direction from which the wind is blowing.

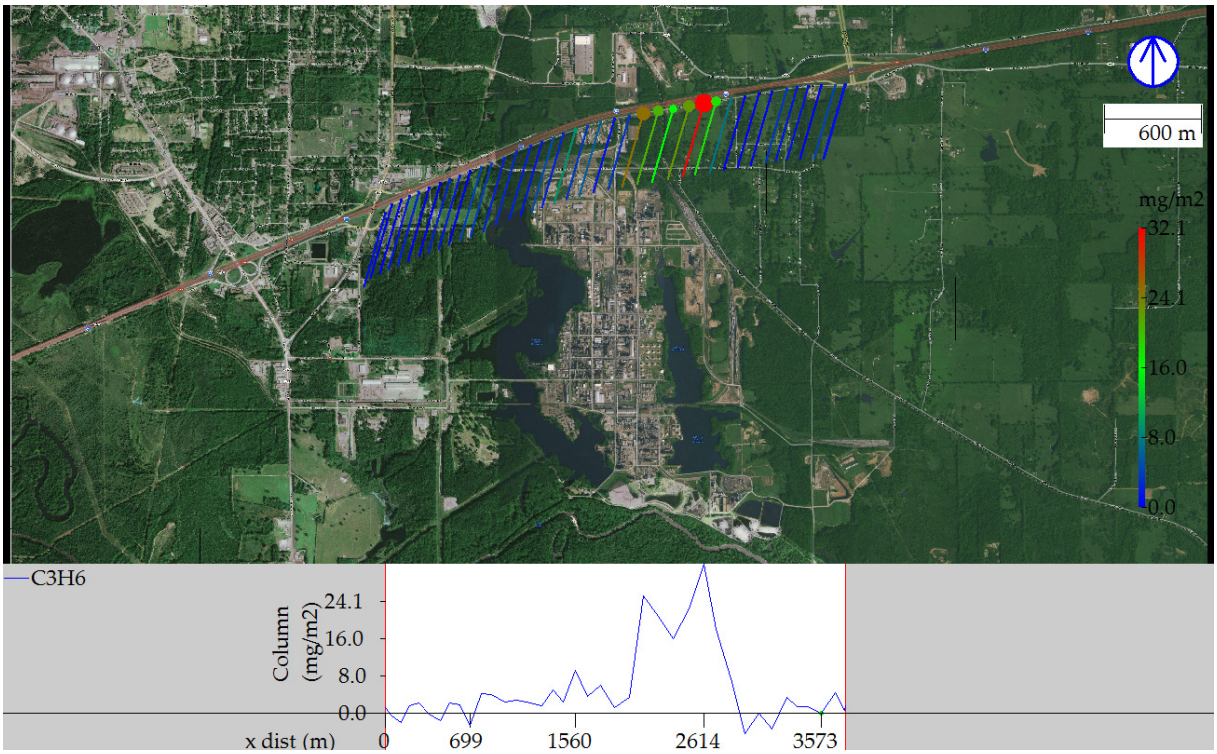

Figure 61 SOF measurement of the propene emission from the Longview plant on the 7 May 2011, 15:36. Each measured spectrum is represented with a point, which color and size indicate the evaluated integrated vertical propene column. The propene column by distance driven through the plume is also shown in the lower part of the figure. A line from each point indicates the direction from which the wind is blowing.

5.5.3 Formaldehyde (HCHO)

Small amounts of formaldehyde from the Longview plant were detected in the four Mobile DOAS transects performed, but the baseline was too uncertain to make a reliable quantification.

5.5.4 Sulfur dioxide (SO_2)

No SO_2 was detected in Longview.

5.5.5 Nitrogen dioxide (NO_2)

Four Mobile DOAS transects were made simultaneously with the SOF measurements. They showed and average NO_2 emission of 176 kg/h with a standard deviation of 51 kg/h. An example measurement is shown in Figure 62 and the measurements are summarized in Table 38.

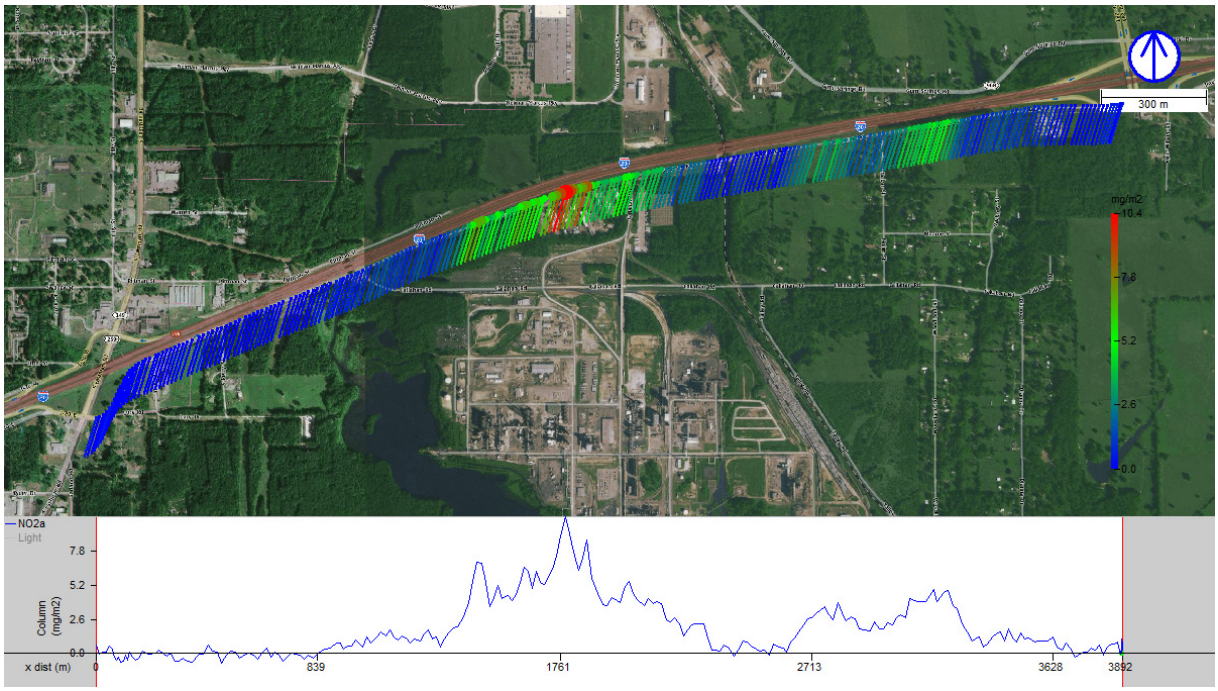

Figure 62 Mobile DOAS measurement of the NO_2 emission from the Longview plant on the 7 May 2011, 15:12. Each measured spectrum is represented with a point, which color and size indicate the evaluated integrated vertical NO_2 column. The NO_2 column by distance driven through the plume is also shown in the lower part of the figure. A line from each point indicates the direction from which the wind is blowing.

Table 38 Summary of NO_2 emission transects in Longview.

Region	Day	N	Start	Stop	Mean (kg/h)	SD (kg/h)	WS (m/s)	Range WD (deg)	
Longview									
	110507	4	144958	154901	175.8	50.5	8.3	196	196
Total		**4**	**144958**	**154901**	**175.8**	**50.5**	**8.3**	**196**	**196**

5.6 Thermal FTIR measurements

During the period 21–26 April 2011 the SOF spectrometer was mounted on a tripod and equipped with a telescope to conduct passive thermal emission measurements. Twenty-four different objects, mostly flares but also a few stack and pipe exhausts, were surveyed around the HSC, Baytown, Mont Belvieu and Texas City areas. The aim of the survey was to pin-point emission sources of ethene and propene in areas where SOF measurements have identified evident emissions of those compounds. The presented results are based on observing the spectral emission signatures in the various exhaust plumes, subtracted by the corresponding upwind thermal backgrounds, see Figure 63. Survey object locations are given in Figure 64 through Figure 67, with more detailed information in Table 39.

Figure 63 Thermal emission measurements of a flare exhaust plume. The down-wind flare emission signal is subtracted with the up-wind flare thermal background signal. The aiming cross is approximately the centre of the viewing infrared emission telescope.

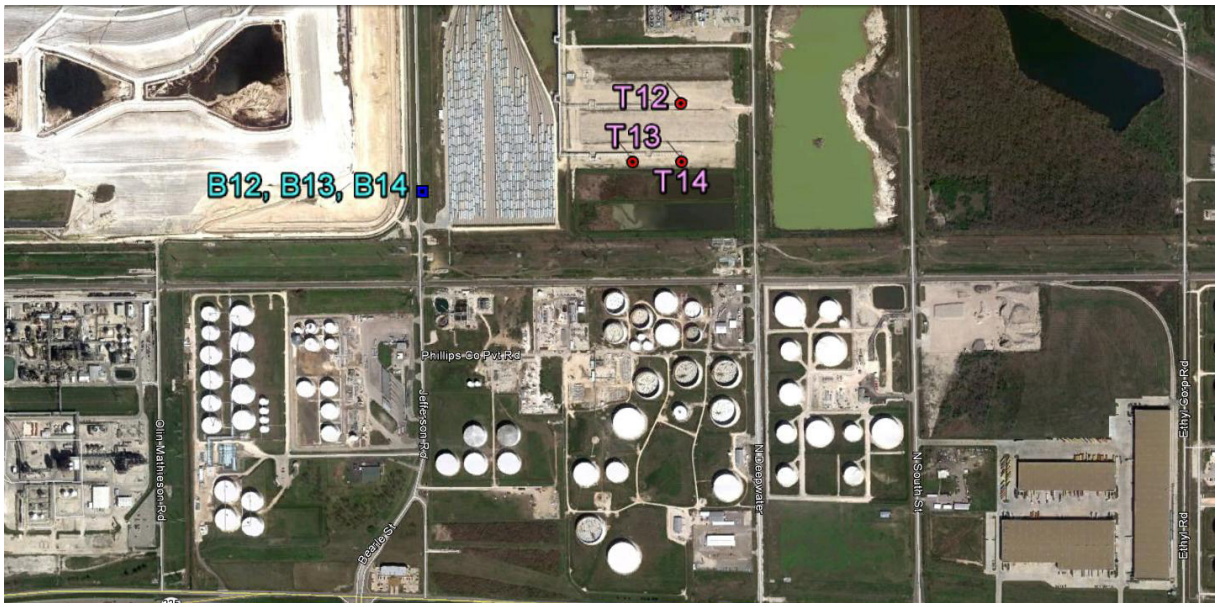

Figure 64 Thermal emission measurement objects around Jefferson Rd in HSC, just north of highway 225. The blue square (B12, 13, 14) indicates the base position of the infrared telescope, whereas red circles (T12, 13, 14) correspond to three different flares. See Table 39 for more detailed information. Note how the flare shadows emerge out of the red circles.

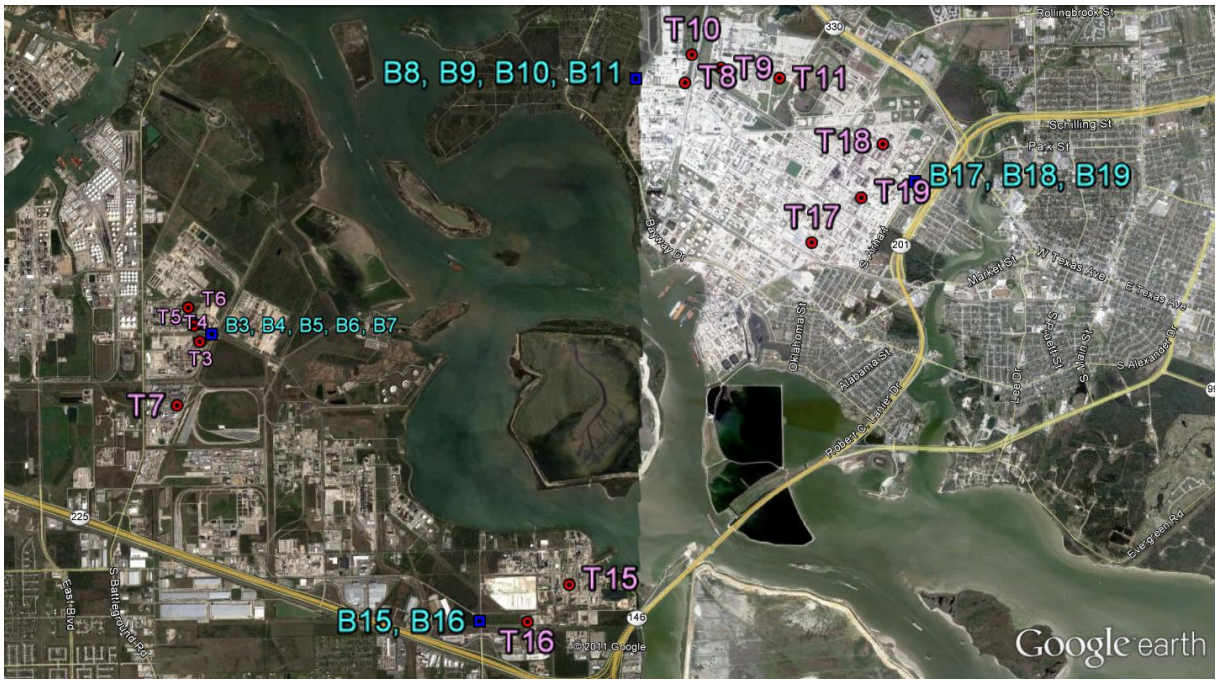

Figure 65 Thermal emission measurement objects around Battleground Rd / Miller Cut Off Rd in HSC (left), Strange Rd (down mid) and Baytown (up right). The blue squares indicate the base positions (B) of the infrared telescope, whereas red circles (T) indicate the corresponding thermal emission survey objects. See Table 39 for more detailed information.

Figure 66 Thermal emission measurement objects around Mont Belvieu (north part). The blue squares indicate the base positions (B) of the infrared telescope, whereas red circles (T) indicate the corresponding thermal emission survey objects. See Table 39 for more detailed information.

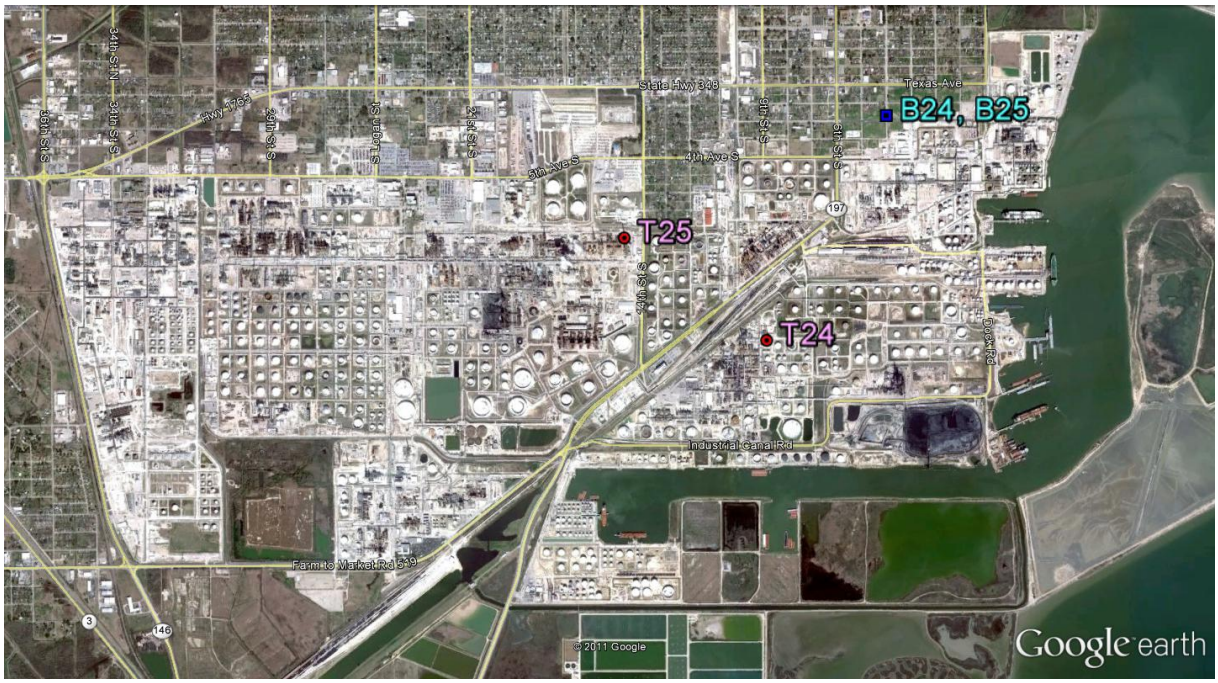

Figure 67 Thermal emission measurement objects around Texas City. The blue squares indicate the base positions (B) of the infrared telescope, whereas red circles (T) indicate the corresponding thermal emission survey objects. See Table 39 for more detailed information. Due to geographical security restrictions following a major power outage in the area, measurements had to be done from long range here.

Detailed information for the surveyed objects is given in Table 39. The so called view base position indicates the position of the thermal FTIR spectrometer, whereas object position corresponds to the position of the surveyed object. In practice the viewing telescope was directed somewhat off these positions, up-wind for the background measurements and down-wind for the exhaust plume measurements. The observed thermal emission signals are binned into three groups: **Distinct** (strong emission fingerprint), ***Weak*** (evident to barely detectable emission fingerprint) and **ND** (compound not detectable in the observed emission signal). Four objects showed distinct ethene emission (for one of them this distinct ethene emission was detected on two separate days, T1 and T20), and two flares showed distinct propene emission. Six other ethene sources and three propene sources were found showing weaker emission signatures.

The scope of this survey was to identify any presence of ethene and propene at flare stacks and pipe exhausts in areas identified by SOF measurements to have substantial alkene emissions. In order to obtain quantitative information from these measurements, a deeper analysis is required, attributing plume temperature (from the relative emission strengths of different emission lines) and including black body radiance calibration. Such calibrations were obtained during the measurements, but the quantitative analysis work is not within the scope of this report.

Figure 68 through Figure 71 show examples of ethene and propene thermal emission signatures detected along with more detailed location maps and visual views of the various objects.

Table 39 Objects in the HSC, Baytown, Mont Belvieu and Texas City area surveyed by passive thermal emission FTIR during April 2011. Object ID's are given in various maps in this chapter. Observed thermal emission signatures for ethene (C_2H_4) and propene (C_3H_6) are binned into **Distinct** (strong emission fingerprint), ***Weak*** (evident to barely detectable emission fingerprint) and ND (compound not detectable in the observed emission signal).

Object ID	Date	Time	View base pos LAT	View base pos LON	Object pos LAT	Object pos LON	Range (m)	Dir	Therm. signal C_2H_4	Therm. signal C_3H_6
T1 [a]	21-apr	15:41	29.871377	-94.919947	29.871331	-94.914900	488	90	**Distinct**	ND
T2 [a]	21-apr	16:36	29.871377	-94.919947	29.877307	-94.911872	1018	50	ND	ND
T3 [a]	22-apr	13:11	29.726250	-95.081000	29.725413	-95.082468	167	237	**Distinct**	**Distinct**
T4 [a]	22-apr	13:34	29.726250	-95.081000	29.727288	-95.082998	225	300	ND	ND
T5 [a]	22-apr	13:52	29.726250	-95.081000	29.727172	-95.083271	243	295	ND	ND
T6 [b]	22-apr	13:45	29.726250	-95.081000	29.729145	-95.083936	430	319	ND	ND
T7 [a]	22-apr	13:59	29.726250	-95.081000	29.718439	-95.085339	964	206	ND	ND
T8 [a]	23-apr	19:24	29.754220	-95.027469	29.753764	-95.021263	601	95	**Distinct**	**Distinct**
T9 [a]	23-apr	19:44	29.754220	-95.027469	29.755413	-95.016717	1046	83	ND	ND
T10 [a]	23-apr	19:51	29.754220	-95.027469	29.756839	-95.020400	742	67	ND	ND
T11 [a]	23-apr	19:57	29.754220	-95.027469	29.754285	-95.009321	1753	90	***Weak***	***Weak***
T12 [a]	24-apr	14:31	29.721128	-95.182696	29.722861	-95.176860	596	71	***Weak***	***Weak***
T13 [a]	24-apr	13:51	29.721128	-95.182696	29.721711	-95.177947	463	82	ND	ND
T14 [a]	24-apr	14:13	29.721128	-95.182696	29.721716	-95.176841	570	83	**Distinct**	ND
T15 [a]	24-apr	16:48	29.694829	-95.047188	29.698802	-95.035868	1179	68	ND	***Weak***
T16 [b]	24-apr	17:02	29.694829	-95.047188	29.694742	-95.041142	585	91	ND	ND
T17 [a]	24-apr	18:07	29.742950	-94.992240	29.736263	-95.005280	1462	239	***Weak***	ND
T18 [b]	24-apr	18:27	29.742950	-94.992240	29.747046	-94.996288	602	319	ND	ND
T19 [b]	24-apr	18:42	29.742950	-94.992240	29.741179	-94.999022	677	253	ND	ND
T20 [a]	25-apr	18:43	29.868540	-94.919262	29.871331	-94.914900	521	54	**Distinct**	ND
T21 [a]	25-apr	19:03	29.868540	-94.919262	29.863359	-94.909127	1133	120	ND	ND
T22 [ac]	25-apr	19:22	29.868540	-94.919262	29.864032	-94.913359	750	131	ND	ND
T23 [a]	25-apr	19:30	29.868540	-94.919262	29.859596	-94.910674	1292	140	***Weak***	ND
T24 [acd]	26-apr	12:30	29.382448	-94.899468	29.370472	-94.906802	1513	208	***Weak***	ND
T25 [acd]	26-apr	13:18	29.382448	-94.899468	29.375938	-94.915513	1724	244	***Weak***	ND

[a] Flare exhaust
[b] Stack/Pipe exhaust(s)
[c] Approximate object location
[d] Long view range due to geographical restrictions, possibly other sources contributing

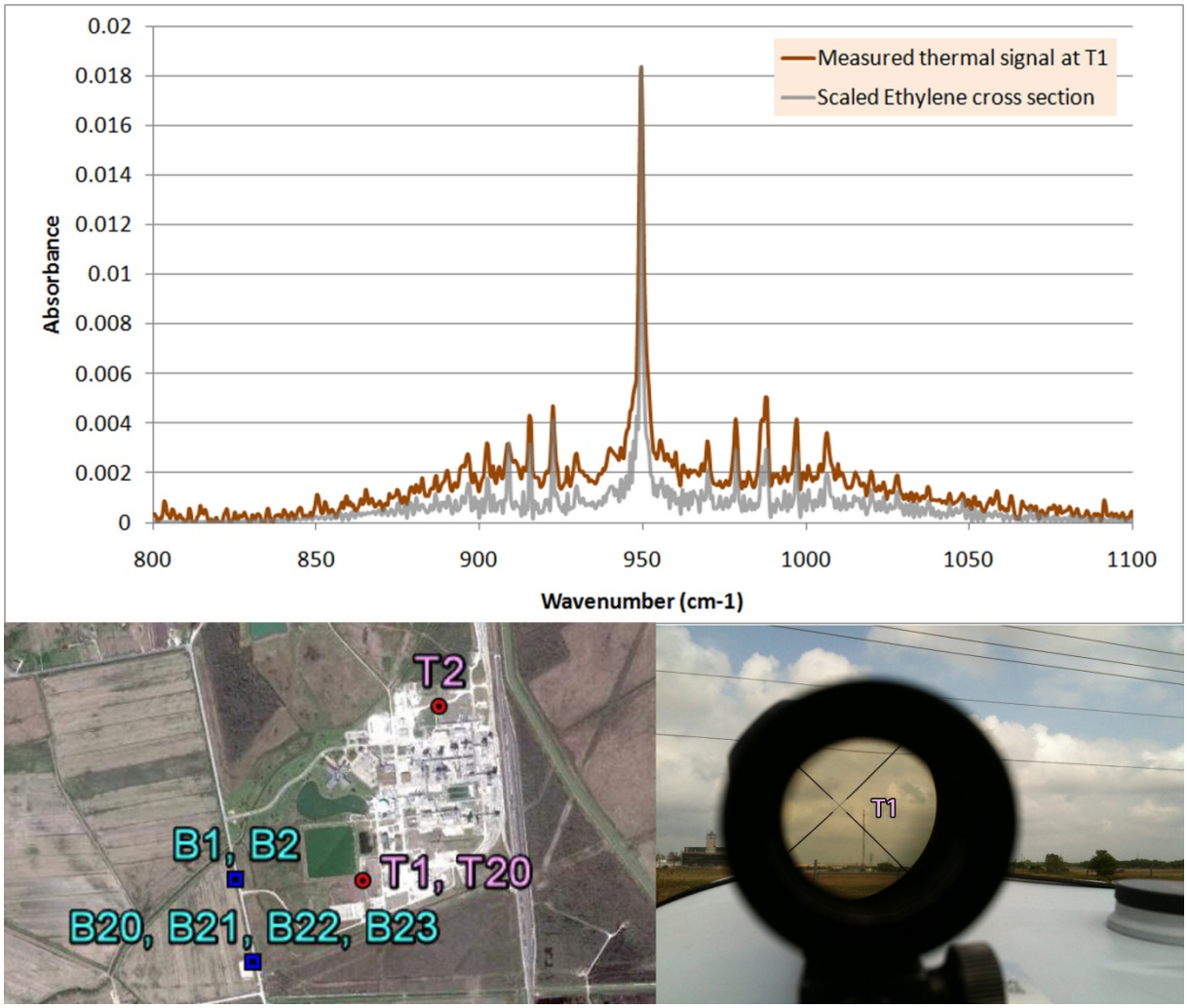

Figure 68 Thermal emission signal acquired at flare T1 in the Mont Belvieu area. The blue squares indicate the base positions (B) of the infrared telescope, whereas red circles (T) indicate the corresponding thermal emission survey objects. See Table 39 for more detailed information. A distinct ethene signature was observed in the exhaust plume, as seen in the upper part of the figure showing the measured thermal emission signal along with the ethene cross section fingerprint. (Wavenumber 1000 cm^{-1} corresponds to wavelength 10 µm). The aiming scope view (mounted on top of the FTIR) is seen down right.

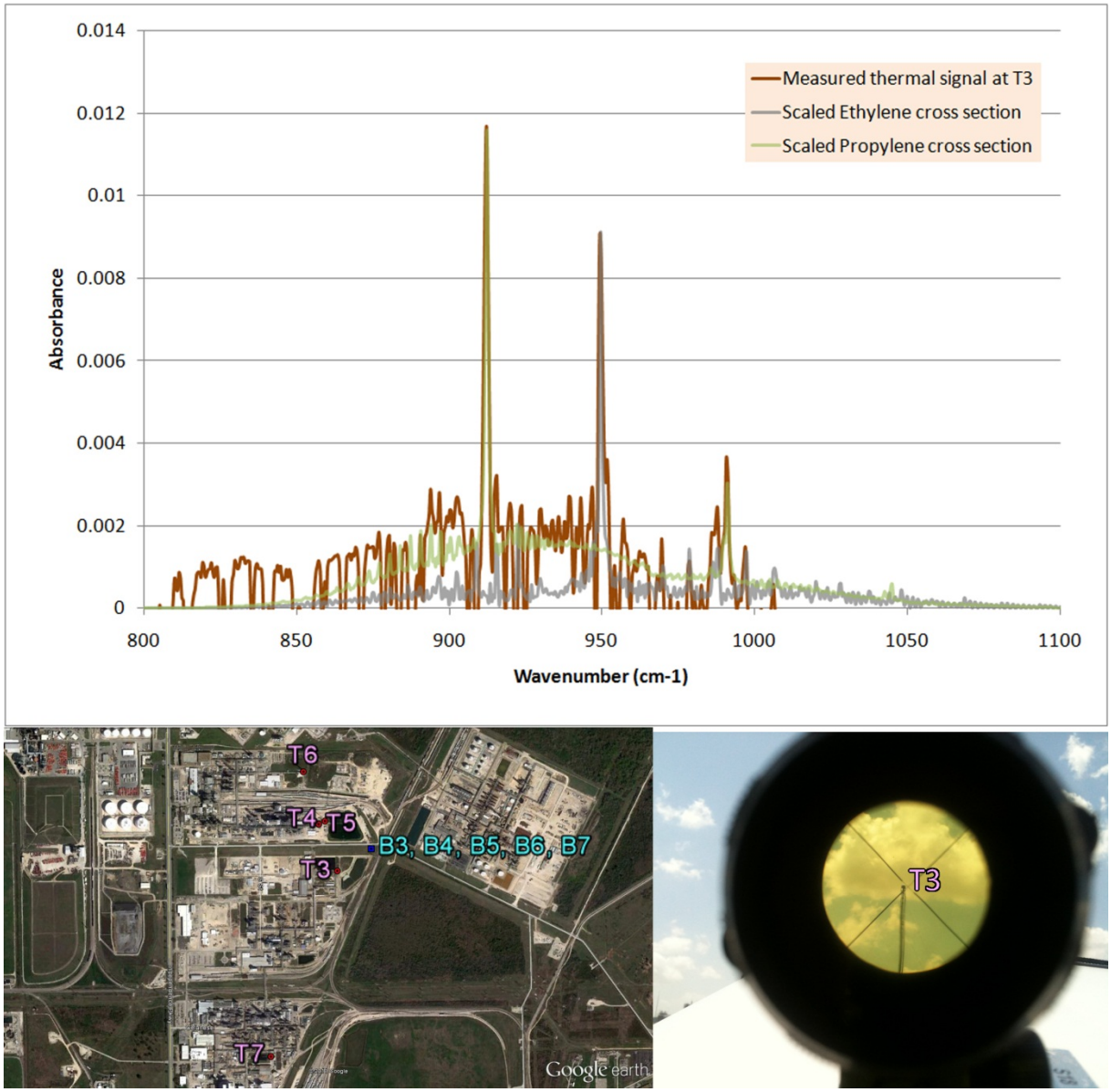

Figure 69 Thermal emission signal acquired at flare T3 around Miller Cut Off Rd in the Battleground area (HSC). The blue squares indicate the base positions (B) of the infrared telescope, whereas red circles (T) indicate the corresponding thermal emission survey objects. See Table 39 for more detailed information. Distinct ethene and propene signatures were observed in the exhaust plume, as seen in the upper part of the figure showing the measured thermal emission signal along with the ethene and propene cross section fingerprints. (Wavenumber 1000 cm^{-1} corresponds to wavelength 10 µm). The aiming scope view (mounted on top of the FTIR) is seen down right.

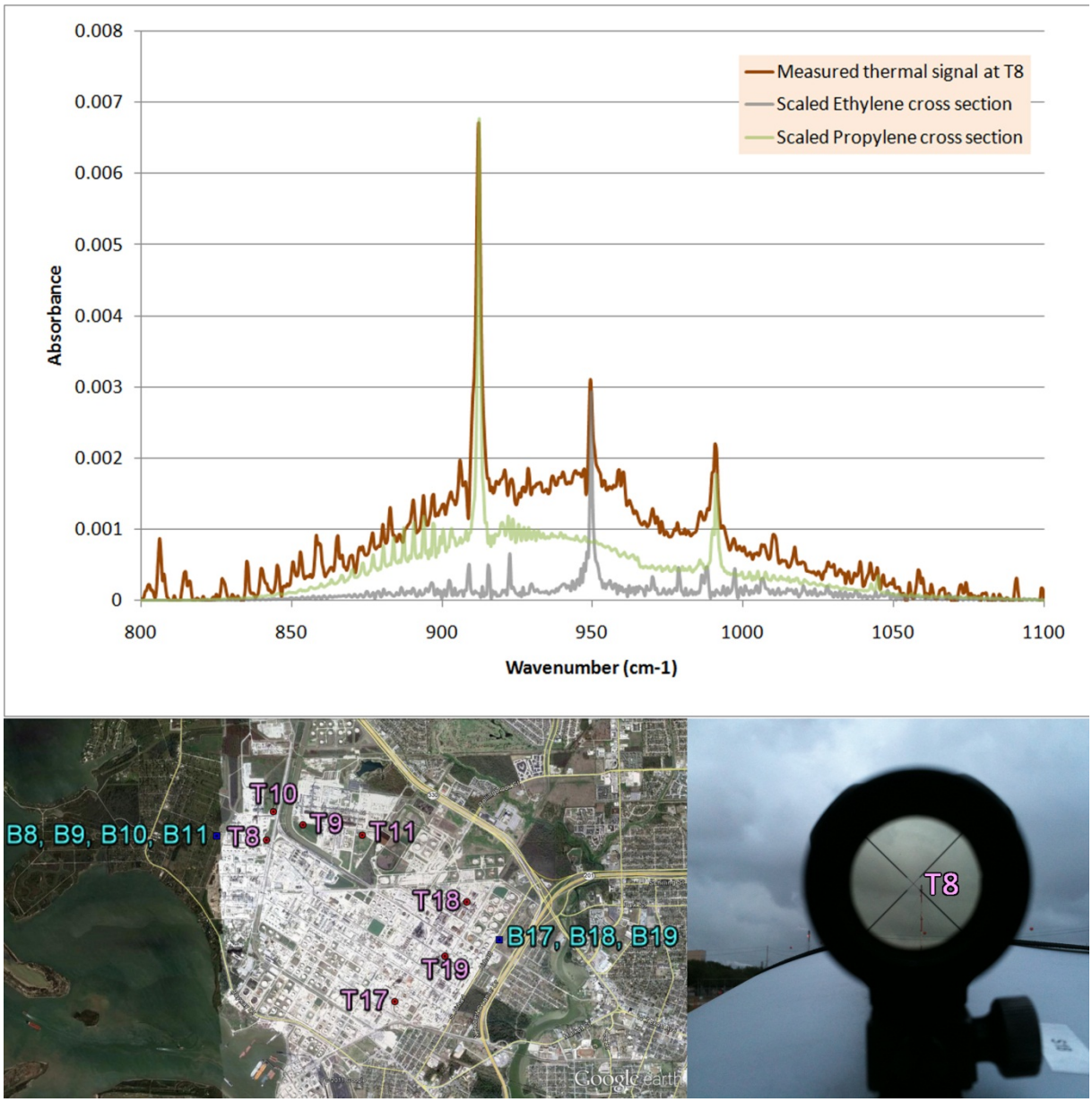

Figure 70 Thermal emission signal acquired at flare T8 in the Baytown area (HSC). The blue squares indicate the base positions (B) of the infrared telescope, whereas red circles (T) indicate the corresponding thermal emission survey objects. See Table 39 for more detailed information. Distinct ethene and propene signatures were observed in the exhaust plume, as seen in the upper part of the figure showing the measured thermal emission signal along with the ethene and propene cross section fingerprints. (Wavenumber 1000 cm^{-1} corresponds to wavelength 10 µm). The aiming scope view (mounted on top of the FTIR) is seen down right.

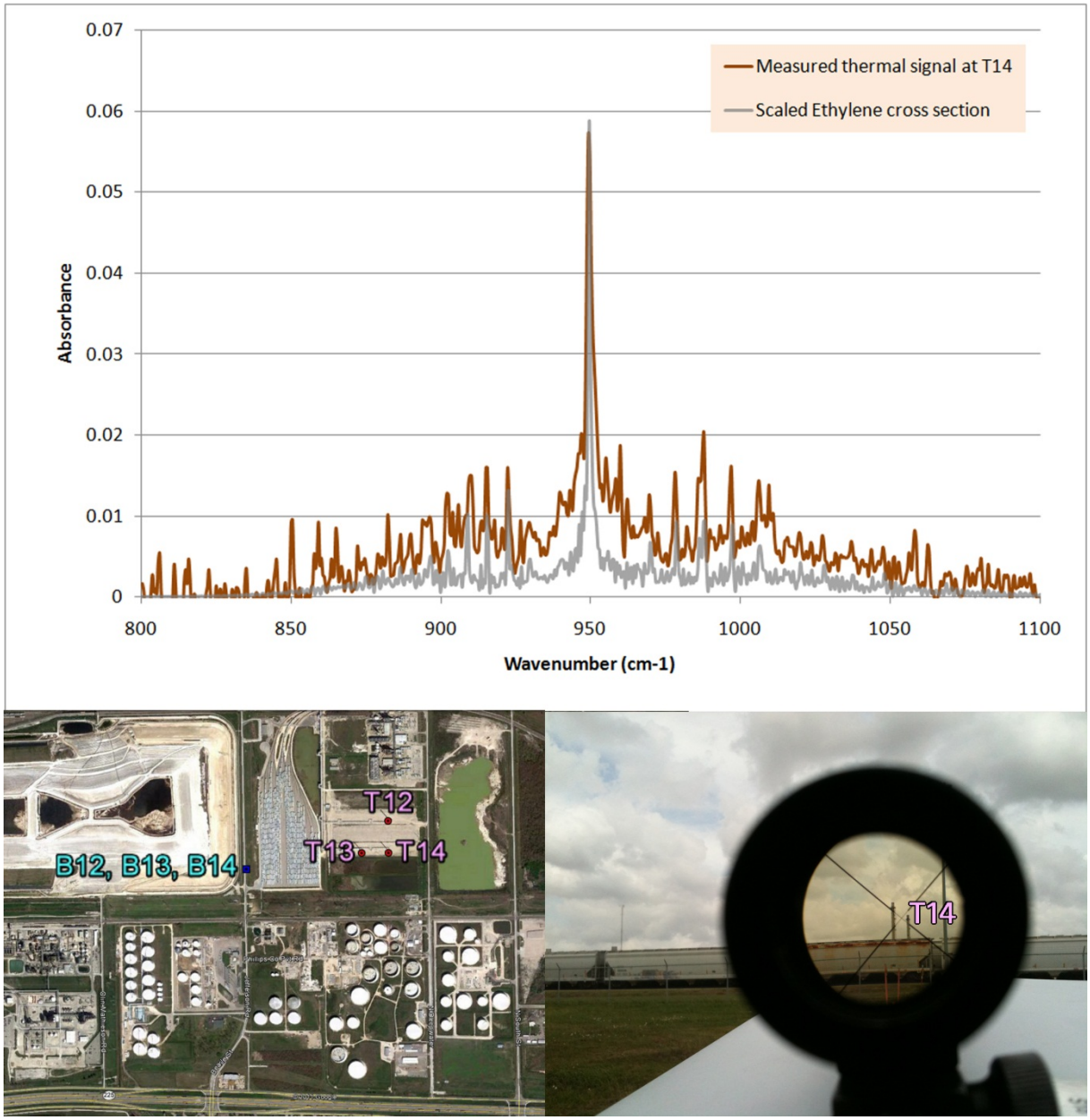

Figure 71 Thermal emission signal acquired at flare T14 located at Jefferson Rd in the HSC area. The blue squares indicate the base positions (B) of the infrared telescope, whereas red circles (T) indicate the corresponding thermal emission survey objects. See Table 39 for more detailed information. A distinct ethene signature was observed in the exhaust plume, as seen in the upper part of the figure showing the measured thermal emission signal along with the ethene cross section fingerprint. (Wavenumber 1000 cm^{-1} corresponds to wavelength 10 μm). The aiming scope view (mounted on top of the FTIR) is seen down right.

5.5. Canister measurements SE Texas

The figures and tables below show canister samples taken downwind of various petrochemical and refinery complexes in SE Texas. The sample locations corresponded to hotspot locations identified by the MeFTIR measurements until May 18 and later on from locations identified by the SOF measurements. It can be seen in the tables that the most abundant species here are alkanes, which would be expected since this is refinery areas.

Figure 72 Location of canister samplings in the vicinity of Port Arthur.

Table 40 The 10 most abundant NMHCs in upwind and downwind areas of the Pt Arthur. (May 17 2011).

10 most abundant NMHCs[1] (at downwind site)	Downwind (can#32)[2] (20:40–20:41 CDT)	Upwind (can#69,23)[3] (21:41–21:43 CDT)	Difference (downwind - upwind)
n-butane	3.16	0.11 (±0.02)	+3.05
n-pentane	2.16	0.05 (±0.01)	+2.11
i-pentane	1.96	0.06 (±0.02)	+1.90
propane	1.43	0.30 (±0.06)	+1.13
i-butane	1.29	0.09 (±0.00)	+1.20
ethane	0.96	1.83 (±0.23)	-0.87
n-hexane	0.96	0.01 (±0.00)	+0.95
2-me-pentane	0.52	ND	≥ +0.42
n-heptane	0.49	ND	≥ +0.49
3-me-pentane	0.44	ND	≥ +0.44

[1] in [ppbv]
[2] valid data of one can available
[3] average of duplicates; in brackets half difference between duplicates

Table 41 The 10 most abundant NMHCs in upwind and downwind areas of the Pt Arthur. (May 17 2011).

10 most abundant NMHCs[1] (at downwind site)	Downwind (can#74)[2] (21:10–21:14 CDT)	Upwind (can#69,23)[3] (21:41–21:43 CDT)	Difference (downwind - upwind)
i-pentane	11.36	0.06 (±0.02)	+11.30
ethane	7.63	1.83 (±0.23)	+5.80
n-butane	6.48	0.11 (±0.02)	+6.37
n-pentane	4.67	0.05 (±0.01)	+4.62
i-butane	3.97	0.09 (±0.00)	+3.88
propane	2.11	0.30 (±0.06)	+1.81
3-me-pentane	2.10	ND	≥ +2.00
2-me-pentane	1.76	ND	≥ +1.66
t-2-butene	1.64	0.04 (±0.02)	+1.60
ethene	1.28	0.37 (±0.14)	+0.91

[1] in [ppbv]
[2] valid data of one can available
[3] average of duplicates; in brackets half difference between duplicates

Table 42 The 10 most abundant NMHCs in upwind and downwind areas of the Pt Arthur. (May 17 2011).

10 most abundant NMHCs[1] (at downwind site)	Downwind (can#68,58)[2] (22:53–22:54 CDT)	Upwind (can#69,23)[2] (21:41–21:43 CDT)	Difference (downwind - upwind)
Ethane	45.16 (±0.34)	1.83 (±0.23)	+43.33
cyc-hexane	6.38 (±0.06)	ND	≥ +6.28
Propene	3.13 (±0.05)	0.12 (±0.02)	+3.01
Propane	2.26 (±0.01)	0.30 (±0.06)	+1.96
Ethene	2.43 (±0.39)	0.37 (±0.14)	+2.06
i-butane	1.38 (±0.03)	0.09 (±0.00)	+1.29
n-butane	0.84 (±0.02)	0.11 (±0.02)	+0.73
Acetylene	0.54 (±0.02)	0.08 (±0.00)	+0.46
Benzene	0.55 (±0.01)	0.02 (±0.00)	+0.53
i-pentane	0.49 (±0.03)	0.06 (±0.02)	+0.43

[1] in [ppbv]
[2] average of duplicates; in brackets half difference between duplicates

Table 43 The 10 most abundant NMHCs in upwind and downwind areas of the Pt Arthur. (May 17 2011).

10 most abundant NMHCs[1] (at downwind site)	Downwind (can#10,57)[2] (23:42–23:44 CDT)	Upwind (can#69,23)[2] (21:41–21:43 CDT)	Difference (downwind - upwind)
n-butane	4.59 (±0.04)	0.11 (±0.02)	+4.48
Ethane	4.53 (±0.04)	1.83 (±0.23)	+2.70
n-pentane	4.46 (±0.15)	0.05 (±0.01)	+4.41
i-pentane	4.37 (±0.22)	0.06 (±0.02)	+4.31
Propane	3.89 (±0.22)	0.03 (±0.06)	+3.86
Propene	1.80 (±0.14)	0.12 (±0.02)	+1.68
n-hexane	1.79 (±0.01)	0.01 (±0.00)	+1.78
i-butane	1.19 (±0.01)	0.09 (±0.00)	+1.10
1-butene	1.02 (±0.08)	0.08 (±0.00)	+0.94
3-me-pentane	0.93 (±0.07)	ND	≥ +0.83

[1] in [ppbv]
[2] average of duplicates; in brackets half difference between duplicates

Table 44 The 10 most abundant NMHCs in upwind and downwind areas of the Pt Arthur. (May 18 2011).

10 most abundant NMHCs[1] (at downwind site)	Downwind (can#27,56)[2] (00:21–00:22 CDT)	Upwind (can#69,23)[2] (21:41–21:43 CDT)	Difference (downwind - upwind)
Ethane	9.44 (±0.47)	1.83 (±0.23)	+7.61
Ethene	7.08 (±0.70)	0.37 (±0.14)	+6.71
n-butane	5.06 (±0.08)	0.11 (±0.02)	+4.95
Propane	4.87 (±0.20)	0.30 (±0.06)	+4.57
Propene	3.35 (±0.25)	0.12 (±0.02)	+3.23
n-pentane	2.03 (±0.01)	0.05 (±0.01)	+1.98
i-pentane	1.77 (±0.02)	0.06 (±0.02)	+1.71
cyc-hexane	1.55 (±0.01)	ND	≥ +1.54
i-butane	1.38 (±0.04)	0.09 (±0.01)	+1.29
n-hexane	0.68 (±0.03)	0.01 (±0.00)	+0.67

[1] in [ppbv]
[2] average of duplicates; in brackets half difference between duplicates

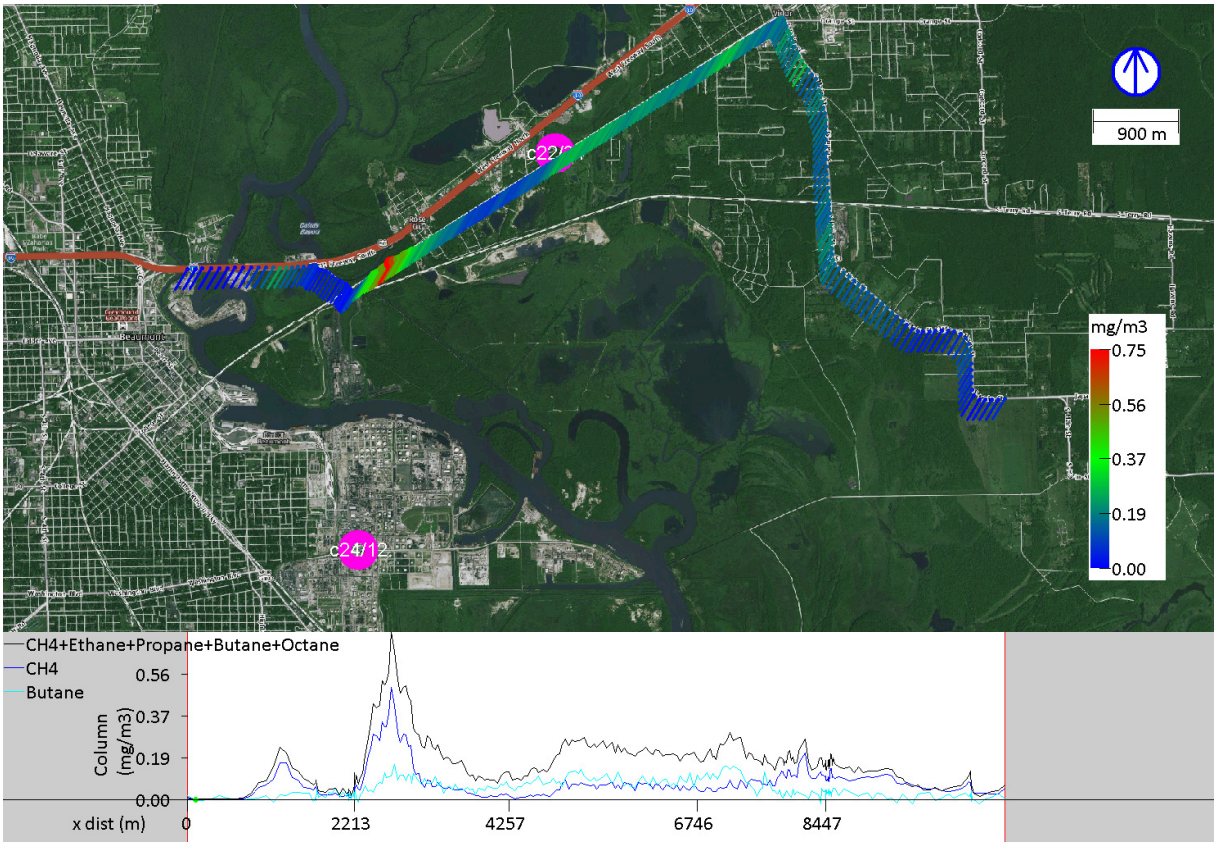

Figure 73 Location of canister samplings in the vicinity of the Beaumont industrial complex, area 2 in Figure 47. In addition a MeFTIR measurement downwind of the facility, carried out between 2 to 3 am is shown.

Table 45 The 10 most abundant NMHCs downwind areas of the Beaumont industrial complex at two distances (May 18 2011).

10 most abundant NMHCs[1] (at downwind site)	Inside Beaumont source (can#12)[2] (01:38–01:40 CDT)	Downwind (can#22,34)[3] (03:07-03:09 CDT)
i-butane	65.08	5.45 (±0.20)
ethane	45.48	10.67 (±0.10)
propane	27.72	8.88 (±0.22)
n-butane	15.17	4.48 (±0.10)
i-butene	12.26	0.81 (±0.10)
c-2-butene	8.81	0.01 (±0.00)
t-2-butene	8.40	0.05 (±0.02)
1-butene	6.97	0.09 (±0.00)
propene	5.01	0.52 (±0.08)
i-pentane	4.35	7.12 ((±0.01)

[1] in [ppbv]
[2] valid data of one can available
[3] average of duplicates; in brackets half difference between duplicates

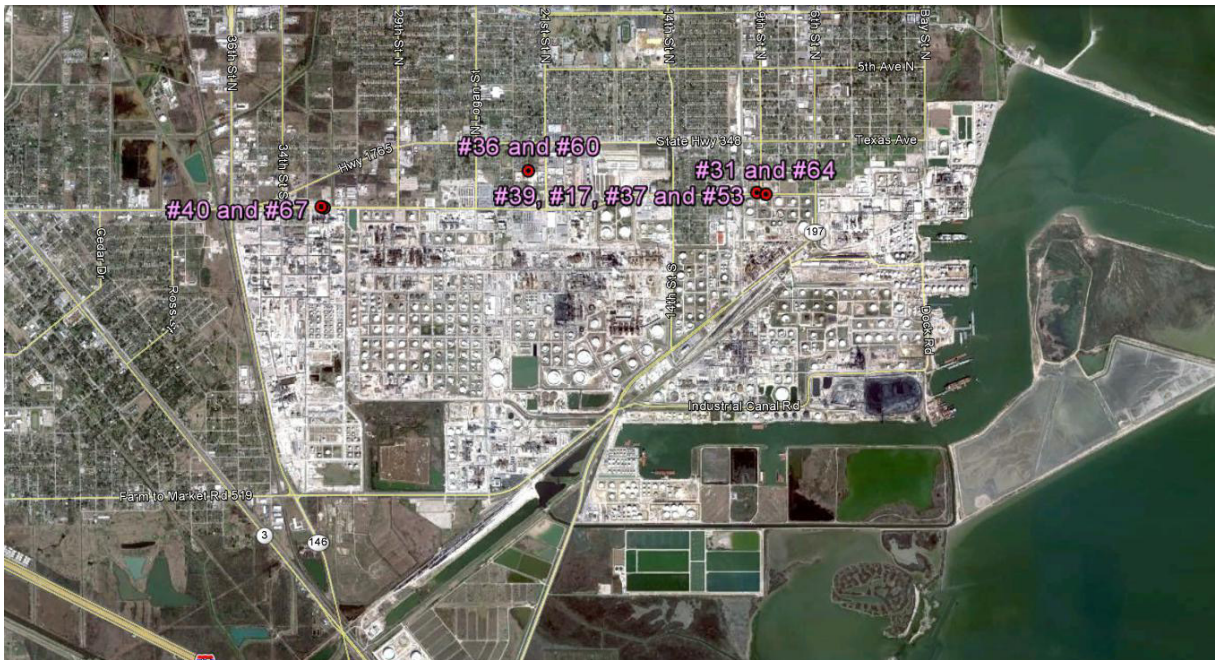

Figure 74 Location of canister samplings in the vicinity of Texas City.

Table 46 The 10 most abundant NMHCs downwind of the Eastern edge of Texas City (June 10, 2011 and June 18, 2011).

10 most abundant NMHCs[1] (at downwind site)	Downwind (can#31,64)[2] (06/10/2011, 15:42–15:44 CDT)	10 most abundant NMHCs[1] (at downwind site)	Downwind (can#53,37,17)[3] (06/18/2011 12:13–12:16 CDT)
propane	38.39 (±0.15)	ethane	17.84 (±1.12)
n-butane	33.16 (±1.32)	propane	13.33 (±0.66)
i-pentane	27.97 (±1.49)	n-butane	10.35 (±0.70)
n-pentane	16.71 (±0.80)	i-pentane	7.90 (±0.33)
i-butane	16.42 (±0.86)	n-pentane	6.77 (±0.16)
ethane	14.39 (±0.10)	ethene	5.26 (±0.20)
2-me-pentane	4.78 (±0.40)	i-butane	4.94 (±0.46)
n-hexane	5.49 (±0.45)	n-hexane	2.21 (±0.05)
3-me-pentane	4.70 (±0.30)	propene	2.08 (±0.33)
me-cyc-hexane	3.10 (±0.39)	3-me-pentane	1.41 (±0.09)

[1] in [ppbv]; [2] average of duplicates; in brackets half difference between duplicates
[3] average of three canisters; in brackets half difference between maximum and minimum values

Table 47 The 10 most abundant NMHCs downwind of the center of Texas City (June 10, 2011).

10 most abundant NMHCs[1] (at downwind site)	Downwind (can#36,60)[2] (06/10/2011, 16:37–16:39 CDT)
ethane	9.55 (±1.04)
propane	2.54 (±0.11)
ethene	2.76 (±0.73)
acetylene	1.27 (±0.02)
n-butane	1.16 (±0.09)
i-pentane	0.95 (±0.01)
i-butane	0.87 (±0.02)
n-pentane	0.72 (±0.04)
propene	0.95 (±0.43)
n-hexane	0.19 (±0.00)

[1] in [ppbv]; [2] average of duplicates; in brackets half difference between duplicates
[3] average of three canisters; in brackets half difference between maximum and minimum values

Table 48 The 10 most abundant NMHCs downwind of the Western edge of Texas City (June 10, 2011 and June 18, 2011).

10 most abundant NMHCs[1] (at downwind site)	Downwind (can#40,67)[2] (06/10/2011, 17:37–17:38 CDT)	10 most abundant NMHCs[1] (at downwind site)	Downwind (can#65,42,72)[3] (06/18/2011 14:28–14:31 CDT)
ethane	15.03 (±0.21)	ethane	23.88 (±0.54)
ethene	5.67 (±0.59)	propane	13.86 (±0.20)
propane	4.50 (±0.06)	propene	13.53 (±0.19)
propene	4.00 (±0.10)	ethene	8.58 (±1.12)
n-butane	2.41 (±0.00)	n-butane	2.21 (±0.02)
i-butane	0.70 (±0.01)	1-butene	1.26 (±0.02)
3-me-hexane	0.88 (±0.19)	i-butane	0.98 (±0.04)
benzene	0.69 (±0.00)	3-me-hexane	0.86 (±0.04)
n-hexane	0.64 (±0.01)	cyc-pentane	0.40 (±0/05)
i-pentane	0.61 (±0.01)	i-pentane	0.41 (±0.01)

[1] in [ppbv]; [2] average of duplicates; in brackets half difference between duplicates
[3] average of three canisters; in brackets half difference between maximum and minimum values

Figure 75. Location of canister samplings in Mont Belvieu.

Table 49 The 10 most abundant NMHCs downwind of Mont Belvieu (June 14, 2011 and June 16, 2011).

10 most abundant NMHCs[1] (at downwind site)	Downwind (can#33,48)[2] (06/14/2011, 14:16–14:19 CDT)	10 most abundant NMHCs[1] (at downwind site)	Downwind (can#30,61)[2] (06/16/2011 16:01–16:03 CDT)
ethane	1.33 (±0.03)	ethane	2.79 (±0.01)
i-pentane	0.81 (±0.01)	propane	1.81 (±0.06)
n-pentane	0.73 (±0.00)	ethene	1.19 (±0.16)
propane	0.46 (±0.06)	propene	1.02 (±0.03)
ethene	0.37 (±0.05)	n-butane	0.68 (±0.05)
n-butane	0.29 (±0.01)	i-butane	0.34 (±0.03)
i-butane	0.15 (±0.00)	i-pentane	0.24 (±0.02)
2-me-pentane	0.10 (±0.00)	n-pentane	0.18 (±0.03)
propene	0.09 (±0.00)	1-butene	0.17 (±0.03)
3-me-pentane	0.09 (±0.00)	i-butene	0.14 (±0.03)

[1] in [ppbv]
[2] average of duplicates; in brackets half difference between duplicates

Table 50 The 10 most abundant NMHCs downwind of the center of Mont Belvieu (June 14, 2011).

10 most abundant NMHCs[1] (at downwind site)	Downwind (can#26,18)[2] (06/14/2011, 15:31–15:32 CDT)
ethane	2.87 (±0.09)
propane	0.63 (±0.00)
i-pentane	0.58 (±0.02)
propene	0.51 (±0.04)
n-pentane	0.41 (±0.00)
n-butane	0.39 (±0.00)
ethene	0.41 (±0.13)
i-butane	0.21 (±0.01)
i-butene	0.12 (±0.01)
toluene	0.09 (±0.00)

[1] in [ppbv]
[2] average of duplicates; in brackets half difference between duplicates

Figure 76 Location of canister samplings in the vicinity of Baytown.

Table 51 The 10 most abundant NMHCs in upwind and downwind areas of Baytown. (June 11 2011).

10 most abundant NMHCs[1] (at downwind site)	Downwind (can#43,73)[2] (17:53–17:54 CDT)	Upwind (can#29)[3] (17:09–17:11 CDT)	Difference (downwind - upwind)
ethane	7.84 (±0.02)	1.54	+6.30
ethene	3.35 (±0.57)	1.41	+1.94
propane	3.23 (±0.03)	0.32	+2.91
propene	1.38 (±0.01)	0.31	+1.07
n-butane	0.81 (±0.02)	0.18	+0.63
i-pentane	0.45 (±0.00)	0.39	+0.06
n-pentane	0.44 (±0.01)	0.35	+0.09
i-butane	0.34 (±0.00)	0.14	+0.20
i-butene	0.21 (±0.01)	0.19	+0.02
n-hexane	0.11 (±0.01)	0.07	+0.04

[1] in [ppbv]
[2] average of duplicates; in brackets half difference between duplicates
[3] valid data of one can available

Table 52 The 10 most abundant NMHCs in upwind and downwind areas of Baytown. (June 16 2011).

10 most abundant NMHCs[1] (at downwind site)	Downwind (can#22,55,57)[2] (19:50–19:52 CDT)	Upwind (can#13,14,23)[2] (19:12–19:15 CDT)	Difference (downwind - upwind)
propene	14.13 (±1.58)	0.19 (±0.03)	+13.94
propane	2.40 (±0.13)	0.09 (±0.06)	+2.31
ethane	2.18 (±0.05)	0.70 (±0.08)	+1.48
ethene	1.64 (±0.17)	0.86 (±0.19)	+0.78
n-hexane	0.43 (±0.01)	0.04 (±0.00)	+0.39
n-butane	0.36 (±0.03)	0.05 (±0.02)	+0.31
1-butene	0.33 (±0.01)	0.08 (±0.01)	+0.25
i-butane	0.24 (±0.06)	0.02 (±0.00)	+0.22
i-pentane	0.26 (±0.02)	0.16 (±0.01)	+0.10
toluene	0.23 (±0.02)	0.13 (±0.03)	+0.10

[1] in [ppbv]
[2] average of three canisters; in brackets half difference between maximum and minimum values

6. Emissions of methane and other VOCs in the Fort Worth area

MeFTIR tracer correlation measurements were made for various hotspots in the Fort Worth area, including gas well pads, compressor facilities and gas treatment plants. The sources were chosen from hotspots identified from mobile measurements carried out in the Fort Worth area. Many of the largest sources identified are shown in Figure 77. Sites for tracer measurements were chosen to be representative of sources in the area and for their accessibility with the given wind direction.

From the MeFTIR measurements it was possible to measure emissions of methane, ethane, and CO. Although ethane emissions are directly measured with the tracer method, presented results are derived from the ratio between ethane and methane in the peak of the plume. Since plume ethane concentrations are a factor 10 lower than methane this approach offers an advantage particularly for measurements of low emissions. The tracer measurements were complemented by canister measurements of ethane and other species, downwind of the sites. Fluxes for the other species in the canister measurements are calculated by a simple ratio with ethane. Furthermore, SOF measurements were made for test purposes, but since CH_4 is difficult measure with this method and the other species have low emissions these data have not been evaluated.

With the mobile measurements we found several sources (see Figure 77 and Table 53) from which tracer releases were carried out to estimate their emissions of methane, ethane and CO and for which canister samples were collected in the plume. In addition, distinct methane emissions were measured from an oil drilling operation, a compressor station north of E Peden Rd, other wells, a food factory and from a digging operation which broke a pipeline. Results from the tracer correlation measurements of the sites in Figure 77 are shown in section 6.1 and the canister measurements results are shown in section 6.2. Figure 78 shows the measurements made for the more northerly sites. For CO it should be noted that it is impossible to completely eliminate interference from mobile sources (e.g. trucks) as measurements were made in traffic, even if on less frequently travelled roads and times.

Figure 77 Overview of the sources measured in by MeFTIR and canister in the Forth Worth area.

Figure 78 Overview of the tracer measurements in the northern portion of the Fort Worth area. Apparent column height is proportional to measured methane concentration. North is to the right in the image.

Table 53 Overview of the sources measured in by MeFTIR and canister in the Fort Worth area and measured methane emissions.

#	Name	Site	Comment	CH_4 (kg/h)	C_2H_6/CH_4 (% m/m)	C_2H_6 (kg/h)	CO kg/h
1	FM 1220	Compressor station, well pad and treatment facility	2 meas. days. Large emissions from well on May 10, potentially due to regeneration. 6 compressors	172	7.7 (tanks) 6.2 (all)	10.7	8
2	Hicks Field Rd	Treatment plant and compressor station	12 compressors	150	6.8	10.3	37±23
3	Blue Mound Rd	Treatment plant and compressor station	6 compressors	120	5.0	6.0	
4	Northern cross Rd	Well pads and mobile compressor	2 condensate tanks, 1 compressor	8	ND	0	0.4±0.4
5	Meacham Blvd	Compressor station, and gas separators and well pad	1 compressor	17	8.2	1.4	0.6±0.4
6	Long Avenue	Compressor station	3 compressors	8	12.6	1.0	10±2
7	Eagle Mt Rd	Well pads, distribution pipes	In the vicinity of compressor station and power station	6	8.4	0.5	1.1±1.1
8	E Peden Rd (1)	Well pad	2 condensate tanks	~1	ND	0	0.1±0.05
9	E Peden Rd 2	Well pad	3 condensate tanks and potentially leaking pipeline	~1	17.4 (pipeline)	0.1	0.1±0.0
10	Bonds Ranch Rd	Well pad	2 tanks	~1	ND	0	0±0.17

6.1 Mobile extractive FTIR and tracer correlation

The individual tracer correlation measurements from the sites in Table 53 are shown below in Table 54 and partly discussed in the figure texts. Of the three largest sources of methane emissions, only one (Hicks Rd site) was within the area covered in the Fort Worth Air Quality Study (ERG 2011). Ethane emissions were also noted from these sites as well as other sites with compressors.

Table 54 Summary of tracer measurements and methane emissions. N is the number of measurements, SD is the standard deviation.

Site	Day	N	Start Time	Stop Time	Emission (kg/h)	SD (kg/h)
FM1220						
	110510	9	164747	172357	221.3	35.7
	110512	5	144502	151118	82.6	26.7
Total		**14**	**144502**	**172357**	**171.8**	**75.9**
Hicks Field Rd						
	110512	7	160544	171716	149.7	88.0
Blue Mound						
	110515	5	201742	214053	119.6	34.8
Northern Cross						
	110510	5	103548	105315	8.1	2.4
Bonds Ranch Rd						
	110514	5	194703	195827	1.0	0.4
Meacham Blvd						
	110510	9	113400	121413	17.8	4.4
	110511	5	214337	220149	14.5	2.5
Total		**14**	**113400**	**220149**	**16.6**	**4.0**
Long Ave						
	110511	3	225618	231300	7.8	1.4
EagleMountain (Well & Pipes)	110513	5	180804	191614	6.2	4.5
E Peden Rd 1						
	110515	3	170721	175723	1.0	0.3
E PedenRd 2						
	110515	2	192452	193142	1.3	0.1

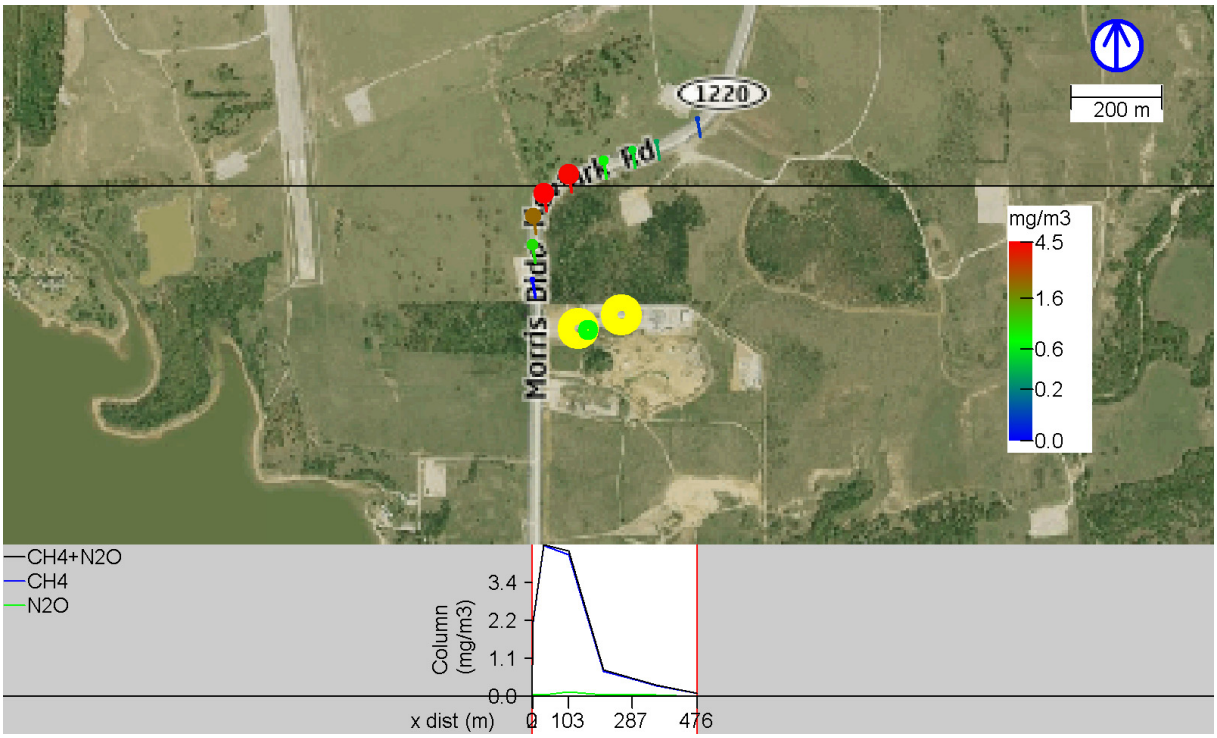

Figure 79 Methane and N2O (tracer) measured by MeFTIR downwind (SSE wind) of a well pad and a compressor plant on FM 1220, close to Kenneth Copeland airfield on May 10 (same data as Figure 18). The emission sources are shown in yellow while the tracer release position is shown as a green dot. On this day there were high emissions from the condensate tanks at the well pad, left yellow circle, which can be regeneration of gas drying liquid.

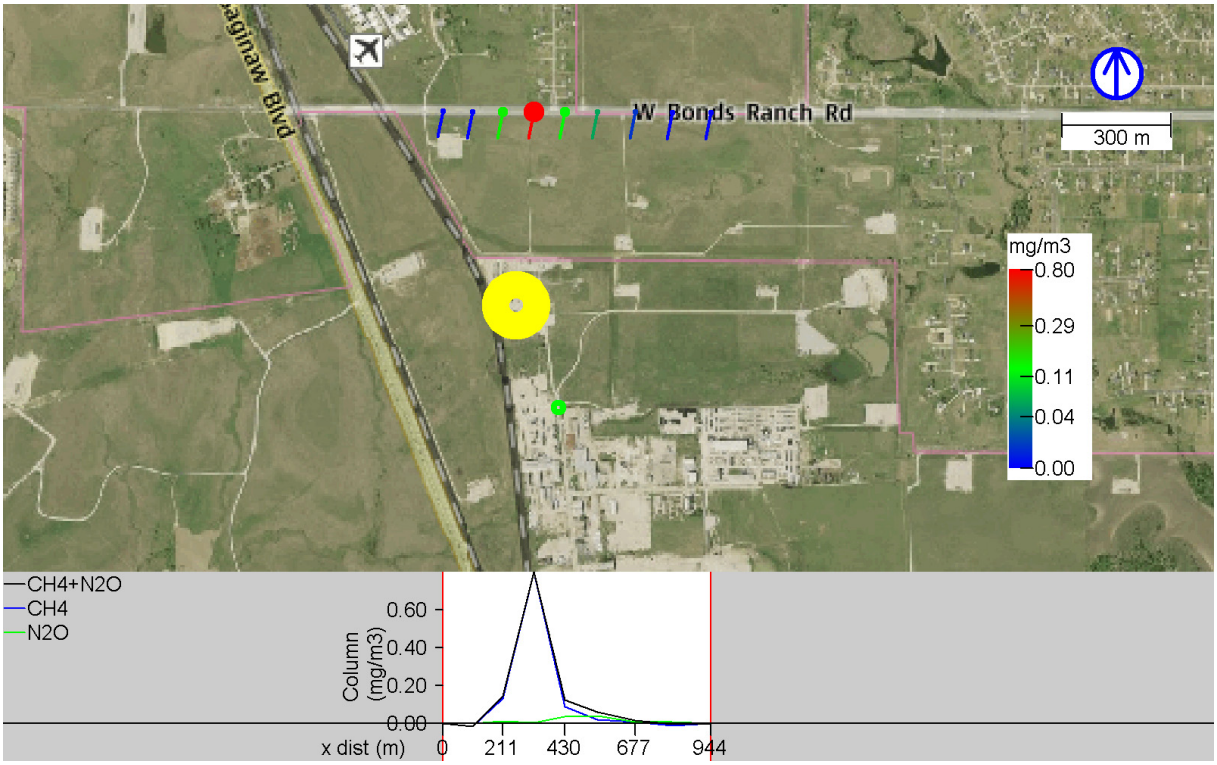

Figure 80 Methane and N2O (tracer) measured by MeFTIR downwind of a gas treatment plant close to Hicks Field Rd. – This site corresponds to FWAQS (ERG 2011) largest emitter. The emission source is shown in yellow and the tracer release in green. Since the tracer was position upwind, rather far from the source, the emissions may be overestimated.

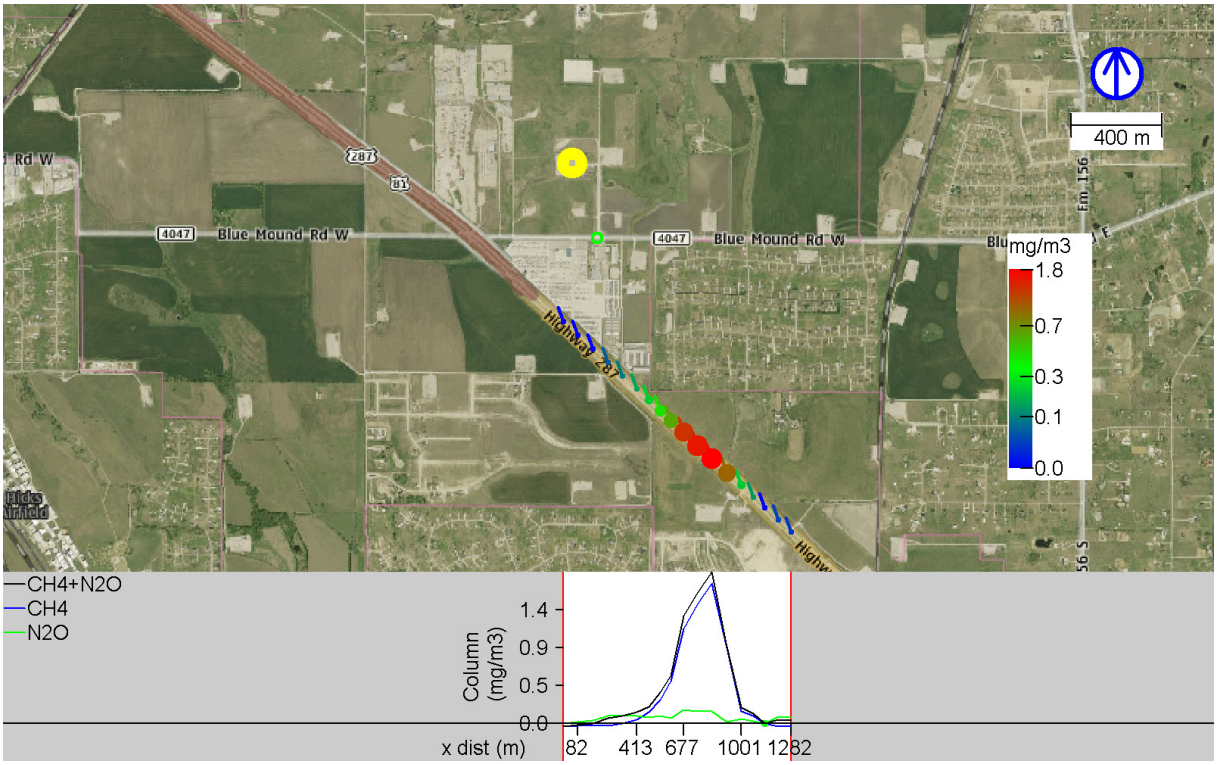

Figure 81 Methane emissions measured by MeFTIR and tracer correlation from the treatment plant on Blue Mound Rd. The emission source is shown in yellow and the tracer release in green. The tracer release point was relocated for the later measurements due to a change in wind direction.

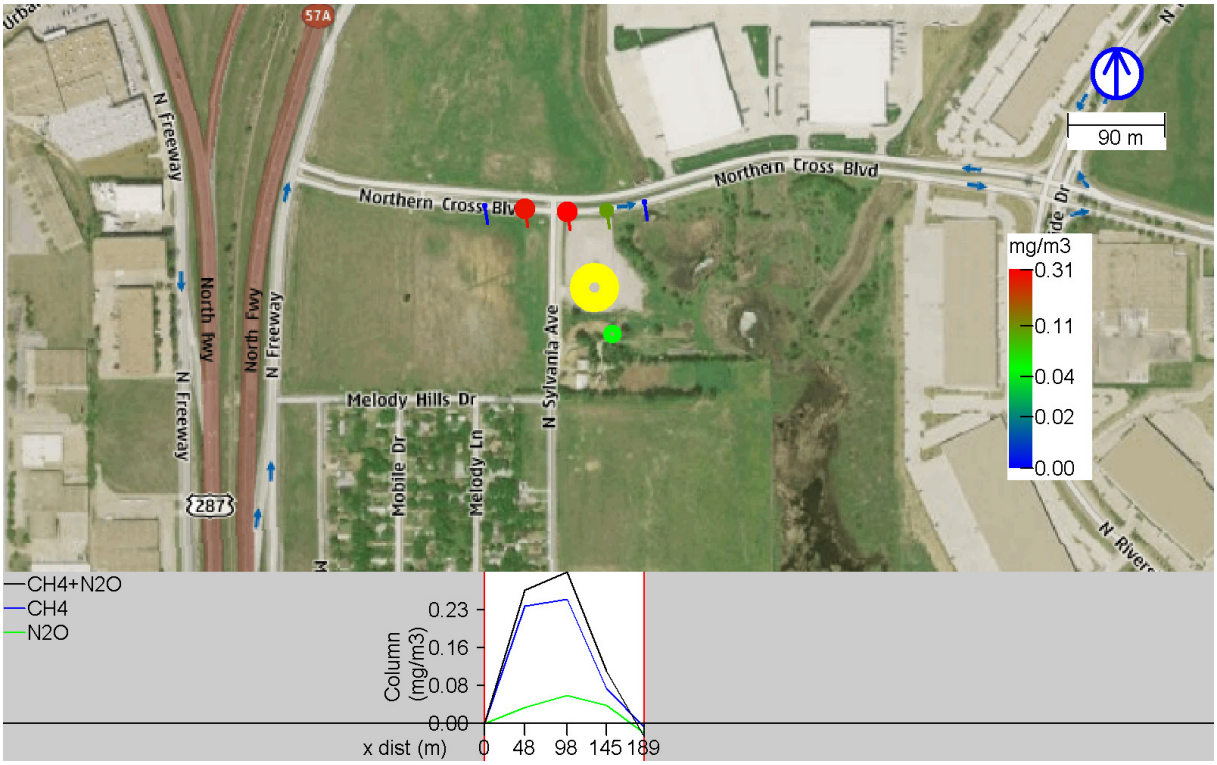

Figure 82 Methane emissions measured by MeFTIR and tracer correlation from a well pad with a mobile compressor on Northern cross Rd –The emission source is shown in yellow and the tracer release in green.

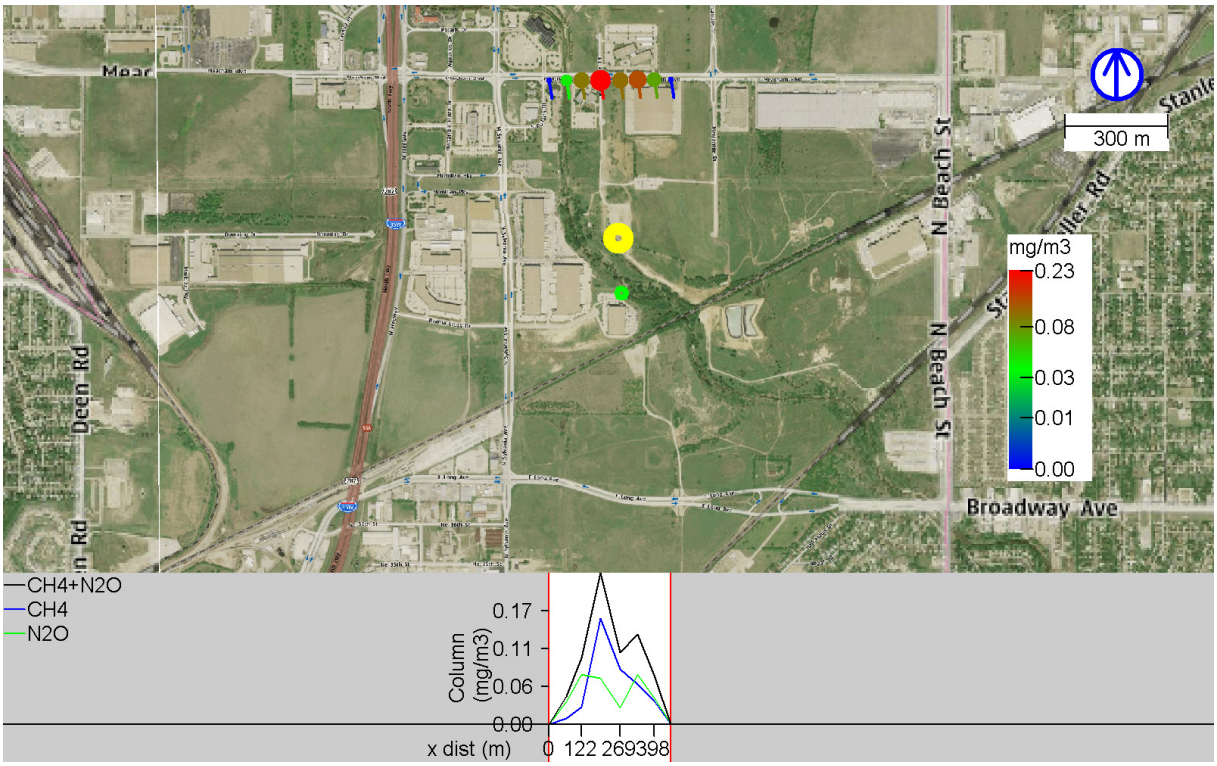

Figure 83 Methane emissions measured by MeFTIR and tracer correlation from a compressor station and well near Meacham Blvd, 110510. –The emission source is shown in yellow and the tracer release in green. On 110511 the tracer was released to the east of the site.

Figure 84 The compressor and separators near Meacham Blvd.

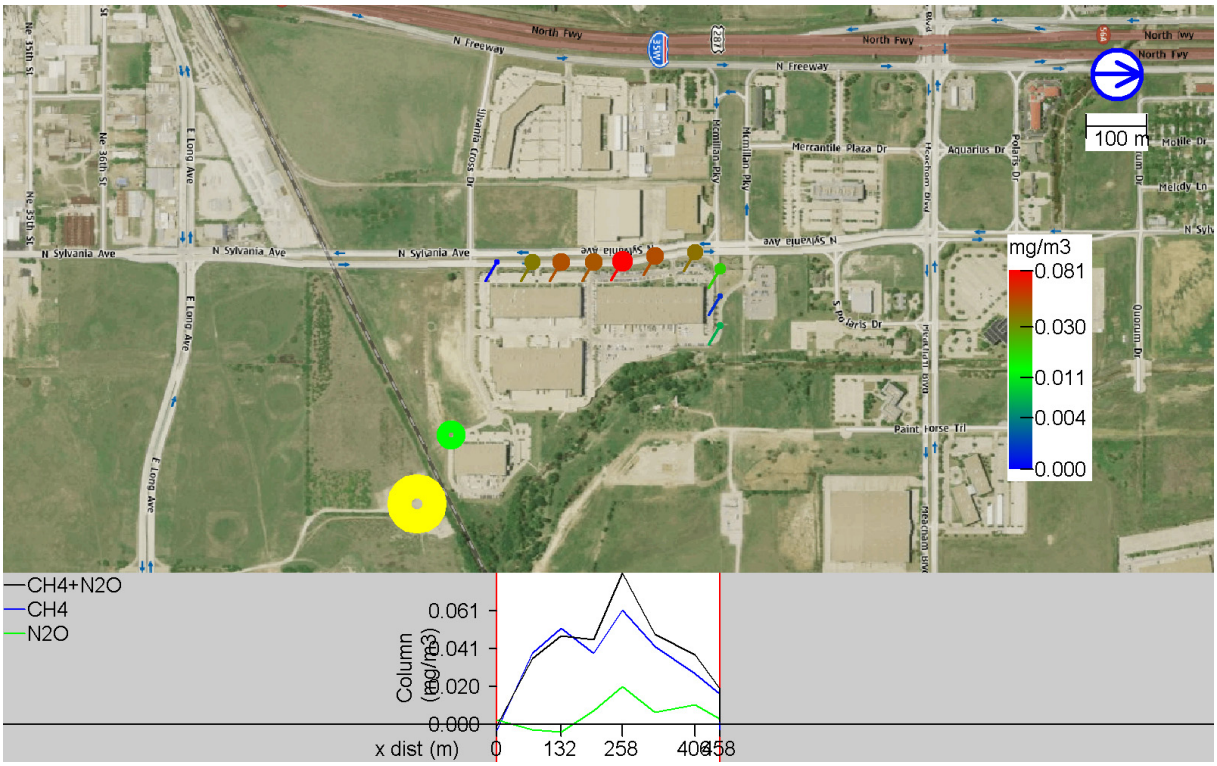

Figure 85 Methane emissions measured by MeFTIR and tracer correlation from a compressor station and well on Long avenue. –The emission source is shown in yellow and the tracer relase in green.

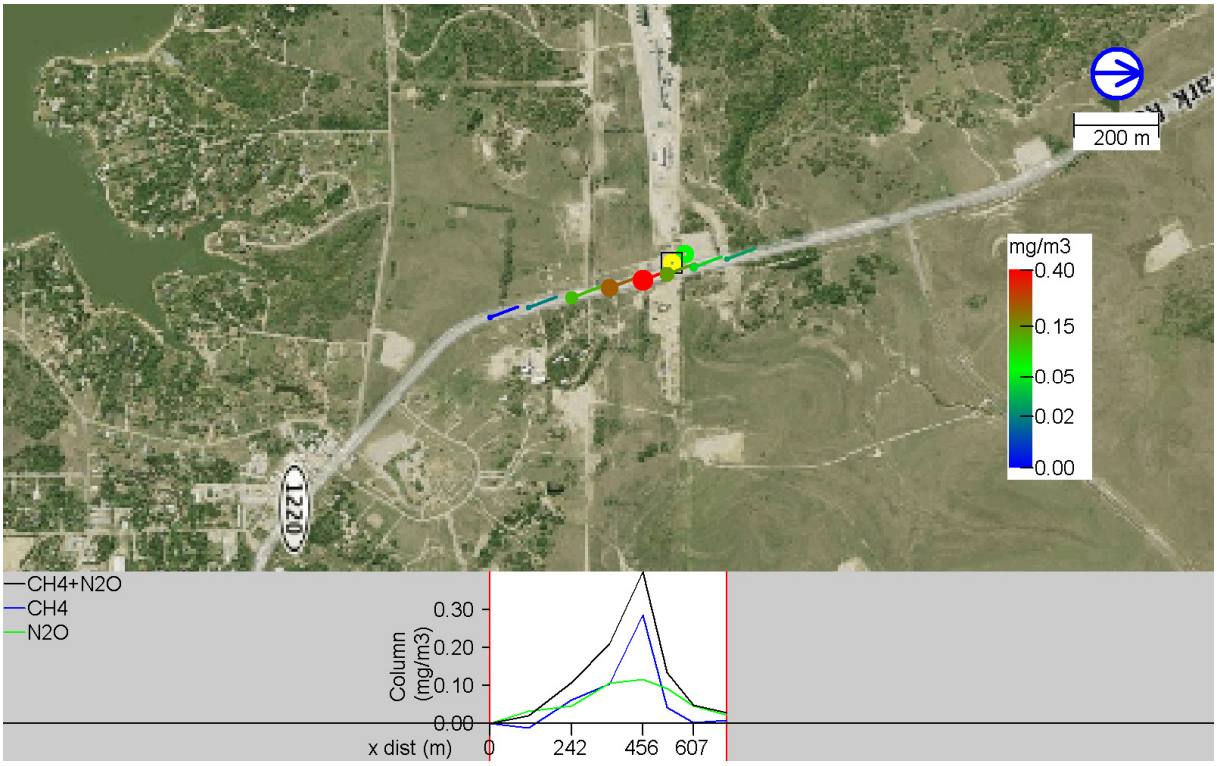

Figure 86 Methane and N2O (tracer) measured by MeFTIR downwind of well pads and a gas distribution system close to Eagle Mt Rd, in the vicinity of the Eagle Mt compressor plant. The emission source is shown in yellow while the tracer release position is shown as a green dot.

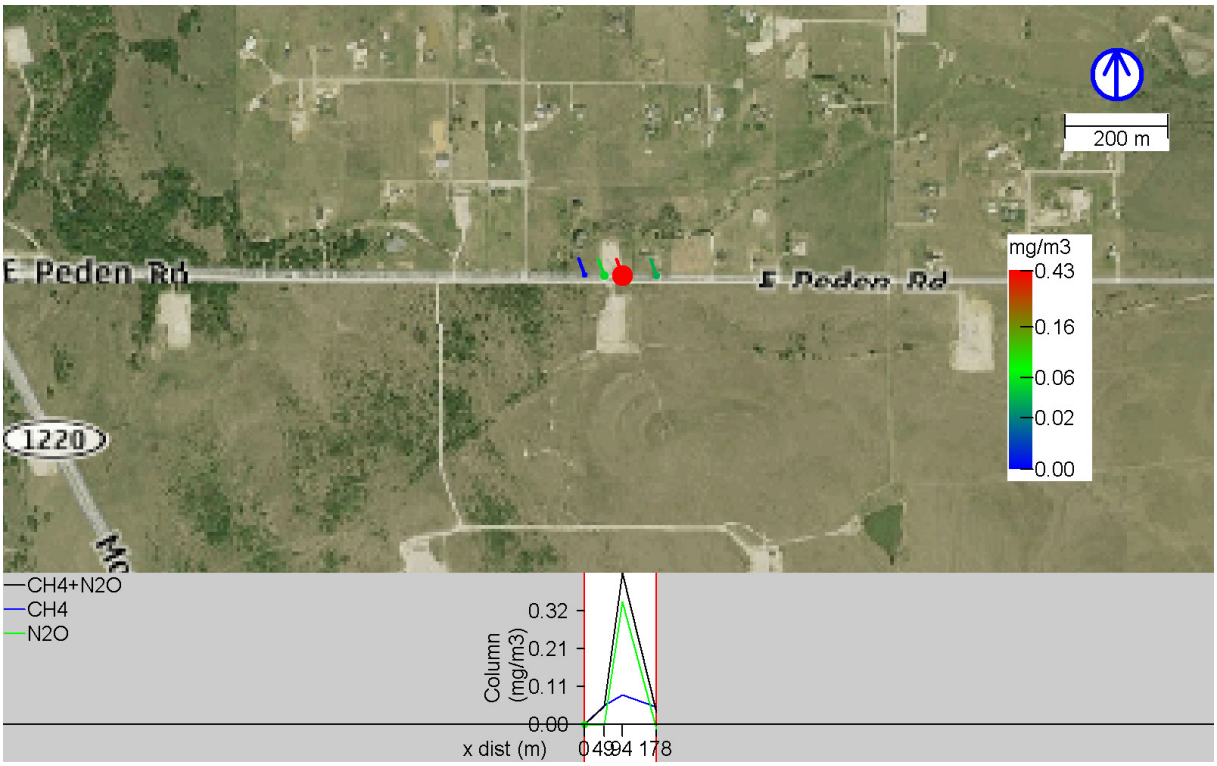

Figure 87 Methane and N2O (tracer) measured by MeFTIR downwind of a well pad on E Peden Rd (1). Tracer release and source location are not indicated but are located at the red dot (highest concentration).

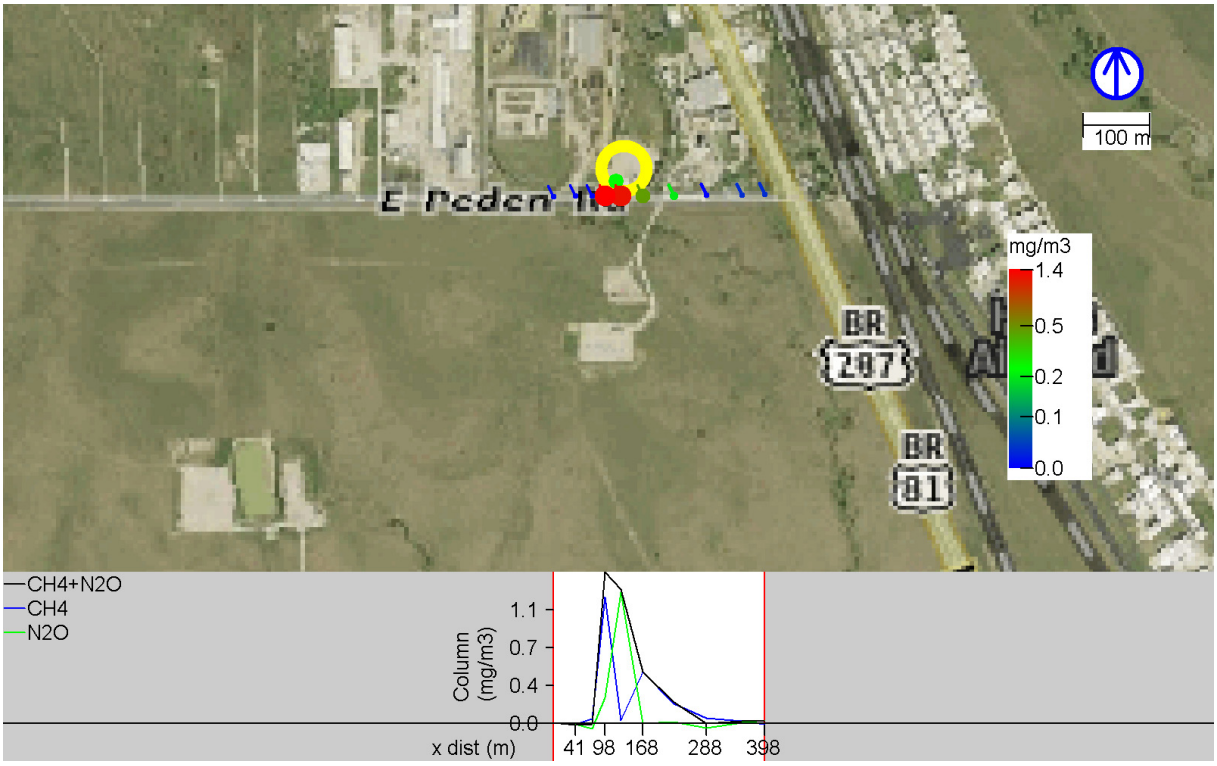

Figure 88 Methane and N2O (tracer) measured by MeFTIR downwind of a well pad on E Peden Rd (2). The emission source is shown in yellow while the tracer release position is shown as a green dot.

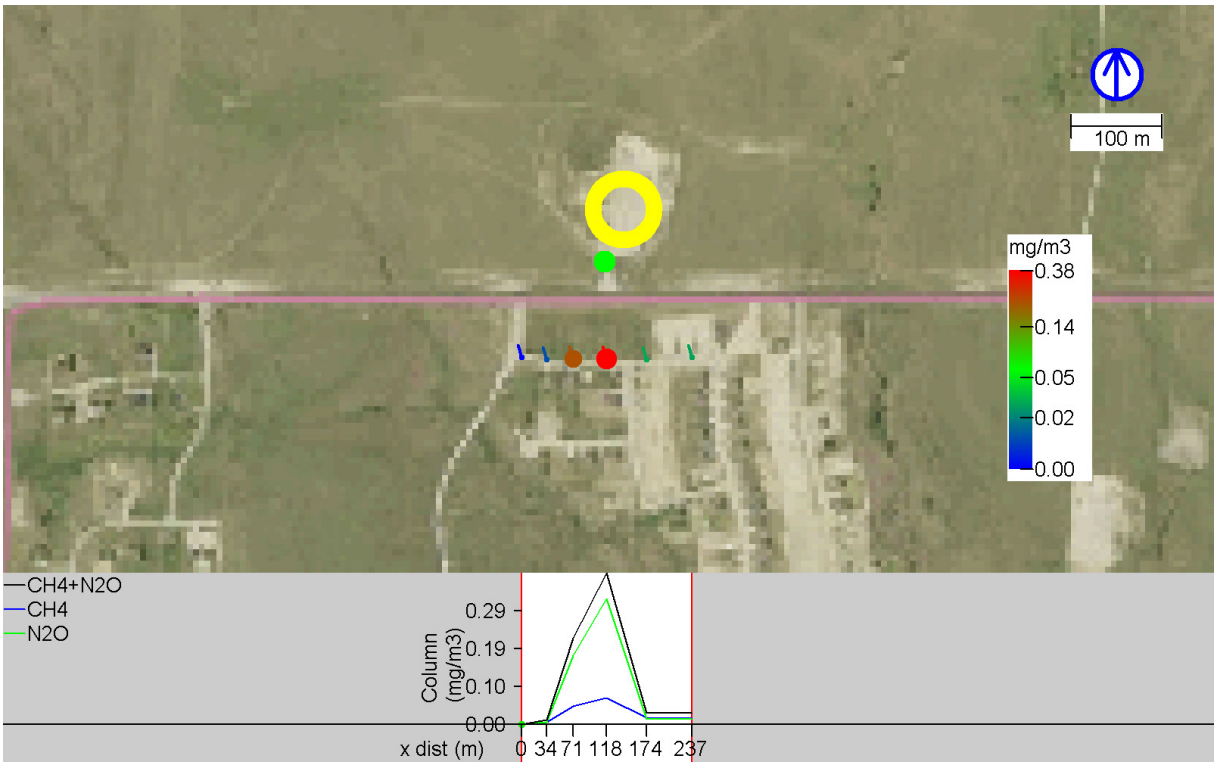

Figure 89 Methane and N2O (tracer) measured by MeFTIR downwind of a well pad on Bonds Ranch Rd. The emission sources is shown in yellow while the tracer release position is shown as a green dot.

6.2 Canister Measurements in Fort Worth

The figures and tables below show canister samples taken downwind of various sources in the Fort Worth area. The sample locations correspond to hotspot locations identified by the MeFTIR. It can be seen in the tables that the most abundant species here are alkanes, which would be expected since that is they are the main components of natural gas. In most measurements we sampled one or several times in the plume from the sources while measuring real time with the MeFTIR, and then an additional canister was sampled upwind.

Figure 90 Location of canister samplings in the vicinity of the compressor station on FM1220. Arrow indicates wind direction.

Table 55 The 10 most abundant NMHCs in upwind and downwind areas of the FM1220 compressor station and well pads. (May 10, 2011). The sample is mostly influenced by ventilation of a condensate tank (flashing emission) in a well pad.

10 most abundant NMHCs[1] (at downwind site)	Downwind (can#65,18)[2] (17.53–17:55 CDT)	Upwind (can#37,72)[2] (19:25–19:27 CDT)	Difference (downwind - upwind)
ethane	308.21 (±4.15)	13.49 (±0.26)	+294.72
ethene	61.72 (±2.31)	1.12 (±0.01)	+60.60
propane	11.11 (±0.41)	3.49 (±0.06)	+7.62
n-butane	1.10 (±0.05)	1.12 (±0.09)	-0.02
propene	1.01 (±0.10)	0.27 (±0.03)	+0.74
i-butane	0.81 (±0.01)	0.68 (±0.01)	+0.13
i-pentane	0.49 (±0.04)	0.59 (±0.01)	-0.10
acetylene	0.41 (±0.01)	0.41 (±0.01)	0.0
n-pentane	0.31 (±0.01)	0.43 (±0.01)	+0.12
isoprene	0.31 (±0.04)	0.29 (±0.03)	-0.02

[1] in [ppbv]
[2] average of duplicates; in brackets half difference between duplicates
Comments:

- Rain and stagnant wind for upwind sample
- Most of the downwind emission came from a vent on a nearby condensate tank (regeneration of drying fluid)

Table 56 The 10 most abundant NMHCs in upwind and downwind areas of the FM1220 compressor site. (May 10, 2011). Mixture of plumes from well pad, storage tanks and compressor station.

10 most abundant NMHCs[1] (at downwind site)	Downwind (can#73,61)[2] (18.20–18:22 CDT)	Upwind (can#37,72)[2] (19:25–19:27 CDT)	Difference (downwind - upwind)
ethane	39.30 (±0.53)	13.49 (±0.26)	+25.81
propane	3.35 (±0.32)	3.49 (±0.06)	-0.14
ethene	2.13 (±0.08)	1.12 (±0.01)	+1.01
n-butane	0.87 (±0.14)	1.12 (±0.09)	-0.25
i-butane	0.48 (±0.02)	0.68 (±0.01)	-0.20
i-pentane	0.40 (±0.02)	0.59 (±0.01)	-0.19
propene	0.40 (±0.09)	0.27 (±0.03)	+0.13
acetylene	0.38 (±0.02)	0.41 (±0.01)	-0.04
n-pentane	0.31 (±0.02)	0.43 (±0.01)	-0.12
isoprene	0.26 (±0.02)	0.29 (±0.03)	-0.03

[1] in [ppbv]
[2] average of duplicates; in brackets half difference between duplicates

Table 57 The 10 most abundant NMHCs in upwind and downwind areas of the FM1220 Compressor Station (May 10, 2011). Primarily compressor station plume.

10 most abundant NMHCs[1] (at downwind site)	Downwind (can#42)[2] (19.03–19:05 CDT)	Upwind (can#37,72)[3] (19:25–19:27 CDT)	Difference (downwind - upwind)
ethane	19.13	13.49 (±0.26)	+5.64
propane	3.69	3.49 (±0.06)	+0.02
ethene	1.44	1.12 (±0.01)	+0.32
n-butane	1.08	1.12 (±0.09)	-0.04
i-butane	0.65	0.68 (±0.01)	-0.03
i-pentane	0.50	0.59 (±0.01)	-0.09
acetylene	0.49	0.41 (±0.01)	+0.08
n-pentane	0.39	0.43 (±0.01)	-0.04
toluene	0.30	0.32 (±0.02)	-0.02
propene	0.26	0.27 (±0.03)	-0.01

[1] in [ppbv]
[2] valid data of on can available
[3] average of duplicates; in brackets half difference between duplicates

Figure 91 Location of canister samplings upwind and downwind of a well pad and pipe manifold in the vicinity of Eagle Mountain Road Compressor Station. Arrow indicates wind direction.

Table 58 The 10 most abundant NMHCs in upwind and downwind areas of a well pad and pipe manifold in the vicinity of Eagle Mountain Road Compressor Station. (May 13, 2011).

10 most abundant NMHCs[1] (at downwind site)	Downwind (can#59,66)[2] (19.38–19:39 CDT)	Upwind (can#63)[3] (19:57–19:59 CDT)	Difference (downwind - upwind)
ethane	9.41 (±0.14)	4.25	+5.16
propane	1.86 (±0.02)	1.08	+0.78
n-butane	0.65 (±0.00)	0.48	+0.17
ethene	0.35 (±0.05)	0.46	-0.11
i-butane	0.29 (±0.03)	0.18	+0.11
n-pentane	0.28 (±0.01)	0.13	+0.15
i-butene	0.26 (±0.15)	0.18	+0.08
i-pentane	0.25 (±0.01)	0.42	-0.17
propene	0.13 (±0.00)	0.13	0.00
n-hexane	0.11 (±0.00)	0.09	+0.02

[1] in [ppbv]
[2] average of duplicates; in brackets half difference between duplicates
[3] valid data of on can available

Figure 92 Location of canister samplings in the vicinity of a well pads on Bond ranch Rd (Eagle Mt). The Eagle Mt Compressor Station also blew in as a background, for can 67 and 011. Arrow indicates wind direction.

Table 59 The 10 most abundant NMHCs in upwind and downwind areas of a well in the vicinity of a well facility on Bond ranch Rd (Eagle Mt). The Eagle Mt Compressor Station also blew in as a background, for can 67 and 011. (May 14, 2011).

10 most abundant NMHCs[1] (at downwind site)	Downwind (can#31,60)[2] (20.08–20:10 CDT)	Upwind (can#67,11)[2] (19:25–19:27 CDT)	Difference (downwind - upwind)
ethane	28.33 (±0.26)	10.68 (±1.85)	+17.91
propane	4.95 (±0.12)	4.33 (±0.09)	+0.50
n-butane	1.42 (±0.00)	1.73 (±0.01)	-0.30
ethene	1.12 (±0.35)	0.36 (±0.09)	+1.11
i-butane	0.61 (±0.01)	0.56 (±0.00)	+0.06
n-pentane	0.48 (±0.02)	0.63 (±0.20)	-0.17
i-pentane	0.41 (±0.01)	0.63 (±0.02)	-0.21
propene	0.36 (±0.16)	0.40 (±0.01)	-0.20
n-hexane	0.17 (±0.00)	0.70 (±0.02)	-0.53
i-butene	0.13 (±0.02)	0.16 (±0.02)	-0.05

[1] in [ppbv]
[2] average of duplicates; in brackets half difference between duplicates

Table 60 The 10 most abundant NMHCs in upwind and downwind areas of the Eagle Mt Compressor Station (May 14, 2011).

10 most abundant NMHCs[1] (at downwind site)	Downwind (can#31,60)[2] (20.08–20:10 CDT)	Upwind (can#9)[3] (21:12–21:14 CDT)	Difference (downwind - upwind)
ethane	28.33 (±0.26)	13.59	+15.00
propane	4.95 (±0.12)	5.63	-0.80
n-butane	1.42 (±0.00)	1.89	-0.46
ethene	1.12 (±0.35)	0.88	+0.59
i-butane	0.61 (±0.01)	0.67	-0.05
n-pentane	0.48 (±0.02)	0.67	-0.21
i-pentane	0.41 (±0.01)	0.63	-0.21
propene	0.36 (±0.16)	0.36	-0.16
n-hexane	0.17 (±0.00)	0.25	-0.08
i-butene	0.13 (±0.02)	0.16	-0.05

[1] in [ppbv]
[2] average of duplicates; in brackets half difference between duplicates
[3] valid data of on can available

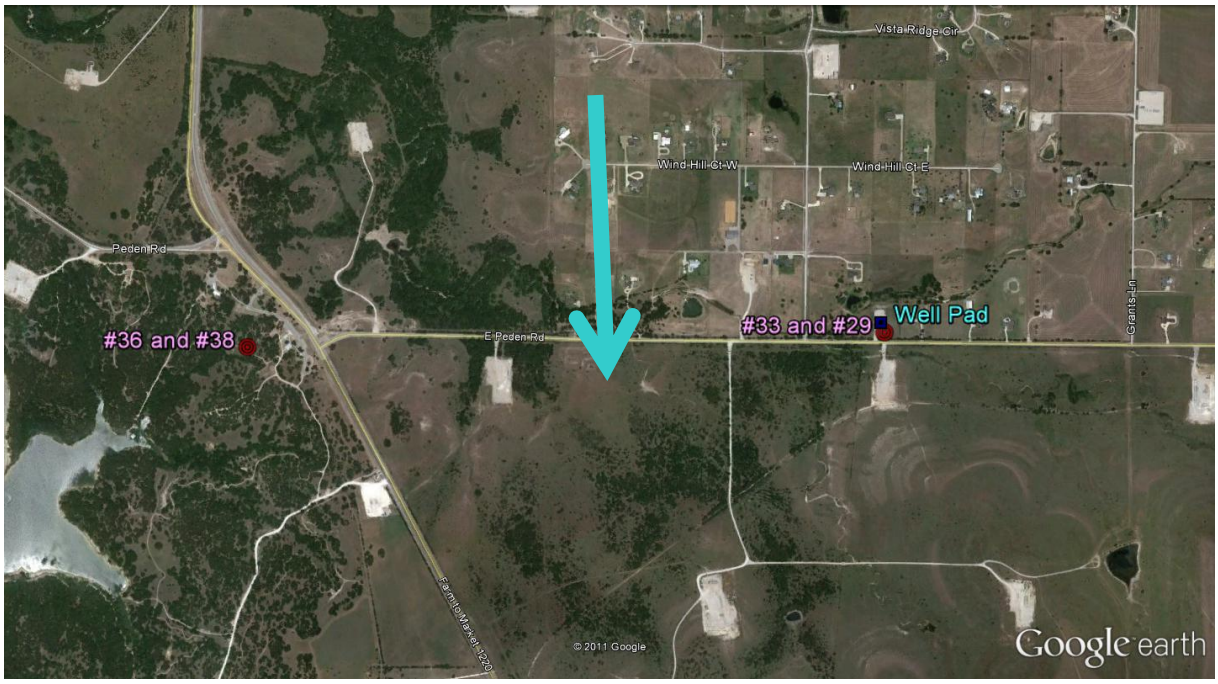

Figure 93 Location of canister samplings in the vicinity of a well facility on E Peden Rd. Arrow indicates wind direction.

Table 61 The 10 most abundant NMHCs in the vicinity of a well on E Peden Rd. (May 15, 2011). Actual wind at the time was northwesterly, thus difference between cans does not denote contribution solely from the well possibly also from sites to the NW.

10 most abundant NMHCs[1] (at downwind site)	Plume (can#29,33)[2] (17.25–17:27 CDT)	Background (can#38,36)[2] (18:25–18:27 CDT)	Difference (plume - background)
ethane	16.31 (±0.10)	5.93 (±0.15)	+10.38
propane	5.42 (±0.13)	2.15 (±0.05)	+3.27
me-cyc-hexane	4.51 (±0.08)	0.03 (±0.00)	+4.48
n-butane	2.43 (±0.03)	1.05 (±0.01)	+1.38
cyc-hexane	1.95 (±0.19)	0.02 (±0.00)	+1.93
n-hexane	1.81 (±0.03)	0.11 (±0.01)	+1.70
n-pentane	1.74 (±0.02)	0.32 (±0.01)	+1.42
i-pentane	1.39 (±0.01)	0.29 (±0.01)	+1.10
3-me-hexane	1.16 (±0.07)	0.03 (±0.01)	+1.13
2,2,4-trime-pentane	1.11 (±0.03)	0.02 (±0.00)	+1.09

[1] in [ppbv]
[2] average of duplicates; in brackets half difference between duplicates

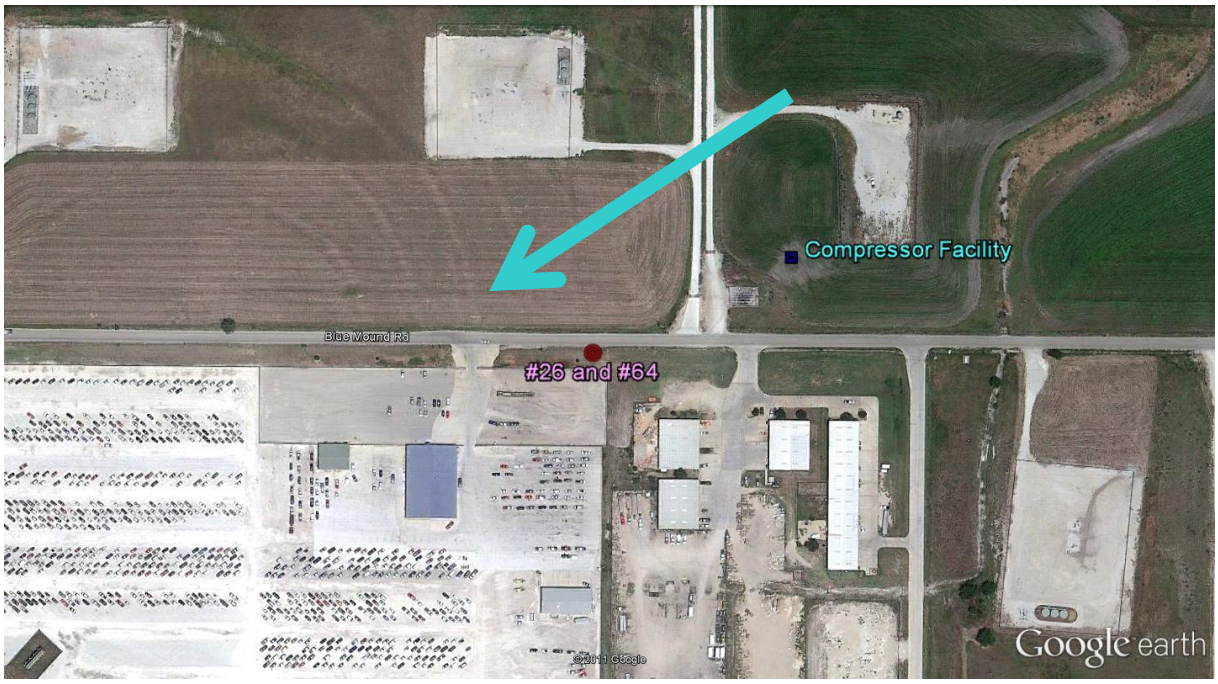

Figure 94 Location of canister samplings downwind of the Blue Mound compressor facility. Arrow indicates wind direction.

Table 62 The 10 most abundant NMHCs in upwind and downwind areas of the Blue Mound compressor Station (May 15, 2011).

10 most abundant NMHCs[1] (at downwind site)	Downwind (can#64,26)[2] (20.20–20:22 CDT)
ethane	8.95 (±0.18)
propane	1.70 (±0.12)
ethene	0.68 (±0.03)
n-butane	0.50 (±0.01)
i-butane	0.22 (±0.00)
i-pentane	0.21 (±0.01)
toluene	0.19 (±0.00)
n-pentane	0.18 (±0.00)
i-butene	0.12 (±0.01)
propene	0.11 (±0.01)

[1] in [ppbv]
[2] average of duplicates; in brackets half difference between duplicates

Figure 86 Location of canister samplings downwind (can #46 and #16) and upwind (can #17 and #14) of the Hicks Field Rd compressor station and treatment plant close to Hicks Field Rd. Arrow indicates wind direction.

Table 63 Three most abundant NMHCs in downwind relative to upwind of the Hicks Field Rd compressor Station and treatment facility. (May 12, 2011). (other species were higher in the background)

10 most abundant NMHCs[1] (at downwind site)	Downwind (can#46,16)[2] (CDT)	Upwind (can#17,14)[2] (CDT)	Difference (downwind - upwind)
ethane	13.20(±0.1)	4.58(±0.28)	8.63(±0.3)
propane	1.24(±0.01)	0.79(±0.05)	0.45(±0.05)
ethene	0.74(±0.02)	0.41(±0.09)	0.33(±0.09)

7. Discussion

7.1 Comparison with emissions inventories

7.1.1 Description of emission inventories

To put the emissions measured with SOF and Mobile DOAS into perspective, they have been compared with data extracted from the TCEQ's State of Texas Air Reporting System (STARS) database for 2009, the most recent year available. The database contains point source emissions speciated to a varying degree. As an example, the data set for Harris County, which includes most of greater Houston (and Houston Ship Channel, but not Texas City or Mont Belvieu), contains 11 595 point sources distributed over 268 industrial sites. These 11 595 point sources are reported to emit on average approximately 6 different contaminants each and altogether 927 different species are reported in the Harris County data set. Most of these contaminants refer to specific chemical compounds, often specifying which isomer, but some contaminants are more vague, like "ALKENES-U" (meaning unclassified alkenes), "COKER FEED" (meaning the raw material used in a coker unit) or "VOC-UNCLASSIFIED" (could be almost anything).
In the following sections, the emissions measured with SOF and Mobile DOAS will be compared to sums of emissions from this database. These are the sums of all emissions of one or several contaminants (depending on the species measured) from all sources located in the area the measured emission is originating from.
All emissions are reported in tonnes over the whole year, which has been converted to kg/h under the assumption that the emissions are uniform over the whole year. Temporal variations in the emission rates are of course one reason for discrepancy in these comparison.

7.1.2 Alkanes

The alkane evaluations of SOF measurements are made in the 2725-3005 cm^{-1} region where practically any species with a C-H bond interferes. However, for most species this interference is fairly weak, and alkanes and alcohols are the only groups of species that would be expected contribute significantly. The first category to compare the alkane measurements to is therefore the sum of all alkanes and alcohols. Contaminants describing various generic petroleum products like "CRUDE OIL" and "KEROSENE" have also been included in this category since they can be expected to consist of mostly alkanes. The secondary category that have been included in this comparison consist of contaminants that are vaguely classified but may be alkanes, like "CONDENSATE" and "VOC-UNCLASSIFIED". The third category in the comparison consists of all species with at least on C-H bond. This includes alkanes, alkenes, aromatics, alcohols, aldehydes, ketones, halogenated hydrocarbons, amines etc. This category is included since very large emissions of these species could potentially have a significant effect on the alkane measurements even if they are not alkanes or alkene.
The total emissions of contaminants in these three categories from each of the areas for which alkane emission measurements are presented in Chapter 5.5 is shown in Table 64. This is compared to the average alkane emission measured for each area and a ratio of the measured emission to the sum of the alkane+alcohols and the unspeciated VOCs category is calculated.

Table 64 Total emissions reported in STARS in three categories; alkanes+alcohols, unspeciated VOCs and Total VOCs, compared to the measured alkane emissions from all areas investigated. All emissions in kg/h. The ratio of the measured alkane emissions to the sum of the alkane+alcohols and the unspeciated VOCs category is also shown.

Region	Area	2009 Emission inventories			Measured alkane emissions	Ratio
		Alkanes+ alcohols	Unscpeciated VOCs	Total VOCs		
Texas City	All	212	106	411	2342	7.4
Mont Belvieu	All	203	41	354	1319	5.4
HSC	Sector 1	58	88	177	1569	10.7
	Sector 2	240	40	371	4154	14.8
	Sector 3	97	52	281	2411	16.2
	Sector 4	66	16	229	1058	12.9
	Sector 5	7	12	60	956	50.3
	Sector 6	1	3	34	894	223.5
	Sector 7	128	42	293	1749	10.3
	All	597	254	1445	11569	13.6
BPA	Area 1	2	3	6	266	53
	Area 2	80	51	181	1758	13.4
	Area 3	46	8	58	1711	31.7
	Area 4	9	3	27	657	54.8
	Area 5	26	33	88	883	15.0
	Area 6	54	32	111	1588	18.5
	Area 7	39	66	114	549	5.2
	Area 8	3	0	4	-	-
	All	260	197	590	7412	16.2
Longview	All	54	33	292	841	9.7

7.1.3 Alkenes

The ethene and propene evaluations are focused on much narrower and more specific absorption lines and hence are not significantly susceptible to interference from other species. For this reason, the three categories ethene, propene and other alkenes have been summed up for comparisons. The ethene and propene categories only include these species respectively while other alkenes include all hydrocarbons with one or several double bonds, except those with aromatic components or substitutions of element other than hydrogen and carbon. The latter category also includes unspeciated alkenes. The total reported emissions in these categories for the areas where alkenes where measured are presented in Table 65 together with the measured emissions of ethene and propene and the ratios of measured emissions to reported emissions for ethene and propene.

Table 65 Total emissions reported in STARS in three categories; ethene, propene and other alkenes, compared to the measured ethane and propene emissions from all areas investigated. All emissions in kg/h. The ratio of measured emissions to reported inventory emissions is also shown for both ethene and propene.

Region	Area	2009 Emission inventories			Measured ethene	Ratio	Measured propene	Ratio
		Ethene	Propene	Other alkenes				
Texas City	West	1.0	2.9	6.5	97	97.0	-	-
	Mid	1.6	2.2	13.1	47	29.4	56	25.5
	East	1.1	2.5	1.1	33	30.0	-	-
	All	3.8	7.6	20.6	177	46.6	56	7.4
Mont Belvieu	North	5.2	3.8	6.9	292	56.2	58	15.3
	South	46.6	20.2	0.5	-	-	-	-
	Southwest	13.1	3.7	4.4	253	19.3	-	-
	All	64.8	27.7	11.7	545	8.4	-	-
HSC	Sector 1	0.6	1.2	4.3	-	-	-	-
	Sector 2	19.0	20.2	25.7	133	7.0	76	3.8
	Sector 3	18.3	16.3	30.9	165	9.0	149	9.1
	Sector 4+5+6	26.4	22.8	14.7	246	9.3	241	10.6
	Sector 7	9.7	16.6	18.1	68	7.0	97	5.8
	All	73.8	77.1	93.7	612	8.3	563	7.3
BPA	Area 1	0.0	0.1	0.0	-	-	-	-
	Area 2	1.4	2.6	4.9	-	-	-	-
	Area 3	0.0	0.0	0.0	-	-	-	-
	Area 4	5.3	2.2	0.3	93	17.5	20	9.1
	Area 5	8.9	7.4	3.4	28	3.1	-	-
	Area 6	6.3	6.2	2.7	34	5.4	13	2.1
	Area 7	1.9	1.5	0.8	24	12.6	21	14.0
	Area 8	0.0	0.1	0.2	-	-	-	-
	All	23.8	20.1	12.1	179	7.5	54	2.7
Longview	All	113.2	31.6	6.8	452	4.0	282	8.9

7.1.4 SO_2 and NO_2

Two categories have been retrieved from the STARS database for comparison with SO_2 and NO_2. The first one includes “SULFUR DIOXIDE” and “SULFUR OXIDE-U” while the second one includes “NITRIC OXIDE”, “NITROGEN DIOXIDE” and “NITROGEN OXIDES”. However, the first category is heavily dominated by “SULFUR DIOXIDE” while the second one is dominated by “NITROGEN OXIDES”. Comparing the first category too measured SO_2 emissions should be straightforward but comparing the second one to measured NO_2 emissions deserves a caveat. Not all nitrogen oxides emitted will be NO_2 when measured. Some of it will be NO and the ratio will vary. NO_2 is also heavier than NO and if NO_x emissions are reported with their mass rate as NO, this rate will increase as it is converted to NO_2. Hence larger discrepancies would be anticipated for the NO_x – NO_2 comparison.
These two categories have been summed up for all areas and are presented together with the measured emissions in Table 66. The ratios measured SO_2 to reported SO_2 and measured NO_2 to reported NO_x is also shown.

Table 66 Total emissions reported in STARS in two categories; SO_2 and NO_x, compared to the measured SO_2 and NO_2 emissions from all areas investigated. All emissions in kg/h. The ratio of measured emissions to reported inventory emissions is also shown for both SO_2 and NO_2 (the ratio of measured NO_2 to reported NO_x in the latter case).

Region	Area	2009 emission inventories		Measured SO_2	Ratio	Measured NO_2	Ratio
		SO_2	NO_x				
Texas City	West+Mid	258	308	1186	4.65	439	1.42
	East	69	79	103	1.49	53	0.67
	All	327	387	1289	3.94	492	1.27
Mont Belvieu	North	8	101	-	-	145	1.44
	South	3	66	-	-	-	-
	Southwest	4	25	-	-	-	-
	All	15	192	-	-	305	1.58
HSC	Sector 0	454	6	565	1.24	-	-
	Sector 1+2	782	348	345		628	1.80
	Sector 3+4	528	361	854	1.62	617	1.71
	Sector 5	2	140	-	-	115	0.82
	Sector 6	17	16	-	-	90	5.63
	Sector 7	183	428	564	3.08	379	0.89
	All	1967	1297	2328	1.18	1829	1.41
BPA	Area 1	2	36	-	-	66	1.83
	Area 2	150	272	282	1.88	360	1.32
	Area 3	0	3	-	-	-	-
	Area 4	0	86	-	-	72	0.84
	Area 5	18	133	71	3.94	189	1.42
	Area 6	22	321	-	-	418	1.30
	Area 7	176	244	354	2.01	267	1.09
	Area 8	745	50	904	1.21	49	0.98
	All	1114	1145	1611	1.47	1421	1.24
Longview	All	2	207	-	-	176	0.85

These measurement results and reported emissions have been further compiled on region level together with similar data from the SOF campaigns in southeast Texas 2006 and 2009. From these results it might be possible to start discussing if there have been changes over the years. One of the most striking changes is probably the drop in propene emissions from the Ship Channel after the first campaign. In 2006 there was large variability in propene, mainly around Battleground Road and Deer Park and the average emissions were inflated by relatively few measurements, which might be considered extraordinary events. Even discounting these upset events propene emissions were higher. This fact, coupled with propene inventories for the Ship Channel that were also significantly higher for 2006 than for the other years, suggests that the emissions were actually significantly higher in 2006.

Table 67 Compilation of measurements from three different SOF campaigns in southeast Texas together with reported emissions for three different years.

Source region	**Species**	**SOF/DOAS 2011 (kg/h)**	**SOF/DOAS 2009 (kg/h)**	**SOF/DOAS 2006 (kg/h)**	**Inventory 2009 (kg/h)**	**Inventory 2006 (kg/h)**	**Inventory 2004 (kg/h)**
Total HSC	Ethene	612	580	804	74	64	60
	Propene	563	624	1653	77	140	80
	Alkane	11569	10134	11528	851	1483	1500
	SO_2	2328	3364		1967	2585	2552
	NO_2	1829			1297*		
Mont Belvieu	Ethene	545	429	443	65	81	45
	Propene		310	488	28	35	12
	Alkane	1319	1837	863	244	190	261
	NO_2	305	168		192*	189*	268*
Texas City	Ethene	177	118	83	4	7	9
	Propene	56	54	ND	8	9	11
	Alkane	2342	2598	2889	318	372	240
	SO_2	1209	834		327	596	613
	NO_2	492	283		387*	452*	883*
Beaumont / Port Arthur	Ethene	179			24		
	Propene	54			20		
	Alkane	7412			457		
	SO_2	1611			1114		
	NO_2	1421			1145*		
Longview	Ethene	452			113		
	Propene	282			32		
	Alkane	841			87		
	NO_2	176			207*		

*** NO_x is reported**

7.2 Flaring

Out of 24 possible emission sources surveyed with thermal FTIR measurements, 4 showed distinct emissions of ethene and/or propene; and 6 showed weaker signs of emissions. All sources showing distinct or weak emission signals were flares, while only 20 of the sources surveyed were flares. Even though the flares surveyed were only a fraction of all flares in these areas, one flare with a distinct emission signal was found in nearly every area where significant ethene and propene emissions were measured with SOF.

No attempt to quantify the emissions detected with the thermal FTIR measurements was made; this was beyond the scope of the project. However, large emissions would probably be required for detection at such large distances as the measurements were typically made.

Emissions rates reported for flare sources are typically calculated by multiplying the flows sent to the flares by 1 minus the assumed combustion efficiency, typically 98–99 %. The 2010 TCEP Comprehensive Flare Study showed that this high combustion efficiency is difficult to maintain while also complying with demands for no visible smoke from the flame. It was argued that many flares might achieve significantly lower combustion efficiency under normal operating conditions, which would give significantly larger emissions than reported. SOF measurements from 2006, 2009 and 2011 have all showed significantly higher emissions of ethene and propene from refineries and petrochemical facilities than what is reported. Underperforming flares is one possible explanation or partial explanation for this. The results from the TCEQ Comprehensive Flare Study and the fact that distinct ethene and propene signal is detected in thermal FTIR measurements at such large distance makes this an attractive explanation, although it is by no means proven.

7.3 Natural gas production in Fort Worth

In the Fort Worth study it was found that the largest continuous gas sources, related to natural gas production, are the treatment facilities combined with large compressor stations (6-12 compressors). Three such facilities were measured with MeFTIR, tracer gas releases and canister sampling and typical emissions are 100 kg/h of methane, 40 kg/h of CO, 10 kg/h of ethane, 1 kg/h of ethane and 0.4 kg/h of ethene, see Table 68.

Another emission source category is small compressor stations (1-3 compressors). These have order of magnitude lower emissions than the combined treatment facilities and compressor stations, obtained from measuring 3 individual stations, see Table 68.

A third important emission category is well pads, i.e. well sites where the natural gas is extracted from the ground and the condensates are separated from the natural gas into a tank. In the Fort Worth area there are around 10000 such well sites. The continuous emissions from the well pads appears to be around 1 kg/h of methane, 0.1 kg/h of ethane and little else, as obtained from measurements of three different well pads, Table 68. However, gases dissolved in the condensate are regularly flashed out by venting the condensate tanks (flashing emissions). Other studies (Bar-Illan 2008a and 2008b and ERG) from the Fort Worth and Denver area indicates that flashing emission from well pads can account for more than 60% of the total emissions.

In this study flashing emissions from a condensate tank were measured on one occasion with emissions of 140 kg/h methane, 10 kg/h ethane and 2 kg/h of ethene and other species; see Table 68. Noteworthy, is the high ethene content (20% of the ethane) that was measured in the canisters with good reproducibility and high abundance above the background (60 ppb). This species is of large interest since it is a precursor for tropospheric ozone formation. To our knowledge ethene emissions have not been reported by others, for instance Sullivan et al. (2010) who carried out similar canister measurements in the Fort Worth area. The reason for this is unclear but differences include the canister sampling method. In this study the canister sampling was carried out at overpressure, while in the standard procedure the sample is extracted into a vacuum pumped canister. The higher pressure prevents wall effects, enabling reactive species to survive longer in the canister.

Another question is how frequent such flashing emission events are, since only one was encountered during the study. It should be noted, that smaller ethene emissions were also detected for gas treatment facilities, (0.4 kg/h.). Since there are only a few such plants this source of ethene can not cause any significant impact on ozone formation, however.

Table 68 Overview of the sources measured with MeFTIR and canisters in the Fort Worth area and measured methane emissions. Methane and CO emissions were measured in real time from MeFTIR and tracer gas (section 6.1, uncertainty 20-30%) while the ethane was derived from average ratios of methane to ethane measured by MeFTIR (6.2). All other species X were derived from canister samples using the obtained X/ ethane ratio and then further using the derived ethane MeFTIR emission. The canister species shown correspond to species for which the downwind values were *significantly* (difference larger than intra canister variability higher than upwind values).

#	**Name**	**Site**	**Comment**	**Emission (kg/h)**
1	FM 1220	Compressor station, and treatment facility	6 compressors (May 12 emissions only)	CH_4: 82.6 CO: 8 C_2H_6: 5.1 C_3H_8: 0.03 C_2H_4: 0.27 C_3H_6: 0.00
1	FM 1220	Well pad close to treatment facility. Open valve on condensate tank	Flashing emission. (Difference May 10 – May 12)	CH_4: 138.7 CO: 0 C_2H_6: 10.6 C_3H_8: 0.40 C_2H_4: 2.04 C_3H_6:0.04 C_5H_{12}: 0.01
2	Hicks Field Rd	Treatment plant and compressor station	1 meas day. 12 compressors	CH_4: 150 CO: 37±23 C_2H_6:10.3 C_3H_8: 0.79 C_2H_4:0.37
3	Blue Mound Rd	Treatment plant and compressor station	6 compressors, (Upwind not available)	CH_4: 120 CO: NA C_2H_6: 6
4	Northern cross Rd	Well pads and mobile compressor	2 condensate tanks, 1 compressor	CH_4: 8 CO: 0.4 C_2H_6: NA
5	Meacham Blvd	Compressor station, and gas separators and well pad	1 compressor	CH_4: 17 CO: 0.6 C_2H_6:1.1
6	Long Avenue	Compressor station	3 compressors	CH_4: 8 CO: 10±2 C_2H_6:0.9
7	Eagle Mt Rd	Well pads, distribution pipes	In the vicinity of compressor station and power station	CH_4: 6 CO: 1.1±1.1 C_2H_6:0.5 C_3H_8: 0.11 C_2H_4: 0.00
8	E Peden Rd (1)	Well pad	2 condensate tanks	CH_4: 1 CO: 0.1±0.05 C_2H_6: NA
9	E Peden Rd 2	Well pad	3 condensate tanks and potentially leaking pipeline	CH_4: 1 CO: 0.1 C_2H_6:0.12
10	Bonds Ranch Rd	Well pad	2 tanks	CH_4: 1 CO: NA C_2H_6:NA

7.4 Further studies

The results from this project indicate the need for future studies.

Flares
Several studies have indicated that it is common for flares to underperform in terms of combustion efficiency during normal operating conditions (Mellqvist 2001, Allen 2011). Additionally, the SOF Texas air quality study in 2006 (Mellqvist, 2010) indicated that flaring was a probable cause of high alkene variability in HSC. The thermal emission measurements carried out within this project indicate that 20% of the petrochemical flares exhibit incomplete combustion of alkenes. All in all, it is very interesting to improve the understanding of the impact of flaring on overall VOC emissions. A future study should include improved spectral retrieval software for thermal FTIR measurements to be able to quantify alkenes and should include measurements by both SOF and thermal FTIR to be able to carry out simultaneous measurements.

Real emissions versus emissions inventories
It is interesting to keep on improving industrial emission data of VOCs, NOx and SO2 and to follow their variation over time. One thing to study is whether the lower propene emissions in Mont Belvieu and HSC are real, or just an artefact of too few measurements and problems with propene measurements. Other things to study are other industrial areas in Texas and to repeat previous measurements. A third interesting topic to study further is the relatively high butadiene emissions encountered in Port Arthur.

Flashing emissions from well pads
The ethene emissions observed from flashing emissions in the Fort Worth area should be continued and further investigated since this study is the only one reporting ethene emission. In further studies it is important to carry out ethene measurements also with other methods, in addition to canister sampling, e.g. MeFTIR and SOF. (In this study the MeFTIR ethene channel was not used in Fort Worth due to instrumental problems, but this could be overcome.)

8. Acknowledgements

This work was funded by state of Texas through the Air Quality Research program administered by the University of Austin under project no 10-006. We thank TCEQ for supplying wind data and John Jolly at TCEQ for supplying data from the STARS (State of Texas Air Reporting System) emission inventory.

9. References

Allen, D.T. and V.M. Torres, 2010 TCEQ Flare Study Project, Final Report. 2011.

Arnold S.R., Methven J., Evans M.J., Chipperfield M.P., Lewis A.C., Hopkins J., McQuaid J.B., Watson N., Purvis R.M., Lee J.D., Atlas E.L., Blake D.R., Rappenglück B. (2007): Statistical inference of OH concentrations and air mass dilution rates from successive observations of nonmethane hydrocarbons in single air masses, *J. Geophys. Res.*, 112, D10S40, doi:10.1029/2006JD007594

Babilotte, A., Green, R., Hater, G., Watermolen, T., Staley, B., 2009, Field intercomparison of methods to measure fugitive methane emissions. Proceedings Sardinia 09 Twelfth International Waste Management and Landfill Symposium, CISA Environmental Sanitary Engineering Centre, Cagliari, Italy.

Bar-Ilan A. et al. (2008a), Development of baseline 2006 emissions from oil and gas activity in the Denver-Julesburg Basin, WRAP Phase III report, 34p, available at http://www.wrapair.org/forums/ogwg/PhaseIII_Inventory.html.

Bar-Ilan A. et al. (2008b), Development of the 2010 oil and gas emissions projections for the Denver-Julesburg Basin, WRAP Phase III report, 26p, available at http://www.wrapair.org/forums/ogwg/PhaseIII_Inventory.html.

Bogumil, K. et al., 2003, Measurements of Molecular Absorption Spectra with the SCIAMACHY PreFlight Model: Instrument Caracterization and Reference Data for Atmospheric Remote-Sensing in the 230–2380 nm Region, J. Photoch. Photobio. A, 157, 167–184

Buhr, M., Alvarez, S., Kauffmann, L., Shauck, M., Zanin, G., Alkene/NOy Emission Ratios observed from the Baylor Aztec during the 2006 TexAQS II study and Comparison with results obtained during 2001–2002, Rapid science synthesis workshop, Austin, october 12, 2006

Burrows, J.P et al., 1999, Atmospheric Remote-Sensing Reference Data from GOME: 2. Temperature-Dependent Absorption Cross Sections of O3 in the 231–794 nm Range, Journal of Quantitative Spectroscopy and Radiative Transfer 61, 509–517

Börjesson, G., J. Samuelsson, J. Chanton, R. Adolfsson, B. Galle, and B.H. Svensson. 2009. A national landfill methane budget for Sweden based on field measurements, and an evaluation of IPCC models. Tellus, 61B: 424–435.

Cantrell CA, Davidson JA, McDaniel AH, Shetter RE, Calvert JG. 1990, Temperature dependent formaldehyde cross sections in the near-ultraviolet spectral region. J Phys Chem, 94:3902–8.

De Gouw, J.A., et. al. (2009), Airborne Measurements of Ethene from Industrial Sources Using Laser Photo-Acoustic Spectroscopy, Environmental Science and Technology, 43, 2437–2442.

ERG, Forth Natural gas Air Quality Study Final Report, 2011, www.forthworthgov.org

EPA Handbook: Optical Remote Sensing for Measurement and Monitoring of Emissions Flux, December 2011, Office of Air Quality Planning and Standards , Air Quality Analysis Division Measurement Technology Group , Research Triangle, North Carolina, 27711, editor Dennis K. Mikael, http://www.epa.gov/ttn/emc/guidlnd/gd-052.pdf

Fayt, C. and Van Roozendael, M., 2001. QDOAS 1.00 Software User Manual, BIRA-IASB.

Fish, D.J. and Jones, R.L., 1995. Rotational Raman scattering and the ring effect in Zenith-sky spectra. Geophysical Research Letters, 22(7): 811–814.

Galle, B.; Mellqvist, J., et al., Ground Based FTIR Measurements of Stratospheric Trace Species from Harestua, Norway during Sesame and Comparison with a 3-D Model, JAC, 1999, 32, no. 1, 147–164.

Galle, B., J. Samuelsson, B.H. Svensson, G. Börjesson, "Measurements of methane emissions from landfills using a time correlation tracer method based on FTIR absorption spectroscopy."

Environ. Sci. Technol. 35: 21–25. 2001.

Galle, B., Oppenheimer, C., Geyer, A., McGonigle, A.J.S., Edmonds, M. and Horrocks, L., (2002), A miniaturised ultraviolet spectrometer for remote sensing of SO2 fluxes: A new tool for volcano surveillance, Journal of Volcanology and Geothermal Research, 119 241–254

Gratien, A. et al (2007), UV and IR Absorption Cross-sections of HCHO, HCDO, and DCDO, J. Phys. Chem. A, 111, 11506–11513

Grenfell R.J.P., Milton M.J.T., Harling A.M., Vargha G.M., Brookes C., Quincey P.G., Woods P.T. (2010): Standard mixtures of ambient volatile organic compounds in synthetic and whole air with stable reference values, *J. Geophys. Res*, 115, D14302, doi:10.1029/2009JD012933

Griffith D.W.T., Synthetic calibration and quantitative analysis of gas-phase FT-IR spectra. Applied Spectroscopy, 1996. 50(1): p. 59–70.

Heckel, A., A. Richter, T. Tarsu, F. Wittrock, C. Hak, I. Pundt, W. Junkermann, and J.P. Burrows, MAX-DOAS measurements of formaldehyde in the Po-Valley, Atmospheric Chemistry and Physics, 5, 909–918, 2005.

Hermans, C.et al., Absorption cross-sections of atmospheric constituents: NO_2, O_2, and H_2O, Environ. Sci. Pollut. R. , 6, 151–158, 1999.

Hurley, P.J., Physick W.L., and Luhar A.K., TAPM: A practical approach to prognostic meteorological and air pollution modelling. Environmental Modelling and Software, 2005. 20(6): p. 737.

Johansson, M., C. et al, 2009, Mobile mini-DOAS measurement of the outflow of NO2 and HCHO from Mexico City, Atmos. Chem. Phys., 9, 5647–5653

Kihlman, M. (2005a), Application of solar FTIR spectroscopy for quantifying gas emissions, Technical report No. 4L, ISSN 1652-9103, Department of Radio and Space Science, Chalmers University of Technology, Gothenburg, Sweden.

Kihlman, M., J. Mellqvist, and J. Samuelsson (2005b), Monitoring of VOC emissions from three refineries in Sweden and the Oil harbor of Göteborg using the Solar Occultation Flux method, Technical report, ISSN 1653 333X, Department of Radio and Space, Chalmers University of Technology, Gothenburg, Sweden.

S.-W. Kim,..Mellqvist, J., et al., Evaluations of NOx and highly reactive VOC emission inventories in Texas and their implications for ozone plume simulations during the Texas Air Quality Study 2006S, Atmos. Chem. Phys., 11, 11361–11386, 2011, www.atmos-chem-phys.net/11/11361/ 2011/doi:10.5194/acp-11-11361-2011

Koppmann R., Johnen F.J., Khedim A., Rudolph J., Wedel A., Wiards B. (1995): The influence of ozone on light nonmethane hydrocarbons during cryogenic preconcentration, *J. Geophys. Res.*, **100**, 11383–11391.

Leuchner M., Rappenglück B. (2010): VOC Source-Receptor Relationships in Houston during TexAQS-II, *Atmos. Environ.*, **44**, 4056–4067, doi:10.1016/j.atmosenv.2009.02.029

Mellqvist, J., Application of infrared and UV-visible remote sensing techniques for studying the stratosphere and for estimating anthropogenic emissions, doktorsavhandling, Chalmers tekniska högskola, Göteborg, Sweden, 1999a

Mellqvist, J och Galle, B., Utveckling av ett IR absorptionssystem användande solljus för mätning av diffusa kolväteemissioner, Rapport till Preems miljöstiftelse juli 1999b.

Mellqvist, J., Arlander, D. W., Galle, B. and Bergqvist, B., Measurements of Industrial Fugitive Emissions by the FTIR-Tracer Method (FTM), IVL report, 1995, B 1214.

Mellqvist, J., Flare testing using the SOF method at Borealis Polyethylene in the summer of 2000. 2001, Chalmers University of Technology. (Available at www.fluxsense.se)

Mellqvist, J., J. Samuelsson, C. Rivera, B. Lefer, and M. Patel (2007), Measurements of industrial emissions of VOCs, NH_3, NO_2 and SO_2 in Texas using the Solar Occultation Flux method and mobile DOAS, Project H053.2005, Texas Environmental Research Consortium., Texas. (http://www.harc.edu/projects/airquality/Projects/Projects/H053.2005)

Mellqvist, J.,Berg N. and Dan Ohlsson, 2008a, Remote surveillance of the sulfur content and NOx emissions of ships, Second international conference on Harbours, Air Quality and Climate Change (HAQCC), Rotterdam.

Mellqvist, J., Johansson, J.,Samuelsson, J., Rivera, C., Lefer, B. and S. Alvarez (2008b), Comparison of Solar Occultation Flux Measurements to the 2006 TCEQ Emission Inventory and Airborne Measurements for the TexAQS II, Project No. 582-5-64594-FY08-06 , TCEQ report., Texas. (available at http://www.tceq.state.tx.us/assets/public/implementation/air/am/contracts/reports/da/20081108-comparison_solar_occultation_flux_measurements.pdf)

Mellqvist, J., et al. (2009a), Emission Measurements of Volatile Organic Compounds with the SOF method in the Rotterdam Harbor 2008, available at www.fluxsense.se

Mellqvist, J., J. Samuelsson, J. Johansson, C. Rivera, B. Lefer, S. Alvarez, and J. Jolly (2010), Measurements of industrial emissions of alkenes in Texas using the solar occultation flux method, J. Geophys. Res., 115, D00F17, doi:10.1029/2008JD011682.

Methven J., Arnold S.R., Stohl A., Evans M.J., Avery M., Law K., Lewis A.C., Monks P.S., Parrish D., Reeves C., Schlager H., Atlas E., Blake D., Coe H., Cohen R.C., Crosier J., Flocke F., Holloway J.S., Hopkins J.R., Hübler G., Lee J.D., Purvis R., Rappenglück B., Ryerson T.B., Sachse G.W., Singh H., Watson N., Whalley L., Williams P. (2006): Establishing Lagrangian connections between observations within air masses crossing the Atlantic during the International Consortium for Atmospheric Research on Transport and Transformation experiment, *J. Geophys. Res.*, 111, D23S62, doi:10.1029/2006JD007540

Plass-Dülmer C., Schmidbauer N., Slemr J., Slemr F., D'Souza H. (2006): The European Hydrocarbon Intercomparison Experiment AMOHA Part 4: Canister Sampling of Ambient Air, *J. Geophys. Res.*, 111, D4, D04306, doi:10.1029/2005JD006351

Platt, U., D. Perner, and H.W. Pätz, Simultaneous Measurement of Atmospheric CH2O, O3 and NO2 by Differential Optical Absorption, Journal of Geophysical Research, 84 (C10), 6329–6335, 1979.

Rappenglück B., Schmitz R., Bauerfeind M., Cereceda-Balic F., v. Baer D., Jorquera H., Silva Y., Oyola P. (2005): An urban photochemistry study in Santiago de Chile, *Atmos. Environ.*, 39, 2913–2931, doi:10.1016/j.atmosenv.2004.12.049

Rappenglück B., Apel E., Bauerfeind M., Bottenheim J., Brickell P., Čavolka P., Cech J., Gatti L., Hakola H., Honzak J., Junek R., Martin D., Noone C., Plass-Dülmer Ch., Travers D., Wang T (2006): The first VOC intercalibration exercise within the Global Atmosphere Watch (GAW), *Atmos. Environ.*, 39, 2913–2931, doi:10.1016/j.atmosenv.2004.12.049

Rappengluck, B. et al, 2008a, Analysis of Primary vs. Secondary Fraction of Formaldehyde Houston Area During TexAQS-II, 10th Conference on Atmospheric Chemistry conference, The 88th Annual Meeting (20–24 January 2008), AMS,

Rappenglück, B et al, (2008b): In‐Situ Ground‐Based and Airborne Formaldehyde Measurements during the TRAMP Study; Atmos.Environ., submitted.

Rinsland, C. P., R. Zander, and P. Demoulin (1991), Ground-based infrared measurements of HNO3 total column abundances: long-term trend and variability, *J. Geophys. Res.*, *96*, 9379–9389.

Rivera, C. et al., (2010), Quantification of NO2 and SO2 emissions from the Houston Ship Channel and Texas City during the 2006 Texas Air Quality Study, J. Geophys. Res., 115, D08301, doi:10.1029/2009JD012675

Rivera , C., Application of Passive DOAS using Scattered Sunlight for quantification of gas emission from anthropogenic and volcanic sources (2009a), Dissertation, ISBN 978-91-7385-317-0, ISSN 0346

Rivera, C., J.A. Garcia, B. Galle, L. Alonso, Y. Zhang, M. Johansson, M. Matabuena, and G. Gangoiti (2009b), Validation of optical remote sensing measurement strategies applied to industrial gas emissions, Int. J. Remote Sens., vol 30, no 12, p3191–3204.

Rivera, C., et al. (2009c),Tula industrial complex (Mexico) emissions of SO2 and NO2 during the MCMA 2006 field campaign using a mobile mini_DOAS system, Atmos. Chem. Phys., 9, 6351–6361, 2009.

Rothman et al. (2003), HITRAN 2000, Journal of Quantitative Spectroscopy and Radiative Transfer, vol. 82, pp. 5–44.

Ryerson, T. B., et al. (2003), Effect of petrochemical industrial emissions of reactive alkenes and NOx on tropospheric ozone formation in Houston, Texas, J. Geophys. Res., 108(D8), 549 4249, doi:10.1029/2002JD003070.

Samuelsson, J., Börjesson, G., Svensson, B., Galle, B., Metan från avfallsupplag i Sverige (Methane from landfills in Sweden), final report to the Swedish Energy Agency, projekt nr P10856-4, December 2005a. In Swedish (www.stem.se), can be ordered from Studsviksbiblioteket, 611 82 Nyköping, Sweden, www.lib.kth.se/SB/service/stemavf.html.

Samuelsson, J., et. al., VOC measurements of VOCs at Nynas Refinery in Nynäshamn 2005b *(Utsläppsmätningar av flyktiga organiska kolväten vid Nynas Raffinaderi i Nynäshamn 2005, in Swedish*), Bitumen refinery official report to provincial government 2005, Available at: http://www.fluxsense.se

Schürmann G., Schäfer K., Jahn C., Hoffmann H., Bauerfeind M., Fleuti E., Rappenglück B. (2007): The Impact of NO_x, CO and VOC Emissions on the Air Quality of the Airport Zurich, *Atmos. Environ.*, 41, 103–118, doi:10.1016/j.atmosenv.2006.07.030

Sharpe, S., et al. (2004), Gas-Phase Databases for Quantitative Infrared Spectroscopy, *Applied Optics*, *58*(12).

Slemr J., Slemr F., Partridge R., D´Souza H., Schmidbauer N. (2002): Accurate measurements of hydrocarbons in the atmosphere (AMOHA): three European intercomparisons, *J. Geophys. Res.*, 107, D19, 4409, doi:10.1029/2001JD001357

STARS, Emission inventory data extracted by John Jolly of the Texas Commission on Environmental Quality (TCEQ) from the TCEQ's State of Texas Air Reporting System (STARS) database, on Sept 28, Oct 3, and Oct 4, 2011.

Sullivan, D., et al, Oil and Gas Emissions in the DFW Region, University of Austin report , TCEQ Grant Activities No. 582-8-86245-FY09-03 , Jan , 2010

Taylor, B., and C. Kuyatt, 1994. "Guidelines for Evaluating and Expressing the Uncertainty of NIST Measurement Results." NIST Technical Note 1297 1994 edition. Gaithersburg, MD.

Thoma, E. et al. (2009), Development of EPA OTM 10 for Landfill Applications, in print, Journal of Environmental Engineering

Tucker, S., Marine boundary Layer dynamics and heights during TexAQS 2006: HRDL measurements from the RV Brown, Principal Findings Data Analysis Workshop TexAQS II, Austin, May 29–June 01, 2007. (available at www.tceq.state.tx.us)

URS Corporation, 2004. Passive FTIR Phase I Testing of Simulated and Controlled Flare Systems. Final report prepared for the Texas Commision on Environmental quality (TCEQ), 12100 Park 35 Circle, Austin, TX 78753

Vandaele A.C., C. Hermans, P.C. Simon, M. Carleer, R. Colin, S. Fally, M.F. Mérienne, A. Jenouvrier, and B. Coquart, Measurements of the NO2 absorption cross-section from 42000 cm-1 to 10000 cm-1 (238–1000 nm) at 220 K and 294 K, J.Q.S.R.T., 59, 171–184 (1998)

Veillerot M., Locoge N., Galloo J.C., Guillermo R. (1998): Multidimensional capillary gas chromatography for the monitoring of individual non-methane hydrocarbons in air, *Analysis Magazine*, **26**, M38–M43.

Walmsley, H. L., and S. J. O'Connor (1998), The accuracy and sensitivity of infrared differential absorption lidar measurements of hydrocarbon emissions from process units. *Pure Appl. Opt.*, *7*, 907–925.

Wert, B. P., et al. (2003), Signatures of terminal alkene oxidation in airborne formaldehyde 571 measurements during TexAQS 2000, J. Geophys. Res., 108(D3), 4104, doi:10.1029/2002JD002502, 2003.

Winkler J., Blank P., Glaser K., Habram M., Jambert C., Jaeschke W., Konrad S., Kurtenbach R., Lenschow P., Perros P., Pesch M., Prümke H.-J., Rappenglück B., Schmitz T., Slemr F., Volz-Thomas A. and Wickert B. (2002): Nonmethane hydrocarbon measurements in BERLIOZ: Characterization of the ground-based measurement sites and emission ratios derived from airborne measurements, *J. Atmos. Chem.*, 42, 465–492